Forty years of geostrophic currents in the Ligurian Sea

Journal of the BLACK SEA/MEDITERRANEAN ENVIRONMENT

International Journal a Trimesterly International Publication of Earth, Marine, Environment and Engineering Science

Special Issue 2015 ISSN: 1304-9550

Proceedings of MedCLIVAR 2014 Conference
Understanding Climate Evolution and Effects on Environment and Societies in the Old World Region
METU, ANKARA, TURKEY
23-25 JUNE 2014

Web
www.blackmeditjournal.org, www.tudav.org

Category Link
Pollution, Marine Biology, Physical and Chemical Oceanography, Marine Geology and Geophysics, Maritime Policy, Biological Conservation, Coastal Zone Management

Printed by: Metin Copy Plus (Tel: 0212 527 61 81)
Editorial Address: TUDAV (Turkish Marine Research Foundation), P.O. Box: 10 Beykoz, Istanbul, Turkey. E mail: tudav@tudav.org

Abstracted in: Chemical Abstracts, ASFA (Aquatic Sciences and Fisheries abstracts), Biosis (Biological Abstracts, Biosis Previews)

Journal of the
BLACK SEA/MEDITERRANEAN
ENVIRONMENT

Special Issue 2015

Contents

For the figures in color, please check pdf's on website. (www.blackmeditjournal.org)

Submission of manuscript: Manuscript must be sent electronically to tudav@tudav.org

Subscription: Yearly subscription rate including postal and handling is €50 for individual subscribers and €100 for institutional subscribers. Please contact tudav@tudav.org for subscription.

Cover photograph: Medicane, 7 November 2014 ©EUMETSAT.

INTRODUCTION TO THE SPECIAL EDITION

Proceedings of MedCLIVAR 2014 Conference
Understanding Climate Evolution and Effects on Environment and Societies in the Old World Region
METU, ANKARA, TURKEY
23-25 JUNE 2014

This special volume of the Journal of the Black Sea and Mediterranean Environment has been made possible by special privilege provided by TÜDAV the Turkish Marine Research Foundation. We, the conference organizers and co-editors, express our deepest felt gratitude to Bayram Öztürk, the chief editor of the journal, for his generous support, and as well to Arda Tonay, for handling the production during the leave, to Antarctica, of the chief editor. In addition to us, conference conveners Vincenzo Artale, Giovanni Zanchetta, Murat Türkeş, Gabriel Jordà, Elena Xoplaki, Levent Kurnaz, Andrea Toreti and Serge Planton shared the responsibility as guest co-editors for groups of papers. We also thank Riccardo Buccolieri of Università del Salento and Tuğçe Gül of TÜDAV, serving as technical editors of this volume, for their careful and creative work.

The international MedCLIVAR 2014 Conference "Understanding Climate Evolution and Effects on Environment and Societies in the Old World Region" has been convened at the Cultural and Congress Center of the Middle East Technical University in Ankara during 23-25 June 2014. We thank METU (the Middle East Technical University, Ankara), for providing the venue and services, along with the EGU (European Geosciences Union), AEMET (Agencia Estatal de Meteorologia - State Meteorological Agency, Spain), CMCC (Centro Euro-Mediterraneo sui Cambiamenti Climatici - Euro-Mediterranean Center on Climate Change, Italy), ENEA (Agenzia Nazionale per le Nuove Tecnologie, l'Energia e lo Sviluppo Economico Sostenibile - National Agency for New Technologies, Energy and Sustainable Economic Development, Italy), for providing generous support for the conference. The conference has been the last one in a series of other conferences, summer schools and courses carried out by the MedCLIVAR network of international scientists.

The conference included the following sessions: (1) paleoclimate and the human dimension, (2) the regional climate system: observations and process studies, (3) extreme events, (4) model simulations of climate variability and climate change, (5) impacts of natural and anthropogenic climate change and mitigation/adaptation strategies, covering a wide spectrum of regional mechanisms and problems associated with the earth's climate, based upon up-to-date scientific methodology to understand and predict their environmental and societal effects.

The papers in this special volume are the short 4 page extended abstracts of the original scientific work presented at the conference. They constitute a subset of the conference contributions selected by the editors based on originality and relevance to the above program of the sessions.

We hope this publication in JMBSE will raise our common conscience, encourage and enhance climate research in Turkey as well as in Europe through an integrated research agenda dictated by the approaching climate risks and dangers, which are very real in the Old World region.

J. Black Sea/Mediterranean Environment
Special Issue : 1-4 (2015)

Extreme precipitation events over the Euro-Mediterranean region: projections dependence on daily/sub-daily time scale definition

Enrico Scoccimarro[1,2*], Gabriele Villarini[3], Silvio Gualdi[1,2], Alessio Bellucci[2], Matteo Zampieri[2], Marcello Vichi[4], Antonio Navarra[1,2]

[1] Istituto Nazionale di Geofisica e Vulcanologia (INGV), Bologna, ITALY
[2] Centro Euro-Mediterraneo per i Cambiamenti Climatici (CMCC), Lecce, ITALY
[3] I IHR-Hydroscience & Engineering, The University of Iowa, Iowa City, IA, USA
[4] Department of Oceanography, University of Cape Town, SOUTH AFRICA

[*]**Corresponding author**: enrico.scoccimarro@ingv.it

Abstract

It is well established that climate model projections indicate a tendency towards more extreme daily rainfall events. It is however uncertain how this changing intensity translates at the sub-daily time scales. The main goal of the present study is to examine possible differences in projected changes in intense precipitation events over Europe at the daily and sub-daily (3-hourly) time scales using a state-of-the-science climate model. There are large differences in intense precipitation projections when comparing the results at the daily and sub-daily time scales. Over north-eastern Europe, projected precipitation intensification at the 3-hour scale is lower than at the daily scale. On the other hand, Spain and the western seaboard exhibit an opposite behaviour, with stronger intensification at the daily rather than 3-hour scale. While the mean properties of the precipitation distributions are independent of the analysed frequency, projected precipitation intensification exhibit regional differences.

Keywords: Extreme events, precipitation, Europe

Introduction

The evaluation of changes in intense precipitation events is one of the most important issue related to climate change projection. Most of the analyses performed on intense precipitation events use data stored from climate models with a monthly or daily frequency. Many studies were performed focusing on Europe, using both General Circulation Models (GCMs) and Regional Climate Models (RCMs). They investigated changes in different parts of the precipitation distribution, such as averaged precipitation or intense/extreme events only, on a daily time basis. Less effort has been put in investigating of

extreme events at sub-daily time scale (Lenderink and Meijgaard 2008). The studies so far suggest a general greater increase in sub-daily precipitation intense events when compared to daily projections in a warmer climate. The main goal of the present study is to verify possible differences in projecting future changes in intense precipitation events over Europe based on a daily or a sub-daily time scale.

Material and Methods

The model employed in this work is the Centro Euro-Mediterraneo sui Cambiamenti Climatici coupled atmosphere-ocean general circulation model (CMCC-CM; Scoccimarro *et al.* 2011). The horizontal resolution of the ocean model is 2°×2° with a meridional refinement near the equator, approaching a minimum 0.5° grid spacing. The model has 31 vertical levels, 10 of which lie within the upper 100 m. The atmospheric model component has a T159 horizontal resolution, corresponding to a Gaussian grid of about 0.75° × 0.75°. Two periods are analysed: the period 1986-2005 (PRESENT), corresponding to the last part of the 'historical' CMIP5 simulation, and the period 2081-2100 (FUTURE), run under the high-end 'RCP8.5' scenario. Only winter (December-February, DJF) season is considered. At each grid point, the distribution of precipitation events is evaluated for the target season (DJF) and 20-year PRESENT and FUTURE periods, over Europe, using both daily and 3-hourly accumulation time windows. As a result, two different are obtained, and the corresponding 90^{th} percentiles (90p) are calculated. The 90p threshold is then used to define a "heavy precipitation" event. Dry events (here defined as lower than 0.2 mm/day precipitation events) were not considered when computing the percentiles.

Results

The CMCC-CM model represents the present climate precipitation activity over Europe reasonably well (Scoccimarro *et al.* 2013) both in terms of average and intense precipitation. Over the north eastern part of (black box in Figure 1) the investigated domain, the projected changes in 90p are less pronounced if computed on a 3h time scale compared to what is obtained at the daily time scale (Figure 1). The values of the 90p increase by 20-30% at the 3-hourly scale, while they are up to 60% larger when using the daily data. On the other hand, over Spain (Magenta box in Figure 1), the 3 hourly 90p projections are more pronounced than daily projections.

The discrepancy between the analyses performed at different time scales is better clarified when examining the inventory of intense events identified with the daily and 3-hourly data. More than 50% (up to 70% over the NE domain) of the DJF intense events defined at 3-hourly time scale occur in days that are not identified as intense precipitation days according to the daily-based statistics

(not shown). This finding suggests that 3-hourly and daily events belong to well distinct populations that share a common mean but different distributional properties on the right tails.

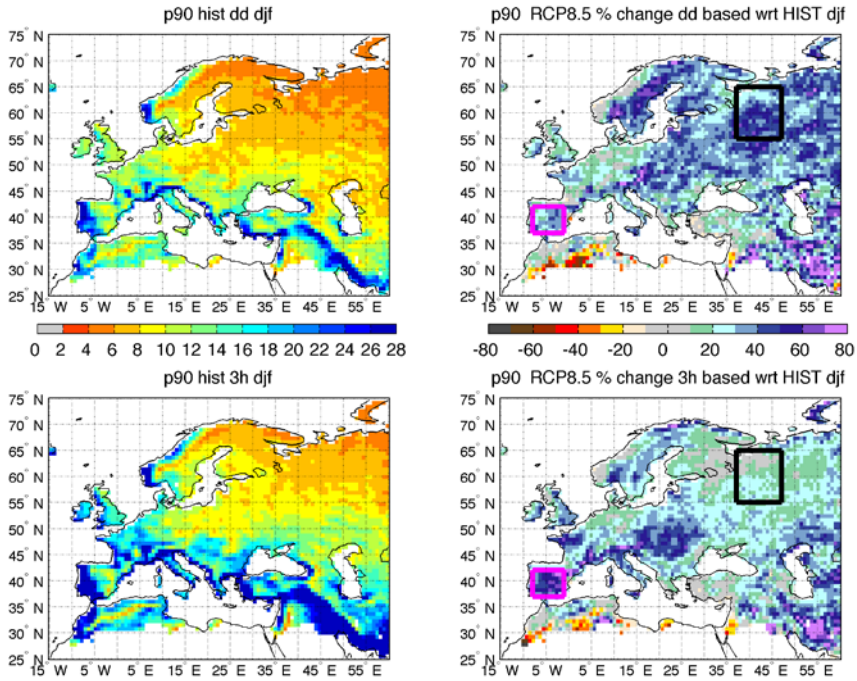

Figure 1. 90th percentile of DJF precipitation computed at daily (upper panels) and 3 hourly (lower panels) time frequency. Left panels represent the historical 90th percentile and the right panels represent the percentage change in FUTURE scenario. Units are [mm/d] for the left panels and [%] for the right panels

Discussion

The time window used to accumulate the precipitation field in the analyses (i.e., daily or 3-hourly) affects the spatial distribution of the projected changes of the 90p. We found that the future projection of 90p is less pronounced at 3 hourly time scale when compared to daily based projections, on the north eastern part of the investigated domain. This can be related to a reduced short term precipitation activity in the future climate. In particular, this is consistent with climate projections suggesting a general weakening of the storm track, both as a reduction in storm numbers and their intensities, in the northernmost part of the Atlantic Ocean and the Norwegian Sea; here a reduction in storm numbers (Bengtsson *et al.* 2006), together with an increase of precipitable water, could reduce the role played by intense short living extra-tropical cyclones in

determining heavy precipitation events changes in a warmer climate. On the other hand, our findings suggest a future increase in intense precipitation events more pronounced at the sub-daily time scale over Spain and over the western European seaboard. Thus, at least over Spain and part of Western Europe, changes in short-duration precipitation extremes may well exceed expectations based on projections relying on daily time series. A multi-model assessment is indeed necessary to corroborate our results, thus we hope this study highlights the importance of storing high frequency (i.e. 3 hourly) model outputs, over long time periods, within international climate modelling frameworks such as future coupled model intercomparison projects.

References

Bengtsson, L., Hodges, K.I., Roeckner, E. (2006) Storm tracks and climate change. *Journal of Climate* 19:3518-3543.

Lenderink, G., van Meijgaard, E. (2008) Increase in hourly precipitation extremes beyond expectations from temperature changes. *Nature Geoscience* 1:511-514.

Scoccimarro, E., Gualdi, S., Bellucci, A., Sanna, A., Fogli, P.G., Manzini, E., Vichi, M., Oddo, P., Navarra, A. (2011) Effects of tropical cyclones on ocean Heat Transport in a high resolution coupled general circulation model. *Journal of Climate* 24(16):4368-4384.

Scoccimarro, E., Gualdi, S., Bellucci, A., Zampieri, M., Navarra A. (2013) Heavy precipitation events in a warmer climate: results from CMIP5 models. *Journal of Climate* 26:7902-7911.

J. Black Sea/Mediterranean Environment
Special Issue: 5-10 (2015)

Dry events in the Mediterranean basin at 5.2 and 5.6 ka as recorded by stable isotopes in Corchia (Italy) and Soreq (Israel) caves speleothems

Giovanni Zanchetta[1*], Mira Bar-Matthews[2], Eleonora Regattieri[1], Russell N. Drysdale[3], Piero Lionello[4], Avner Ayalon[2], Ilaria Isola[5], John C. Hellstrom[6]

[1] Dipartimento di Scienze delle Terra, University of Pisa, Via S. Maria 53, 56126, Pisa, ITALY
[2] Geological Survey of Israel, Jerusalem, ISRAEL
[3] Department of Resource Management and Geography, University of Melbourne, Parkville 3010, AUSTRALIA
[4] Dipartimento Scienze e Tecnologie Biologiche e Ambientali, Università del Salento, Lecce, ITALY
[5] I Istituto Nazionale di Geofisica e Vulcanologia, sez. Pisa, Via della Faggiola 32, 56100, Pisa, ITALY
[6] School of Earth Sciences, University of Melbourne, Victoria 3010, AUSTRALIA

[*]**Corresponding author:** zanchetta@dst.unipi.it

Abstract

Analyses of speleothem $\delta^{18}O$ records from Soreq (Israel) and Corchia (central Italy) caves for the period between ca. 7 to 4 ka BP show two prominent isotopic excursions toward higher values, argued to reflect relatively drier conditions, centred at ca. 5.6 and ca. 5.2 ka. A possible mechanism explaining these two drier events is from comparison with the wind strength proxy record from Hólmsá loess profile in Iceland. This suggests that rainfall decrease was related to a reduced vapour advection from Atlantic towards the Mediterranean connected to northward shift in the Westerlies.

Keywords: speleothems, oxygen isotopes, dry mid-Holocene events, Mediterranean climate

Introduction

The study of past periods of reduced meteoric precipitation in the Mediterranean basin is of particular relevance for the sensitivity and vulnerability of the region to future water shortages due to climate change (Giorgi and Lionello 2008). Oxygen isotope composition of speleothem (cave calcite) is particularly suitable for investigating past hydrological changes over the Mediterranean (Bar-Matthews and Ayalon 2011; Regattieri *et al.* 2014), representing principally a signal of winter water recharge of the caves. In this paper we compare high-

resolution oxygen isotope data from Soreq Cave (Israel) and Corchia Cave (central Italy) (Figure 1) for the period of 7 to 4 ka. The investigated period overlaps the period of Rapid Climatic Changes (RCC) identified by Mayewski *et al.* (2004) between ca. 6000 and 5000 cal yr BP. This is a partial synthesis of data recently published by Zanchetta *et al.* (2014).

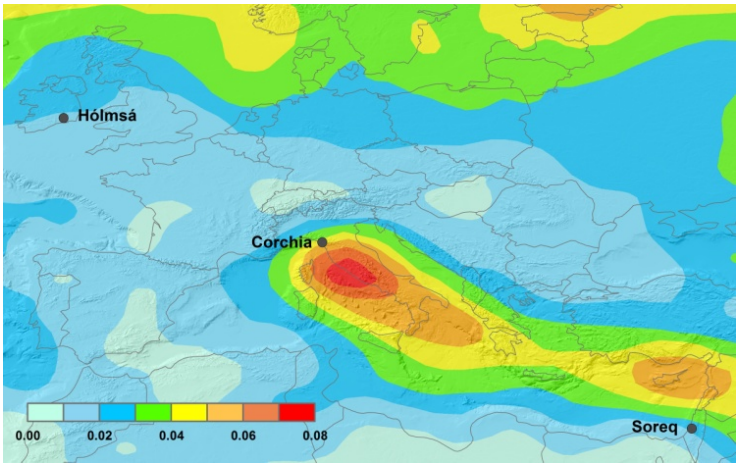

Figure 1. Location map of the studied sites

The figure shows the density track of winter storms according to ERA-interim 1989-2009. Numerical values (number of cyclones/deg^2) represent the average spatial density of cyclone centers in the winter season. Only cyclones with a minimum 1 day duration and 5 hPa depth with respect to the background are included (modified after Lionello *et al.* 2012).

Results and discussion

Both caves and their speleothem isotope records have been described in detail elsewhere (e.g. Bar-Matthews *et al.* 1996; Piccini *et al.* 2008) and will not be discussed further. Specifically, for this work the data are those discussed in Bar-Matthews and Ayalon (2011) obtained from three different, partially overlapping, speleothems, whereas the Corchia record is identical to that reported by Zanchetta *et al.* (2007) for stalagmite CC26. Figure 2 shows the two high resolution $\delta^{18}O$ time series, where two prominent events of increasing oxygen isotope composition are highlighted and centred at ca. 5.2 and 5.6 ka respectively.

In both records, an increase in the $\delta^{18}O$ values of speleothem calcite can be interpreted as a response to a decrease of precipitation, mostly due to the so-called “amount effect” (Zanchetta *et al.* 2007; Bar-Matthews *et al.* 2000), which is particularly relevant in different parts of Mediterranean (Bard *et al.* 2002).

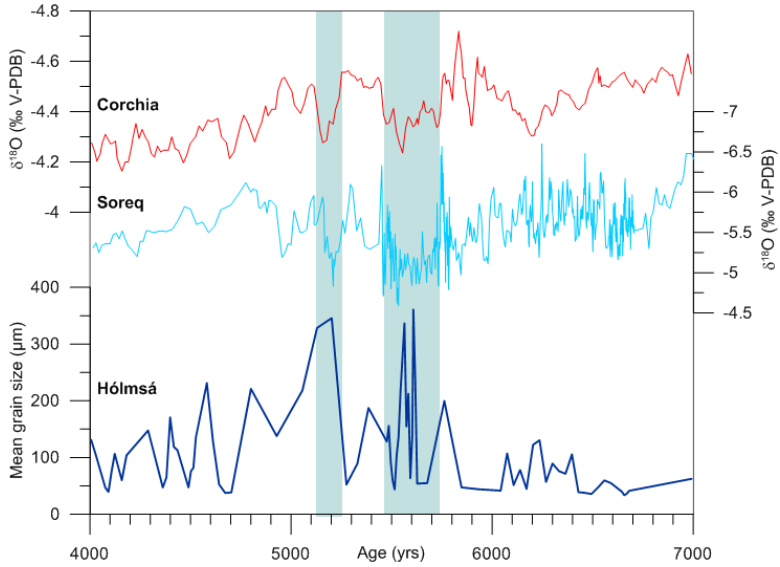

Figure 2. Comparison between $\delta^{18}O$ records from Corchia (Zanchetta *et al.* 2007) and Soreq (Bar-Matthews and Ayalon 2011) Caves and Hólmsá loess profile in Iceland (Jackson *et al.* 2005). Two phases of increasing grain size indicating elevated wind strength occur precisely at 5.2 and 5.6 ka, consistent with increasing zonal westerly flows and reduction of vapour advection in the Mediterranean. Ages are reported as AD 2000.

According to Orland *et al*. (2009), a change of ca. 1‰ in the annual weighted mean $\delta^{18}O$ of the local meteoric precipitation today at Soreq cave corresponds to a ca. 280 mm of change in rainfall. If this relation holds for the past, this implies that between the wettest period investigated (at ca. 5.8 ka) and the driest phase (at ca. 5.6 ka), there could have been a decrease of rainfall of ca. 280 mm. This is a maximum estimate assuming that most of the signal in the calcite is controlled by the "amount effect" and little or no change in influence from other atmospheric processes and from changes in the fractionation factor due to temperature. Detailed data are not yet available from Corchia; however, according to Bard *et al.* (2002) for Corchia area a relation of 1.6±0.2 ‰ per 100 mm/month would be reasonable. This indicates that any corresponding decrease in precipitation may have been less than that estimated for Soreq Cave. The less prominent isotopic shift at Corchia, and the inferred smaller decrease in rainfall relative to Soreq, can be explained by the fact that the Apuan Alps are strictly tied to the Gulf of Genoa cyclogenesis centre and the Apuan Alps act as a very efficient orographic barrier, enhancing rainfall. Moreover, we can infer that during the period of the reduction of vapour advection from the North Atlantic, which can be deduced by the present characteristics of precipitation for Corchia (Reale and Lionello 2013), the contribution of the Mediterranean Sea evaporation progressively becomes more and more significant eastward, which

has the effect to increase the isotopic composition of rainfall at Soreq to a greater degree than at Corchia, amplifying the isotopic differences between the speleothems from the two caves.

Of particular interest is to compare the wind strength proxy record from Hólmsá loess profile in Iceland (Jackson *et al.* 2005). Two phases of elevated wind strength occur precisely at 5.2 and 5.6 ka, consistent with increasing zonal westerly flows, which can correspond to a reduction of vapour advection in the Mediterranean (Figure 2). At Hólmsá, wind intensity is strongly influenced by the strength of westerly flow, with more severe gusts more likely to occur during positive (high-index) NAO. So, it seems that a persistent positive NAO-like condition would explain the presence of the drier periods identified at Corchia and Soreq.

Conclusion

Between ca. 6 and 4 ka Corchia and Soreq Cave speleothem oxygen stable isotope records show a remarkable similarity, and indicate at least two prominent dry events: at 5.6 and 5.2 ka. The first lasted perhaps a few decades to a century, whereas the second probably lasted from ca 5.7 to 5.4 ka.

We suggest that during the period of the two drier events recorded at Soreq and Corchia winter storm trajectories may have changed drastically, with increased zonal westerly flow producing a reduction of moisture advection toward the Mediterranean.

References

Bard, E., Delaygue, G., Rostek, F., Antonioli, F., Silenzi, S., Schrag, D. (2002) Hydrological conditions in the western Mediterranean basin during the deposition of Sapropel 6 (ca. 175 kyr). *Earth Planet. Sc. Lett.* 202: 481-494.

Bar-Matthews, M., Ayalon, A. (2011) Mid-Holocene climate variations revealed by high-resolution speleothems records from Soreq Cave, Israel and their correlation with cultural changes. *The Holocene* 21: 163-171.

Bar-Matthews, M., Ayalon, A., Kaufmann, A. (2000) Timing and hydrological conditions of sapropel events in the eastern Mediterranean, as evident from speleothems, Soreq cave, Israel. *Chem. Geol.* 169: 145-156.

Bar-Matthews, M., Ayalon, A., Matthews, A., Sass, E., Halicz, L. (1996) Carbon and oxygen isotope study of the active water-carbonate system in a karstic Mediterranean cave: implications for paleoclimate research in semiarid regions. *Geochim. Cosmoch. Acta* 60: 337-347.

Giorgi, F., Lionello, P. (2008) Climate change projection for the Mediterranean region. *Glob. Planet. Ch.* 63: 90-104.

Jackson, M.G., Oskarsson, N., Tronnes, R.G., McManus, J.F., Oppo, D.W., Grönvold, K., Hart, S.R., Sachs, J.P. (2005) Holocene loess deposition in Iceland: Evidence for millennial-scale atmosphere–ocean coupling in the North Atlantic. *Geology* 33: 509-512.

Lionello, P., Abrantes, F., Congedi, L., Dulac, F., Gacic, M., Gomis, D., Goodess, C., Hoff, H., Kutiel, H., Luterbacher, J., Planton, S., Reale, M., Schröder, K., Struglia, M.V., Toreti, A., Tsimplis, M., Ulbrich, U., Xoplaki, E. (2012) Introduction: Mediterranean Climate: Background Information in Lionello P. (Ed.) The Climate of the Mediterranean Region. From the Past to the Future, Amsterdam: Elsevier.

Mayewski, P.A., Rohling, E.E., Stafer, J.C., Karlen, W., Maasch, K.A., Meeker, L.D., Meyerson, E.A., Gasse, F., van Kreveld, S., Holmgren, K., Lee-Thorp, J., Rosqvist, G., Rack, F., Staubwasser M., Schneider, R.R., Steig, E.J. (2004) Holocene climate variability. *Quat. Res.* 62: 243-255.

Orland, I.J., Bar-Matthews, M., Kita, N.T., Ayalon, A., Matthews, A., Valley, J.W. (2009) Climate deterioration in the eastern Mediterranean as revealed by ion microprobe analysis of a speleothem that grew from 2.2 to 0.9 ka in Soreq Cave, Israel. *Quat. Res.* 71: 27-35.

Piccini, L., Zanchetta, G., Drysdale, R.N., Hellstrom, J., Isola, I., Fallick, A.E., Leone, G., Doveri, M., Mussi, M., Mantelli, F., Molli, G., Lotti, L., Roncioni, A., Regattieri, E., Meccheri, M., Vaselli, L. (2008) The environmental features of the Monte Corchia cave system (Apuan Alps, central Italy) and their effects on speleothem growth. *Int. Jour. Spel.* 37: 153-172.

Reale, M., Lionello, P. (2013) Synoptic climatology of winter intense precipitation events along the Mediterranean coasts. *Nat. Hazards Earth Syst. Sci.*13:1707-1722.

Regattieri, E., Zanchetta, G., Drysdale, R.N., Isola, I., Hellstrom, J.C., Dallai, L. (2014) Lateglacial to Holocene trace element record (Ba, Mg, Sr) from Corchia Cave (Apuan Alps, central Italy): paleoenvironmental implications. *Jour. Quat. Sc.* 29: 381-392.

Zanchetta, G., Drysdale, R.N., Hellstrom, J.C., Fallick, A.E., Isola, I., Gagan, M., Pareschi, M.T. (2007) Enhanced rainfall in the western Mediterranean during deposition of sapropel S1: stalagmite evidence from Corchia cave (Central Italy). *Quat. Sc. Rev.* 26:279-286.

Zanchetta, G., Bar-Matthews, M., Drysdale, R.N., Lionello, P., Ayalon, A., Hellstrom, J.C., Isola, I., Regattieri, E. (2014) Coeval dry events in the central and eastern Mediterranean basin at 5.2 and 5.6 ka recorded in Corchia (Italy) and Soreq Cave (Israel) speleothems. *Glob. Planet. Ch.* 122:130-139.

J. Black Sea/Mediterranean Environment
Special Issue: 11-14 (2015)

Trend towards earlier spring runoff in Alps

Matteo Zampieri[1*], Enrico Scoccimarro[1,2], Silvio Gualdi[1,2]

[1] Centro Euro-Mediterraneo sui Cambiamenti Climatici (CMCC), Bologna, ITALY
[2] Istituto Nazionale di Geofisica e Vulcanologia (INGV), Bologna, ITALY

[*]**corresponding author:** matteo.zampieri@cmcc.it

Abstract

We analyse the observed long-term discharge time-series of the main Alpine rivers: the Rhine, the Danube, the Rhone and the Po. We found common features in the trend and in the decadal variability of the spring discharge timings. In particular, all the time-series display a similar tendency towards earlier spring peaks of more than two weeks per century, which is mainly explained by the changes in total precipitation and rainfall seasonality.

Keywords: snowmelt, river discharge, precipitation seasonality, MedCLIVAR

Introduction

Spring river discharge can affect water quality and management, flood risk, river navigation and water availability, energy production and natural ecosystems. We present a long-term analysis of the observed discharge timings of the Rhine, the Danube, the Rhone and the Po rivers for the last two centuries and we assess the effects of precipitation seasonality, of its liquid portion (i.e. rainfall) and of snowmelt timing in terms of the long-term trend and of the decadal variability.

Materials and Methods

River discharge monthly time-series have been provided by the Global Runoff Data Center (GRDC, http://www.bafg.de). We used gridded climate datasets of monthly surface observations (HISTALP, Efthymiadis *et al.* 2006), covering the last two centuries. Determination of derived data and of the peak timings are explained in Zampieri *et al.* (2014), where a discussion on the basin climatologies can be found as well. Linear trends are computed with standard least square method.

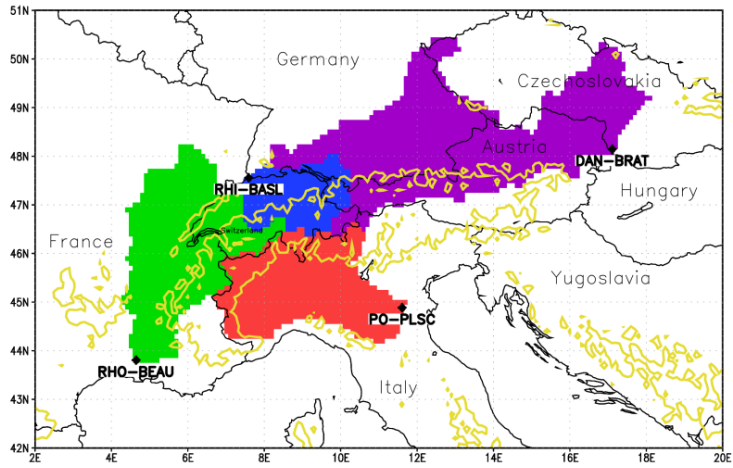

Figure 1. Discharge gauges (black diamonds) and contributing basins of the Rhine in Basel (RHI-BASL), the Danube in Bratislava (DAN-BRAT),the Rhone in Beaucaire (RHO-BEAU) and the Po River in Pontelagoscuro (PO-PLSC)

Results

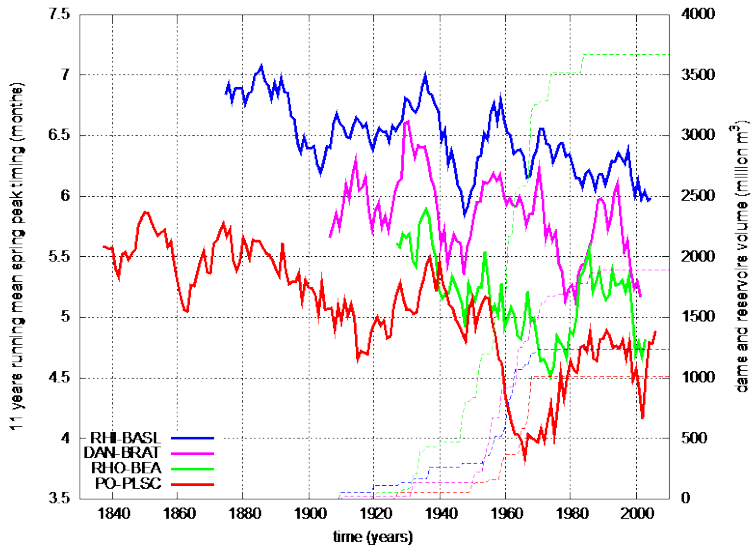

Figure 2. Spring river discharge peak timing time-series. Dashed lines represent the accumulated managed reservoirs volume in the basins (Lehner *et al.* 2011).

The river discharge peak timings time-series show an earlier trend of more than two weeks per century on the northern flank of the Alps, and more than 3 weeks

on the southern flank (see Figure 2 and Table 1). The peak timings time-series exhibit also some similar features of decadal variability among the rivers.

Table 1. Trends of river discharge, total and liquid precipitation, and snowmelt timings. Trends of the seasonal averages of liquid to total precipitation ratio, temperature, and of spring minus winter precipitation.

	RHI-BASL	**DAN-BRAT**	**RHO-BEAU**	**PO-PLSC**
River discharge timing (days/100years)	**-16±1** [a] p<2e-16	**-17±3** p<2e-16	**-22±4** p<2e-16	**-24±2** p<2e-16
Total precip. Timing (days/100years)	**-14±1** p<2e-16	**-15±2** p<2e-16	**-23±2** p<2e-16	3±2 [c] p=0.06
Rainfall timing (days/100years)	0±1 [b] p=0.76	**-11±1** p<2e-16	**-12±2** p=5.8e-13	**-4±1** p<1.6e-4
Snowmelt timing (days/100years)	-2±1 p=0.03	**-4±1** p=4.7e-7	**-5±1** p=4.8e-4	-0±1 p=0.82
MAM liquid/total (%/100years)	**4.5±1.0** p=6.9e-6	**4.6±1.1** p=2.6e-5	**3.6±0.8** p=1.4e-5	**2.5±0.5** p=1.3e-5
MAM temp. (°K/100years)	**0.74±0.14** p=8.1e-7	**0.75±015** p=8.8e-7	**0.70±0.14** p=1.6e-6	**0.70±0.13** p=3.8e-7
MAM-DJF HISTALP Total precip. (mm/day/100years)	**-0.35±0.09** p=6.4e-4	-0.15±0.08 p=0.05	**-0.71±0.09** p=1.3e-11	-0.17±0.08 p=0.04

[a] Results that are significantly different from zero at the 99.9% threshold level (p<0.001) are shown in bold.
[b] Results that are not statistically significant at the 90% (p>0.1) are in normal.
[c] Other values are associated with a significance of between 90% and 99%.

Total precipitation and rainfall are characterised by a tendency towards earlier peaks that are consistent with the trends of the river discharge peak timings for all the basins except the Po (see Table 1). Snowmelt shows a relatively small but significant trend towards earlier peaks. The percentage of liquid precipitation is increasing in all basins, consistently with the warming observed in the Alpine region. The proportion of winter to spring precipitation increases over all basins.

Discussion

We found a consistent earlier spring discharge of more than two weeks per century in the basins located north of the Alps, and more than three weeks per century in the basins located to the south. In our analysis, the long-term trend is mostly explained by the change of seasonality of precipitation and the increase of its liquid portion, while snowmelt timing is better at explaining the decadal fluctuations.

We provide in Figure 2 the basins' estimates of the accumulated reservoirs volumes, which can delay the peaks and affect the variability (Haddeland *et al.* 2006). Most of the structures were built in the 1960s, but they do not appear to affect significantly our time-series. Moreover, it is unlikely that human modification of land could produce the common features that we found in the different basins. Therefore, we think that most of the detected signals are due to climate variability and change.

Acknowledgments

Italian GEMINA and NEXTDATA projects.

References

Efthymiadis, D., Jones, P.D., Briffa, K.R., Auer, I., Böhm, R., Schöner, W., Frei, C., Schmidli, J. (2006) Construction of a 10-min-gridded precipitation data set for the Greater Alpine Region for 1800-2003 *J. Geophys. Res.* 110 D01105

Haddeland, I., Skaugen, T. and D. P. Lettenmaier (2006) Anthropogenic impacts on continental surface water fluxes *Geophys. Res. Lett.* 33 L08406

Lehner, B., Liermann, C., Revenga, C. at el. (2011) Global Reservoir and Dam Database, Version 1 (GRanDv1): Reservoirs, Revision 01. NASA Socioeconomic Data and Applications Center (SEDAC): http://sedac.ciesin.columbia.edu/data/collection/grand-v1

Zampieri, M., Scoccimarro, E., Gualdi, S., A. Navarra (2014) Observed shift towards earlier spring discharge in the main Alpine rivers. *Sci. Total Environ.* doi:10.1016/j.scitotenv.2014.06.036.

J. Black Sea/Mediterranean Environment
Special Issue: 15-20 (2015)

Stable isotopic record from 160 to 121 ka from Tana Che Urla Cave (Apuan Alps, central Italy)

Eleonora Regattieri E.[1*], Ilaria Isola[2], Giovanni Zanchetta[1], Russell N. Drysdale[3], John C. Hellstrom[4]

[1] Dipartimento di Scienze della Terra, Via S. Maria, 53 56126 Pisa, ITALY
[2] Istituto Nazionale di Geofisica e Vulcanologia INGV, Via della Faggiola 32, Pisa, ITALY
[3] Department of Resource Management and Geography, University of Melbourne, Victoria 3010, AUSTRALIA
[4] School of Earth Sciences, University of Melbourne, Victoria 3010, AUSTRALIA

[*]**Corresponding author**: regattieri@dst.unipi.it

Abstract

Two flowstone cores from Tana che Urla Cave (TCU, central Italy), preserve an interval of continuous growth between ca. 159 and 121 ka. Stable isotope time series show an abrupt shift toward lower values at ca. 132 ka, coincident with an increase in growth rate and a marked change in speleothem fabric. This shift is consistent with the profound climate changes associated with the glacial–interglacial transition (i.e. shift to warmer and wetter conditions). The TCU record also shows significant variability (alternation between wetter and drier periods), both for glacial and interglacial portions of the record. Glacial MIS 6 is characterized by a wetter period between ca. 154 and 152 ka, while the early to middle last interglacial period shows several drier events (at ca. 129, 126 and 122 ka) which can be placed in the wider context of climatic instability emerging from North Atlantic marine and NW European terrestrial records.

Keywords: stable isotopes, Tana Che Urla, speleothems, last interglacial

Introduction

The timing and climatic evolution of the last interglacial is of particular interest in the frame of the debate of natural climate variability and length of the current interglacial (Kukla *et al.* 1997; Tzedakis *et al.* 2009). There is increasing evidence that the climate of the last interglacial was unstable relative to the Holocene. This variability was first identified North Atlantic marine sediments (McManus *et al.* 1994; Bond *et al.* 2001; Oppo *et al.* 2001) and, at least for the most prominent events, it propagated into Southern Europe and the Mediterranean basin (Martrat *et al.* 2004; Sprovieri *et al.* 2006; Couchoud *et al.* 2009). In this study we summarize growth rate and stable isotope data from two flowstone cores collected from Tana che Urla Cave (Apuan Alps NW Tuscany,

central Italy, Figure 1), which show continuous growth between ca. 159 and 121 ka. This report condenses what is extensively discussed in Regattieri *et al.* (2014a).

Cave Setting and Material and Methods

Tana che Urla (TCU) is a sub-horizontal spring cave, which opens at 620 m a.s.l. on the south-eastern side of the Pania massif, in the Apuan Alps (central Italy, Figure 1). Detailed description of the cave is available in Regattieri *et al.* (2012, 2014a).

Two cores, TCU-D3 and TCU-D4 (following referred as D3 and D4), were drilled from the same flowstone, located at about 100 m from the entrance. Polished sections of each core were sub-sampled and analysed for stable isotope composition and U/Th dating (see Hellstrom, 2003 for method description). The depth-age model provided was constructed using a Bayesian–Monte Carlo approach following Hellstrom (2006).

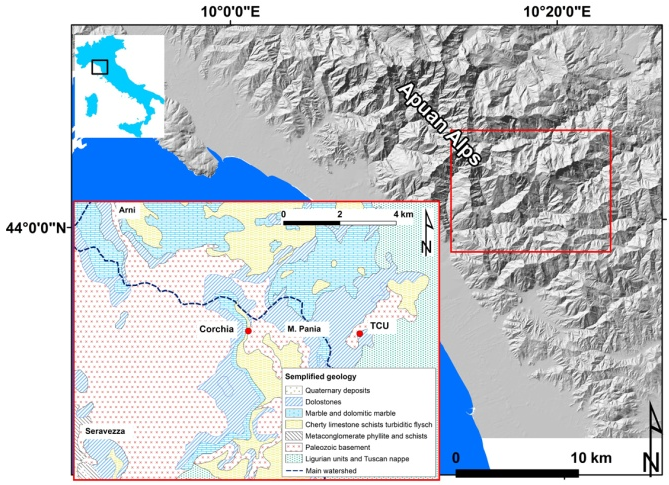

Figure 1. Location map of Tana che Urla and Corchia cave.

Results and Discussion

The Tana che Urla proxy record (stable isotope and growth rate, Figure 2) shows a consistent pattern of variability both at orbital (i.e. glacial-interglacial transition) to suborbital time scales (centennial-to-millennial scale events). For most of the Mediterranean, changes in speleothem $\delta^{18}O$ calcite are thought to mainly reflect changes in the isotopic composition of $\delta^{18}O$ of meteoric precipitation, rather than changes in temperature of deposition. Changes in $\delta^{18}O_p$ could be due to changes in the source of vapor (Bar-Matthews *et al.* 2000) or to

the “amount effect” (Bard *et al.* 2002), with lower/higher values related to wetter/drier periods For central Mediterranean the amount effect is believed to be the main factor driving the final $\delta^{18}O$ of the calcite (Drysdale *et al.* 2005; Zanchetta *et al.* 2007; Regattieri *et al.* 2014b). The basal section of the flowstone, from 158.5±2.7 to 132.2±1.8 ka, corresponding to late MIS 6, shows lower stable isotope values and lower growth rates (Figure 2) indicating generally drier conditions.

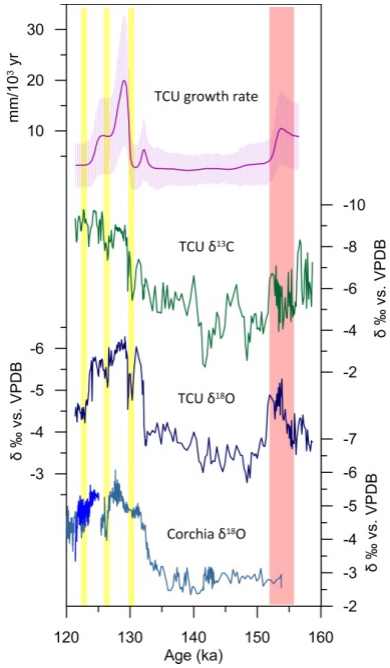

Figure 2. Stable isotopes and growth ratio for TCU-D4 (Regattieri *et al*. 2014a). Drier events during MIS5e are shadowed in yellow, wetter period during MIS6 is shadowed in red. Data from Corchia Cave (CC5 blue, CC7 light blue) are also shown for comparison (Drysdale *et al*. 2005; 2009).

At ca. 132.1±1.8 ka all speleothem properties show an abrupt and prominent change: stable isotope (oxygen and carbon) values decrease rapidly, the growth rates dramatically increase and the brown, clastic calcite is replaced by the white clastic-poor lithofacies (Regattieri *et al.* 2012). This shift indicates enhanced precipitation over the cave catchment at this time, marking the transition between MIS5 and MIS6.

The TCU $\delta^{18}O$ record also shows significant multi-centennial variability between the peak interglacial conditions at ca. 131.0 ka and the hiatus located at ca. 121.4 ka (Figure 2). The lowest isotope values occurred between ca. 130.1 and 123.6 ka, indicating that the wettest period lasted ca. 6 ka. However, this

period is interrupted by two short prominent events indicating reduced precipitation between ca. 130.7 and 129.6 ka, between ca. 126.7 and 125.6 ka and after 123.6 ka, where a new increase of values may suggest that interglacial condition ended. Records for the TCU and Corchia, caves located at higher altitude in the Apuan Alps (Figure 1), display remarkable similarities for this period (Figure 2) (Drysdale *et al.* 2005; 2009).

Conclusions

The growth history and stable isotope geochemistry of two flowstones from Tana che Urla, preserve a continuous record from the last part of the penultimate glacial to the middle part of the last interglacial (ca.159-121 ka). The most prominent feature of the record is a dramatic excursion toward lower isotope values at ca. 131 ka, coincident with a change in the lithology (from brown, detrital-rich to white, detrital-poor calcite) and growth rate. This shift in all speleothem properties indicates enhanced rainfall in the recharge area, related to climatic amelioration at glacial/interglacial transition.

The interglacial part of the record shows substantial variability, with 3 events of reduced moisture at ca. 129.6, 126.0 ka and between 123.6 ka and the first growth interruption at ca. 121.4 ka. This climatic instability during the first part of the last interglacial substantially agrees with the nearby speleothem record from Corchia Cave (Drysdale *et al.* 2009), supporting the regional significance of these events.

References

Bard, E., Delaygue, G., Rostek, F., Antonioli, F., Silenzi, S., Schrag, D.P. (2002) Hydrological conditions over the western Mediterranean basin during the deposition of the cold Sapropel 6 (ca. 175 kyr BP). *Earth Planet. Sc. Lett.* 202: 481-494.

Bar-Matthews, M., Ayalon, A., Kaufmann, A. (2000) Timing and hydrological conditions of sapropel events in the eastern Mediterranean, as evident from speleothems, Soreq Cave, Israel. *Chem. Geol*. 169:145-156.

Bond, G., Kromer, B., Beer, J., Muscheler, R., Evans, M.N., Showers, W., Hoffman, S., Lotti-Bond, R., Hajadas, I., Bonani, G. (2001) Persistent solar influence on North Atlantic climate during Holocene. *Science* 7: 2130-2136.

Couchoud, I., Genty, D., Hoffmann, D., Drysdale, R.N., Blamart, D. (2009) Millennial-scale variability during the Last Interglacial recorded in a speleothem from south-western France. *Quat. Sci. Rew.* 28:3263-3274.

Drysdale, R.N., Zanchetta, G., Hellstrom, J.C., Fallick, A.E., Sanchez-Goni, M.F., Couchoud, I., McDonald, J., Maas, R., Lohmann, G., Isola, I. (2009) Evidence for obliquity forcing of glacial termination II. *Science* 325: 1527-1531.

Drysdale, R.N., Zanchetta, G., Hellstrom, J.C., Fallick, A.E., Zhao, J.X. (2005) Stalagmite evidence for the onset of the Last Interglacial in southern Europe at 129+/−1 ka. *Geophys. Res. Lett.* 32: 1-4.

Hellstrom, J.C. (2003) Rapid and accurate U/Th dating using parallel ion-counting multicollector ICP-MS. J. *Anal. At. Spect.* 18: 1346-1351.

Hellstrom, J.C. (2006) U–Th dating of speleothems with high initial ^{230}Th using stratigraphical constraint. *Quat. Geochr.* 1: 289-295.

Kukla, G., Mcmanus, J.F., Rousseau, D.D., Chuine, I. (1997) How long and how stable was the Last Interglacial? *Quat. Sc. Rev.* 16: 605-612.

Martrat, B., Grimalt, J.O., Lopez-Martinez, C., Chaco, I., Sierro, F.J., Flores, J.A., Zahn, R., Canals, M., Jason, H.C., Hodell, D.A. (2004) Abrupt temperature changes in the Western Mediterranean over the past 250,000 years. *Science* 306: 1762-1765.

McManus, J.F., Bond, G.C., Broecker, W.S., Johnsen, S., Labeyrie, L., Higgins, S. (1994) High-resolution climate records from the North Atlantic during the last interglacial. *Nature* 371: 326-329.

Oppo, D.W., Keigwin, L.D., McManus, J.F. (2001) Persistent suborbital climate variability in marine isotope stage 5 and Termination II. *Paleoceanography* 16: 280-292.

Regattieri, E., Isola, I., Zanchetta, G., Drysdale, R.N., Hellstrom, J.C., Baneschi, I. (2012) Stratigraphy, petrography and chronology of speleothem deposition at Tana che Urla (Lucca, Italy): paleoclimatic implications. *Geogr. Fis. Dinam. Quat.* 35: 141-152.

Regattieri, E., Zanchetta, G., Drysdale, R.N., Isola, I., Hellstrom, J.C., Dallai, L. (2014b) Lateglacial to Holocene trace element record (Ba, Mg, Sr) from Corchia Cave (Apuan Alps, central Italy): paleoenvironmental implications. *J. Quat. Sc.* 29: 381–392.

Regattieri, E., Zanchetta, G., Drysdale, R.N., Isola, I., Hellstrom, J.C., Roncioni, A. (2014a) A continuous stable isotopic record from the Penultimate glacial maximum to the Last Interglacial (160 to 121 ka) from Tana Che Urla Cave (Apuan Alps, central Italy). *Quat. Res.* 82: 450-461.

Sprovieri, R., Di Stefano, E., Incarbona, A., Oppo, D.W. (2006) Suborbital climate variability during Marine Isotopic Stage 5 in the central Mediterranean basin: evidence from calcareous plankton record. *Quat. Sc. Rev.* 25: 2332-2342.

Tzedakis, P.C., Raynaud, D., McManus, J.F., Berger, A., Brovkin, V., Kiefer, T. (2009) Interglacial diversity. *Nat. Geosc.* 2: 751-755.

Zanchetta, G., Drysdale, R.N., Hellstrom, J.C., Fallick, A.E., Isola, I., Gagan, M., Pareschi, M.T. (2007) Enhanced rainfall in the western Mediterranean during deposition of sapropel S1: stalagmite evidence from Corchia Cave (Central Italy). *Quat. Sc. Rev.* 26: 279-286.

J. Black Sea/Mediterranean Environment
Special Issue: 21-24 (2015)

Reliability of uncertainty estimates from climate projection ensembles

Josep Llasses[1*], Gabriel Jordà[1,2], Damià Gomis[1]

[1] IMEDEA (Mediterranean Institute for Advanced Studies), Mallorca, SPAIN
[2] National Oceanography Centre, Southampton, UK

[*]**Corresponding author:** josep.llasses@uib.es

Abstract

We explore the reliability of uncertainties estimated of climate projection ensembles. A Monte-Carlo numerical approach is used to quantify the actual uncertainty of ensembles affected by different, independent uncertainty sources, which is then compared to the uncertainty obtained using current methods. The obtained results can serve as guidance in the design of future projection ensembles with more reliable uncertainty estimates. As an application we explore the relative contribution of each uncertainty source and the reliability of their estimation for a Mediterranean storm surge projection ensemble. In that case the dominant source of uncertainty is the global model (from which atmospheric pressure and winds are downscaled using a regional model) and the natural variability, while the regional model used for the downscaling and the emission scenario are secondary sources. The errors in the calculation of the uncertainties attributed to each source are often higher than the estimated uncertainties themselves (e.g., the relative error of the uncertainty of the global model contribution is 50-60%, being much higher for secondary sources).

Keywords: climate projections, uncertainty, Mediterranean

Introduction

The quantification of uncertainties of climate projections is a crucial issue, as it conditions the confidence of decision makers on the value of adaptation strategies. Different ways to quantify the uncertainty from climate projection ensembles have been proposed, from probabilistic multi-model ensemble approaches (Smith *et al.* 2009) to more complex statistical methodologies. However, very often the quantification of uncertainties from ensembles of model runs is simply related to the spread of the ensemble, without paying much attention to the reliability of the estimation. In particular, the reliability of that approach can be quite low when the ensembles are small, which is usually the case for instance in regional or local climate projections. Here we investigate the reliability of the uncertainty estimates when the ensemble has multiple sources of uncertainty. We also give advices for the design of new ensembles in terms of

the relative contribution of each source of uncertainty to the total uncertainty (Hawkin and Sutton 2009). The modeler community must be aware of where are the highest discrepancies between the projections in order to focus on their reduction. As an application, we apply the proposed methodology to an ensembleof Mediterranean storm surge projections.

Methods

The uncertainty of climate projection ensembles is often computed simply as the spread of the ensemble results. A better way of doing it is identifying the different uncertainty sources and, for each of them, considering the simulations as independent realizations with a Gaussian distribution. In regional climate projection studies, for instance, it is common not to dispose of really independent simulations; however, it is also common to dispose of groups (sub-sets) of independent simulations, each one sampling an uncertainty source. A sub-set of independent simulations is understood here as a group of simulations where all the uncertainty sources but one are fixed. If each uncertainty source is really independent, we can define the "total uncertainty" of the ensemble as the sum of the variance of each uncertainty source:

$$\sigma_{tot}^2 = \sum_i \sigma_i^2$$

We will also be interested in quantifying the relative contribution of each uncertainty source to the total uncertainty and the reliability of such estimate. The relative contribution of each source (C_i) to the total uncertainty is defined as:

$$C_i = \frac{\sigma_i^2}{\sigma_{tot}^2} \pm \delta_i$$

where δ_i is the error of the estimation.

The methodology to calculate the errors is based on a Monte-Carlo approach. Provided that we have N_i simulations in each subset *i* and that the variance of this subset is σ^2_i, we generate a large number of series of N_i numbers with standard deviation σ_i. Then, we compute the relative contribution to the total uncertainty from each Monte-Carlo sample and compare to the exact value in order to have an estimate of the δ_i.

Results and discussion

To analyze the case of having more than one sources of uncertainty we consider a numerical example with two sources ($\sigma_1 = 2\,\sigma_2$). Figure 1a shows the relative error in the calculation of the total uncertainty as a function of the number of simulations of the primary source (N_1) for different numbers of simulations of the secondary source (N_2). The figure shows that if the number of simulations of the primary source is small, it is useless to increase the number of simulations of

the secondary source. Being aware of this can be useful to design new projection ensembles resulting in better estimates of the actual uncertainty. Figure 1b shows the reduction of the total uncertainty resulting from an increase in the number of simulations of each source. In our example, if N1<5 or N2>25, any increase in N1 will improve the reliability of the uncertainty estimate more than any increase in N2. Or conversely, depending on the values of σ_i and N_i, it will not be useful to increase the number of simulations sampling a given uncertainty source.

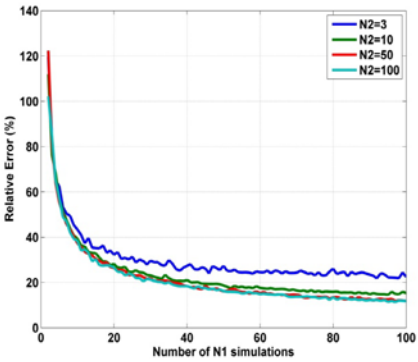

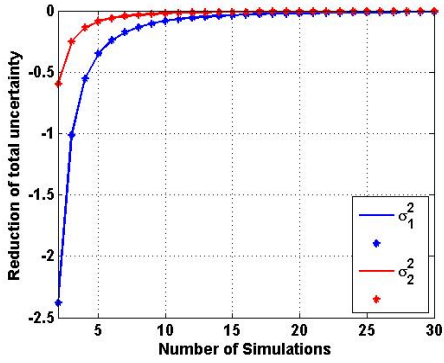

Figure 1a (left): Relative Error in the calculation of the total uncertainty as a function of the number of simulations of the primary source of uncertainty (N1) for different numbers of simulations of the secondary source of uncertainty (N2)
Figure 1b (right): Reduction of total uncertainty as a function of the number of simulations (the blue line refers to N1 and the red line refers to N2)

To apply the methodology to a real case, we consider a storm surge projection ensemble. The domain is the Mediterranean Sea and the target parameter will be the basin mean sea level. This example is representative of actual regional ensembles where the number of simulations is small compared to global ensembles. Figure 2a shows the relative contribution of each uncertainty source to the total uncertainty. The dominant source is the global model (GCM) from which atmospheric pressure and winds are downscaled using a regional model. The GCM contributes with 50-60% of the total uncertainty, while the natural variability contributes with about 20%. The regional model and the scenario choice are of second order of importance. The reliability of the calculation of each contribution is shown in Figure 2b. Note that the uncertainty of the calculation of each contribution is often higher than the contribution itself. If we focus for example on the major source, the GCM, Figure 2b shows that only about 25-30% of the GCM contribution is reliable while almost the same percentage is uncertain (~ 50%).

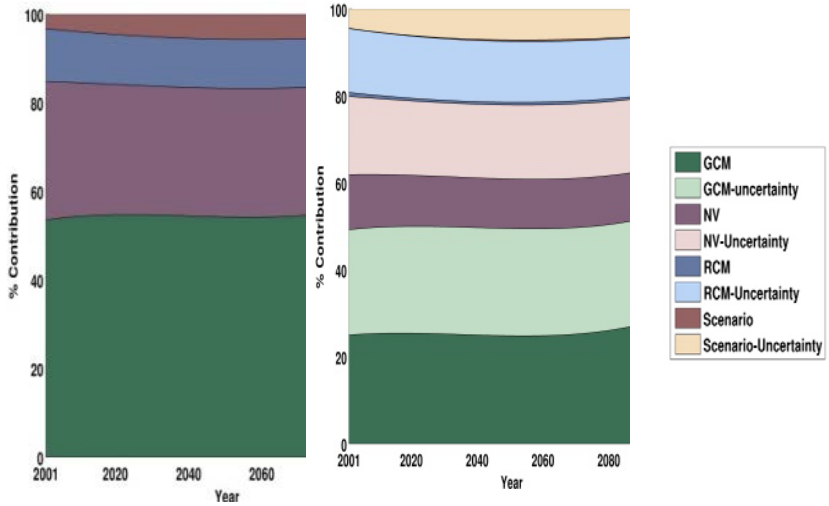

Figure 2a (left): Relative contribution to the total uncertainty of each source.
Figure 2b (right): Same than Figure 2a but including the reliability in the calculation of each uncertainty contribution (after a renormalization)

References

Hawkin, E., Sutton, R. (2009) The potential to narrow uncertainty in regional climate predictions. *Bulletin of the American Meteorological Society* 90: 1095-1107.

Smith, R., Tebaldi, C., Nychka, D., Mearns, L. (2009) Bayesian modeling of uncertainty in ensembles of climate model. *Journal of the American Statistical Association* 104(485): 97-116.

J. Black Sea/Mediterranean Environment
Special Issue: 25-28 (2015)

A Regional Climate Model versus a Surface Energy Balance Model in estimating the evapotranspiration distribution in the semi-arid Konya Basin, Turkey

Mustafa Gökmen[1*], Barış Önol[2], Ömer Lütfi Şen[3]

[1] Ministry of Environment and Urbanisation, Ankara, TURKEY
[2] Department of Meteorological Engineering, ITU, Istanbul, TURKEY
[3] Eurasia Institute of Earth Sciences, ITU, Istanbul, TURKEY

[*]**Corresponding author:** mustaf.gokmen@gmail.com

Abstract

This study presents the comparison of two different approaches for quantifying the spatiotemporal distribution of the evapotranspiration at the regional scale: the simulations by a regional climate model (ICTP-RegCM3), versus the estimations by a remote sensing based surface energy balance model (SEBS). The comparison was carried out in the semi-arid Konya basin. Our results show that while performing similarly in representing the seasonal dynamics, there was considerable difference of average daily ET estimates between the two models, and this difference varied spatially in the region. The difference between the ET outputs can be mainly attributed to the factors including differences in model structures, input parameters and spatial resolutions.

Keywords: regional climate model, ICTP-RegCM3, surface energy balance model, SEBS, evapotranspiration, the Konya Basin

Introduction

In this study, we present a comparison of two different approaches for quantifying the regional distribution of the evapotranspiration: the high resolution simulations by the regional climate model ICTP-RegCM3 (Önol 2012), versus the estimations by a RS-based surface energy balance model SEBS (Gökmen *et al.* 2012). By such a comparison, it is aimed not only to evaluate the two different methods in quantifying the regional evapotranspiration but also two different spatial resolutions of the ET outputs (i.e. ~10 km resolution by ICTP-RegCM3 and ~1 km resolution by SEBS). The comparison carried out in one of the largest endorheic basins in the world, namely the Konya closed basin in Turkey. The basin is a characteristic example of a semi-arid region whose limited water resources are under strong anthropogenic influence.

Materials and Methods

In this study, the ET simulations by Önol (2012) using ICTP-RegCM3 (International Centre for Theoretical Physics Regional Climate Model, Version 3) were used. In the model, which was run at a 10 km resolution for the East Mediterranean domain, ET rates depend on the availability of soil water based on a Biosphere-Atmosphere Transfer Scheme (BATS) by Dickinson *et al.* (1993). Also, the input surface parameters vary geographically, and are specified using look-up tables for the different land cover classes. More detailed information about ICTP-RegCM3 as well as climatology of the reference period, 1961-1990 are given in Bozkurt *et al.* (2012) and Önol (2012).

With respect to the RS-based estimation of the regional ET, we used the physically based and single source Surface Energy Balance System (SEBS) model by Su (2002). SEBS estimates ET using RS retrievals and meteorology data. In this study, we used a modified version of SEBS (Gökmen *et al.* 2012) which integrates soil moisture into the model for better accounting for moisture-limited evapotranspiration regime, which is typical in semi-arid regions.

The study area, The Konya Closed Basin is located in central Anatolia, Turkey, with a surface area of about 54,000 km^2 and elevations from 900 to 3500 m.a.s.l. There are extensive irrigated croplands which are usually surrounded by the vast sparse steppe areas, in the central and downstream plains. The region has a typical arid to semi-arid climate with a long-term average precipitation of 380 mm/year, ranging from 250 mm in the plain parts up to more than 1,000 mm in the mountainous areas (unpublished data from State Hydraulic Works, DSI).

Results

According to Figure 1a, both SEBS and the RCM simulate similar seasonal ET variation, while SEBS is estimating higher than the RCM throughout the year with an average difference of about 0.5 mm/day.

Discussion

Although both SEBS and the RegCM3 simulate similar seasonal dynamics of ET, there is considerable difference of average daily ET estimates between the two models, and this difference varies spatially in the region. The differences can be attributed to several factors including differences in model structures, input parameters and spatial resolutions. Due to the different model structures (RegCM3 using BATS, while SEBS estimates ET based on surface energy balance), the sensitive parameters of the two methods are also rather different. In the case of RegCM3, ET simulations are highly sensitive to the water stress level which is imposed by the land cover input to the model. For example, the few grids which had much larger ET estimates by the RegCM3 (blue grids on

Figure 1d) were the ones assigned as irrigated crops or water surfaces. Therefore, we can claim that an accurate estimation of ET by RegCM3 highly depends on an accurate definition of the dynamic land cover conditions of a region, spatially and temporally. However, though being a high resolution simulation for a RCM, 10 km horizontal resolution of the RegCM3 is still quite coarse in representing the heterogeneous and dynamic land cover characteristics at regional and basin scales. In fact, according to a detailed CORINE land cover mapping study (unpublished data from Ministry of Environment and Forestry of Turkey), the green polygons in Figures 1b-d depict the irrigated croplands and they occupy much larger areas than the one used as input to the RegCM3. In the case of SEBS, the land cover map is not a direct input to the model and ET estimate is most sensitive to the surface temperature and the difference between the surface and air temperature. Further improvements for the regional ET estimations by the two methods can be suggested with further concurrent validations of the methods against the ground-based measurements.

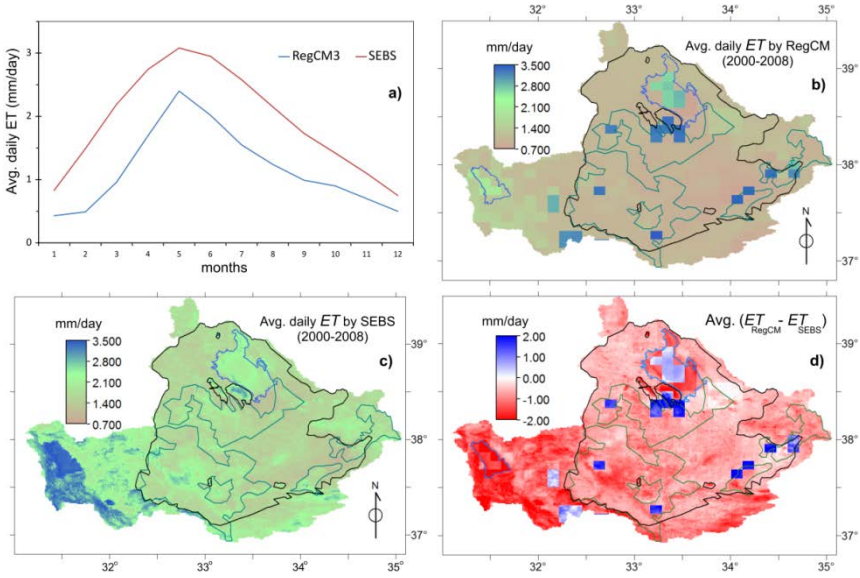

Figure 1a. Seasonal dynamics of the basin-averaged *ET*, **b-c.** distribution of the average *daily ET* and, **d.** distribution of the difference between average *daily ET* during the study period (2000-2008) by RCM and SEBS, respectively.

Figures 1b-d. reveals that, apart from some particular grids of the RCM (the blue coloured areas in Figure 1d; the daily ET estimate by SEBS is generally higher in the basin. While the difference is between 0 to 1 mm/day in the plain areas (inside the bigger black polygon), it can reach up to 2 mm/day in the mountainous upstream parts in the southwest and south of the basin (outside the bigger black polygon).

References

Bozkurt, D., Turunçoğlu, U., Şen, Ö.L., Önol, B., Dalfes, H.N. (2012) Downscaled simulations of the ECHAM5, CCSM3 and HadCM3 for the eastern Mediterranean–Black Sea region. *Clim Dyn* 39 (1-2): 207-225.

Dickinson, R.E., Henderson-Sellers, A., Kennedy, P.J. (1993) Biosphere-Atmosphere transfer scheme (BATS) Version 1E as coupled to the NCAR. *Tech. Rep*. TN-387+STR, NCAR, Boulder, CO.

Gökmen, M., Vekerdy, Z., Verhoef, A., Verhoef, W., Batelaan, O., van der Tol, C. (2012) Integration of soil moisture in SEBS for improving ET estimation. *Remote Sensing of Environment* 121: 261-274.

Önol, B. (2012) Effects of coastal topography on climate: high-resolution simulation with a RCM. *Climate Research* 2:159.

Su, Z. (2002). The SEBS for estimation of turbulent heat fluxes. *Hydrology and Earth System Sciences* 6: 85-99.

J. Black Sea/Mediterranean Environment
Special Issue: 29-32 (2015)

Recent mixed layer warming and deepening in the Mediterranean Sea

Irene Rivetti[1*], Ferdinando Boero[1,2,4], Simonetta Fraschetti[1], Enrico Zambianchi[3], Piero Lionello[1,2]

[1] DiSTeBA, Università del Salento, CoNISMa, 73100, Lecce, ITALY
[2] CMCC Euro-Mediterranean Center on Climate Change, 73100, Lecce, ITALY
[3] Dipartimento di Scienze per l'Ambiente, Università "Parthenope", CoNISMa, 80143, Napoli, ITALY
[4] CNR-ISMAR, 16149, Genova, ITALY

[*]**Corresponding author:** irene.rivetti@unisalento.it

Abstract

This study investigates the link between the occurrence of mass mortalities of benthic invertebrates in the Mediterranean Sea and changes in its thermal stratification. The analysis covers the period 1945-2011 using data from three public sources: MEDAR-MEDATLAS, World Ocean Database, MFS-VOS program. Mass mortalities events have been identified considering studies published from 1945 to 2011. A synthetic description of the evolution of the upper water column is provided in terms of four parameters describing the mixed layer and the seasonal thermocline. Results show that important changes in the uppermost part of the water column have occurred in the last three decades of the analyzed period (1983-2011, when mass mortalities have been reported) with respect to the previous decades (1945-1982, with no recorded mass mortalities): a widespread increase of thickness and temperature of the mixed layer, deepening and cooling of the thermocline base. It is shown that most mass mortalities occurred in seasons with anomalously high mixed layer temperature.

Keywords: mixed layer, seasonal thermocline, mass mortalities, temperature profiles, DYFAMED station, Mediterranean Sea

Introduction

The Sea Surface Temperature (SST) of the Mediterranean Sea is increasing (Nykjaer 2009) and this has been linked to changes in Mediterranean biota (Lejeusne *et al.* 2010). In fact, increasing SST may be associated to stronger thermal stratification and warming of the upper water column, which can result in dramatic events, such as the mass mortalities of benthic invertebrates that have been observed in the last decades (Rivetti *et al.* 2014). Assessing the magnitude of changes of the SST and of the upper water column is critical to understand their effects on marine ecosystems. In this study we assess the

effects of changes in thermal stratification on marine ecosystems, by evaluating changes of selected parameters describing the mixed layer and the seasonal thermocline and their relation with mass mortalities of benthic invertebrates.

Materials and Methods

In this study we have analyzed all the vertical profiles of temperature available for the Mediterranean Sea, including bottles, MBT, XBT and CTD, extracted from the MEDAR/MEDATLAS database (Fichaut *et al.* 2003), the World Ocean Database 2013 (WOD13; Johnson *et al.* 2013) and the Mediterranean Forecasting System-Voluntary Observing Ship program (MFS-VOS; Manzella *et al.* 2007). The analysis has covered the period 1945-2011 and has been focused on summer and autumn. The total number of temperature profiles that have passed a quality control procedure and have been used is 108.079. Data used in this study include also CTDs collected at the DYFAMED station (Ligurian Sea), a Mediterranean long-term observatory, in the period from 1991 to 2008.

The three segments profile model, has been selected among different possibilities as it has been shown to yield robust results for most shapes of temperature profiles (Rivetti *et al.* 2014). This method approximates the upper water column with three segments representing mixed layer, thermocline and deep layer. The parameter values defining these three segments are determined by an optimization procedure that minimizes the root mean square error of the idealized profile with respect to the observations. This computes four parameters: Mixed Layer Depth (MLD), Mixed Layer Temperature (MLT), Thermocline Base Depth (TBD) and Thermocline Base Temperature (TBT).

To describe the ongoing changes in the thermal stratification across the Mediterranean Sea, mean seasonal values of MLD, MLT, TBD and TBT have been computed for the periods 1983-2011 and 1945-1982, and their difference has been binned in boxes of 1° lat × 1° long. The two periods have been chosen considering that mass mortalities have been reported after 1983. Further the MLD and the MLT in the season and location of each mass mortality event have been compared with the corresponding mean MLD and MLT over the period 1945-1982.

Results

Figure 1 shows the spatial distribution of the variations of MLD, TBD, MLT and TBD between the two considered periods in summer.

Most coloured cells show an increase of MLD (Figure 1a) with the exception of the Algerian and of the South Ionian Seas. Also a general increase of TBD is present over most of the basin with the exception of the Aegean, Gulf of Lion,

Catalan Sea (Figure 1b). A clear signal of MLT increase is evident for the whole basin (Figure 1c). The TBT is, instead, generally decreasing (Figure 1d) except in the Central Ionian, the Tyrrhenian, the Balearic and the Algerian Seas. Autumn (not shown) presents a similar pattern of change.

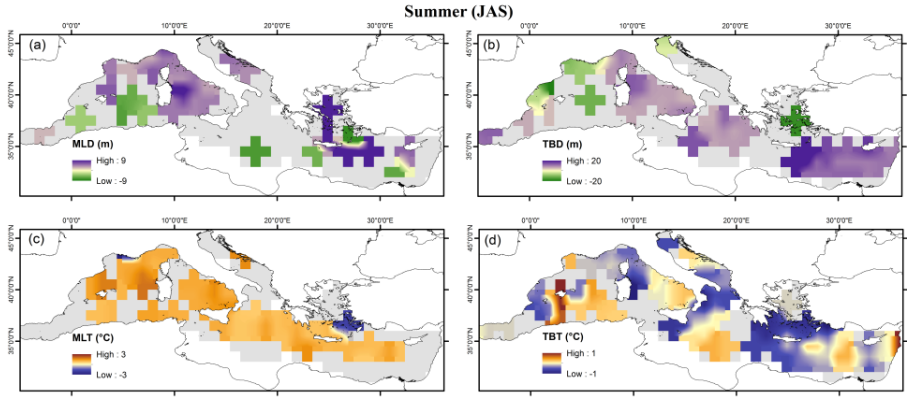

Figure 1. Variations of the MLD (a), of the TBD (b), of the MLT (c) and of the TBT (d) in summer. Depth\temperature variations are computed as difference between average depth\temperature values in the period 1983-2011 and those in the period 1945-1982 in 1°lat x 1°lon cell and tested for statistical significance at the 90%. Significant values are reported as coloured cells, not significant values are reported as grey areas

Considering summer and autumn (Rivetti *et al.* 2014), in 18 out of 26 reported mass mortalities, the MLT during the event was higher than the mean MLT over the period 1945-1982. Further, 10 events occurred when the MLD was deeper than the mean MLD over the period 1945-1982. This result confirms a general link between MLT and mass mortality events.

Discussion

Results, extensively discussed in Rivetti *et al.* (2014), show a widespread increase of thickness and temperature of the mixed layer, deepening and cooling of the thermocline base in the last three decades (1983-2011). Further, in most locations where mass mortalities have been reported the MLT was higher than the mean MLT calculated over the period 1945-1982. In conclusion, our results support a recent warming, which is potentially associated with important environmental changes in the upper layer of the Mediterranean Sea.

References

Fichaut, M., Garcia, M.J., Giorgetti, A., Iona, A., Kuznetsov, A., Rixen, M., Group, M.(2003) MEDAR/MEDATLAS 2002: A Mediterranean and Black Sea

database for the operational oceanography. In: Building the European Capacity in Operational Oceanography: Proceedings 3rd EuroGOOS Conference (eds., H. Dahlin, N.C. Flemming, K. Nittis, S.E. Petersson) *Elsevier Oceanogr. Ser.* 69:645–648.

Johnson, D.R., Garcia, H.E., Boyer, T.P. (2013) World Ocean Database 2013 Tutorial. Sydney Levitus (ed., Alexey Mishonov, technical ed.; NODC) Internal Report 23, NOAA Printing Office, Silver Spring, MD. 25 pp.

Lejeusne, C., Chevaldonne, P., Pergent-Martini, C., Boudouresque, C.F., Perez, T. (2010) Climate change effects on a miniature ocean: the highly diverse, highly impacted Mediterranean Sea. *Trends Ecol Evol* 25: 250-260.

Manzella, G.M.R., Reseghetti, F., Coppini, G., Borghini, M., Cruzado, A., Galli, C., Gertman, I., Gervais, T., Hayes, D., Millot, C., Murashkovsky, A., Ozsoy, E., Tziavos, C., Velasquez, Z., Zodiatis, G. (2007) The improvements of the ships of opportunity program in MFS-TEP. *Ocean Sci* 3: 245-258.

Nykjaer, L. (2009) Mediterranean Sea surface warming 1985-2006. *Clim Res* 39: 11-17.

Rivetti, I., Fraschetti, S., Lionello, P., Zambianchi, E., Boero, F. (in press) Global warming and mass mortalities of benthic invertebrates in the Mediterranean Sea. *Plos One*.

Rivetti, I., Boero, F., Fraschetti, S., Zambianchi, E., Lionello, P. (2014) Mixed layer warming-deepening in the Mediterranean Sea and its effect on the marine environment. (in preparation)

J. Black Sea/Mediterranean Environment
Special Issue: 33-36 (2015)

Impacts of climate change on water demand and yield of Mediterranean crops

Mladen Todorovic[1,*], Piero Lionello[2], Luis S. Pereira[3], Claudia Pizzigalli[4], Sameh Saadi[1], Lazar Tanasijevic[1]

[1] CIHEAM, Mediterranean Agronomic Institute of Bari, Valenzano, ITALY
[2] DISTEBA, University of Salento and CMCC, Lecce, ITALY
[3] CEER, Universidade de Lisboa, Lisbon, PORTUGAL
[4] SAIPEM S.p.a., Ocean Engineering Department, Fano, ITALY

[*]**Corresponding author**: mladen@iamb.it

Abstract

This study focusses on the impact of climate change on water demand and yields of Mediterranean crops (winter wheat, tomato and olive). High resolution climate data, based on the A1B emission scenario, were arranged to represent the mean climate conditions in years 1991-2010 and 2036-2065 and describe climate change over a 50-years span, during which an overall reduction of precipitation and increase of air temperature are expected. As a consequence, net irrigation requirements (NIR) for olives may increase (particularly in Southern Spain), while actual evapotranspiration of rainfed olives would decrease in most areas due to increased water stress. The potentially cultivable areas of winter wheat, tomato and olive trees may substantially increase mostly in the Northern Mediterranean countries. Due to anticipation and shortening of growing season, the NIR may decrease for both wheat and tomato. As a whole, future relative yield losses are expected to be slightly larger than now for rainfed wheat, particularly in the Northern Mediterranean, while they are not expected to change for tomato. Precipitation decrease will be relevant for winter-spring crops and the adoption of supplemental irrigation for winter wheat could become widespread in the future. Locally-tailored (water, land and nutrient) best management practices will play determinant role for crop production.

Keywords: winter wheat, tomato, olive trees, Mediterranean region, crop water requirements, irrigation, yield

Introduction

Agricultural production depends on a complex interaction between the pedo-climatic conditions, availability of resources, cropping pattern and management practices. Climate change is one of the main factors affecting this interrelation through its direct impact on the climatic conditions of cultivation, availability and quality of resources (water and land). Accordingly, the adaptation measures give emphasis on the adoption of cropping pattern and management practices

that fit adequately to the new cultivation condition. This work focusses on the expected impact of climate change on water demand and yields of some characteristic Mediterranean crops, such as winter wheat, tomato and olive trees, indicating possible variation of actual cultivation practices. The results present a synthesis of findings reported in the deliverables of the WASSERMED project (EC-FP7-ENV) and related publications (Tanasijevic *et al.* 2014; Saadi *et al.* 2015).

Materials and Methods

Climate data have been derived from the ENSEMBLES project (EC-FP6-ENV) RCM simulations. The results of RACMO2, driven by ECHAM5, were selected as the most suitable for this analysis. The data refer to A1B SRES scenario and two time periods: a) present, denoted as "year 2000" (average values of simulations for the period 1991-2010), and b) future, denoted "year 2050" (average values of simulations for the period 2036-2065). Monthly values of precipitation, air temperature and relative humidity, solar radiation and wind speed are used. Daily values were generated as described in Saadi *et al.* (2015). Soil data were taken from the harmonized soil database, HWSD version 1.2 (FAO/IIASA/ISRIC/ISSCAS/JRC 2012).

Crop evapotranspiration, irrigation requirements and yield reduction under non-optimal water supply were estimated using the standard FAO approach (Allen *et al.* 1998). More details about soil water balance and applied irrigation scenarios are given in Saadi *et al.* (2015) and Tanasijevic *et al.* (2014). The Geographical Information System (GIS) software (ArcView GIS) was used for data elaboration.

Results and discussion

Climate data for the period 2000-2050 indicated over the Mediterranean an average reduction of annual precipitation (-39.1±55.1 mm $year^{-1}$) and increase of surface air temperature (+1.57±0.27°C). As a result, the areas suitable for cultivation of winter wheat, tomato and olive trees are foreseen to increase prevalently in the Northern Mediterranean countries by 7, 24 and 25%, respectively. Moreover, an increase of annual reference evapotranspiration (Figure 1) of 92.3±42.1 mm (6.7%) is expected (Saadi *et al.* 2015).

Due to temperature increase, a future reduction of the average length of growing season (15 and 12 days for wheat and tomato, respectively) and, consequently, of crop evapotranspiration (6 and 5% for wheat and tomato, respectively) are also expected. Then, net irrigation requirements (NIR) under optimal water supply could be diminished by 11% for wheat and 5% for tomato (Saadi *et al.* 2015).

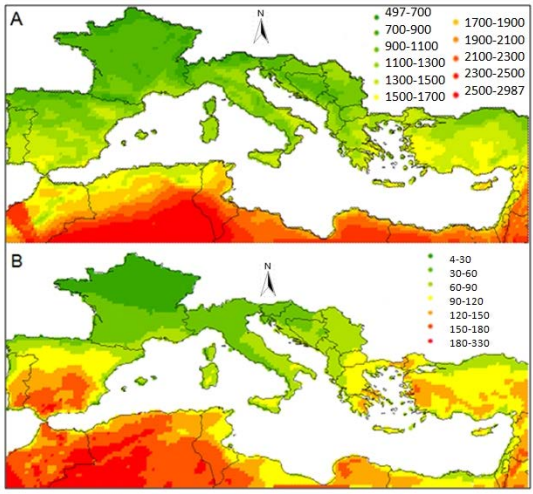

Figure 1. Reference evapotranspiration over the Mediterranean for year 2000 (A) and expected variation in respect to 2050 (B), (mm/year) (Saadi *et al.* 2015)

Shortening of growing season and earlier crop development would negatively affect yield, but could reduce the risk of drought and heat stress (Moriondo and Bindi 2007; Saadi *et al.* 2015). Also rain-fed cultivation of wheat could lead to slight reduction of yield especially in the Northern Mediterranean where the introduction of supplemental irrigation could be required. No particular changes are expected for tomato and other spring summer crops cultivation.

An anticipation of olive flowering by 11±3 days is foreseen. Crop evapotranspiration is expected to increase on average by 8% (51±17 mm season^{-1}) while NIR is foreseen to increase by 18.5% (70±28 mm season^{-1}). The greatest increase of NIR is expected in Southern Spain and north-western Algeria and Morocco (Tanasijevic *et al.* 2014), where available water resources are already limited.

Conclusions

The impact of climate change on agricultural production in the Mediterranean depends on the considered crop and varies throughout the regions. In general, the benefits are expected to be larger in the Northern areas of the Mediterranean, where resources (land and water) are available, while in the Southern regions cultivation could be penalized. The overall effects of climate change could actually reduce water demand in most regions. However, the effects on yield should be seen within a complex management setting that includes the starting day and duration of growing season, the selection of the most adequate varieties

(short or long maturing), CO_2 concentration in the atmosphere and the adoption of locally-tailored best management practices.

References

Allen, R.G., Pereira, L.S., Raes, D., Smith, M. (1998) Crop Evapotranspiration. Guidelines for Computing Crop Water Requirements. FAO Irrig. and Drain. Paper 56, FAO, Rome. 300 pp.

FAO/IIASA/ISRIC/ISSCAS/JRC (2012) Harmonized World Soil Database (version 1.2). FAO, Rome, Italy and IIASA, Laxenburg, Austria.

Moriondo, M., Bindi, M. (2007) Impact of climate change on the phenology of typical Mediterranean crops. *Ital. J. Agrometeorology* 3: 5-12.

Saadi, S., Todorovic, M., Tanasijevic, L., Pereira, L.S., Pizzigalli, C., Lionello, P. (2015) Climate change and Mediterranean agriculture: impacts on winter wheat and tomato crop evapotranspiration, irrigation requirements and yield. Agric. *Water Manage* 147: 103-115.

Tanasijevic, L., Todorovic, M., Pereira, L.S., Pizzigalli, C., Lionello, P. (2014) Impacts of climate change on olive crop evapotranspiration and irrigation requirements in the Mediterranean region. Agric. *Water Manage* 144: 54-68.

J. Black Sea/Mediterranean Environment
Special Issue: 37-40 (2015)

Heat-related impacts of climate change in the East Mediterranean

Christos Giannakopoulos*, Anna Karali, Vassilis Psiloglou, Giannis Lemesios

National Observatory of Athens, Athens, GREECE

***Corresponding author:** cgiannak@meteo.noa.gr

Abstract

This study investigates the heat-related impacts of climate change on public health in the East Mediterranean. Most of the health problems in the East Mediterranean are related mainly to the warming already occurred as well as to extreme weather events such as heatwaves. In addition projections indicate that warming and extreme events will increase in future posing serious threats on human health. To examine the potential negative impacts of climate warming on human life for the greater East Mediterranean area, the HUMIDEX index, employed to express the temperature perceived by people, was examined. HUMIDEX is applied in summer and generally warm periods and describes the temperature felt by an individual exposed to heat and humidity. The analysis revealed a significant increase in the HUMIDEX in future period mainly during summer months.

Keywords: regional climate modeling, climate change, public health, HUMIDEX, Eastern Mediterranean

Introduction

One of the major concerns of climate change is its impact on human health. The Fourth IPCC assessment report (Parry *et al.* 2007) provides evidence that climate change currently contributes to the global burden of disease and premature deaths. In fact, it plays an important role in the spatial and temporal distribution of some of the most deadly infectious diseases such as malaria, dengue fever, tick-borne diseases, etc. It is also affecting the seasonal distribution and concentrations of some allergenic pollen species, and it has increased heat-related as well as extreme weather-related morbidity and mortality (Parry *et al.* 2007).

Eastern Mediterranean is already experiencing some of the impacts of climate change on public health (Paz *et al.* 2010). Most of the health problems in the area are related mainly to the warming already occurred as well as to extreme

weather events such as heat waves, floods, fires, etc. (D'Ippoliti *et al.* 2010). Even if milder winters have the potential to decrease cold-related mortality and morbidity locally (Donaldson *et al.* 2001), the direct and indirect effects of climate change are expected to have adverse impacts on human health and well-being at the global scale in the future, in particular in the Mediterranean (Paz *et al.* 2010). From the 1960's until today, the mean intensity, duration and number of heat wave events in the Eastern Mediterranean, have increased by a factor of around 7.5, 7.5 and 6 respectively posing serious threats to human health (Kuglitsch *et al.* 2010).

Materials and Methods

HUMIDEX is applied in summer and generally warm periods and describes the temperature felt by an individual exposed to heat and humidity. More specifically, the HUMIDEX parameter (in $^{\circ}$C) is calculated by the following equation:

$$T(h) = Tmax + \frac{5}{9} \times (e - 10), \qquad e = 6.112 \times 10^{\left(7.5 \times \frac{Tmax}{(237.7+Tmax)}\right)} \times \frac{h}{100},$$

where *e* is the vapour pressure, *Tmax* is the maximum 2m air temperature ($^{\circ}$C) and *h* is the humidity (%).

Furthermore, 6 classes of HUMIDEX ranges are established to inform the general public for discomfort conditions:
1) <29°C comfortable, 2) 30–34°C some discomfort, 3)35–39°C discomfort; avoid intense exertion, 4) 40–45°C great discomfort; avoid exertion, 5) 46–53°C significant danger; avoid any activity 6) >54°C imminent danger; heart stroke.

All calculations were performed using PRECIS (Providing Regional Climates for Impact Studies) regional Climate Model based on the United Kingdom (UK) Meteorological Office Hadley Centre HadRM3P model (Jones *et al.* 2004). The model simulations were performed at the Cyprus Institute within the framework of the CIMME project (www.cyi.ac.cy/climatechangemetastudy), which studies 'Climate Change and Impacts in the Eastern Mediterranean and Middle East'. In all simulations the period 1961–1990 was used as the base period (control run) providing a reference for comparison with future projections for the period 2040–2069. The future period simulations of the model are based on the IPCC SRES A1B scenario (Nakićenović *et al.* 2000), which provides a good mid-line scenario for carbon dioxide emissions and economic growth (Parry *et al.* 2007).

Results

In the control period (Figure 1), most parts of Greece and Western Turkey appear to have around a month of thermal discomfort. This value reaches 3 or

more months for North Africa and south parts of the Arabian Peninsula. Coastal and island regions appear equally vulnerable.

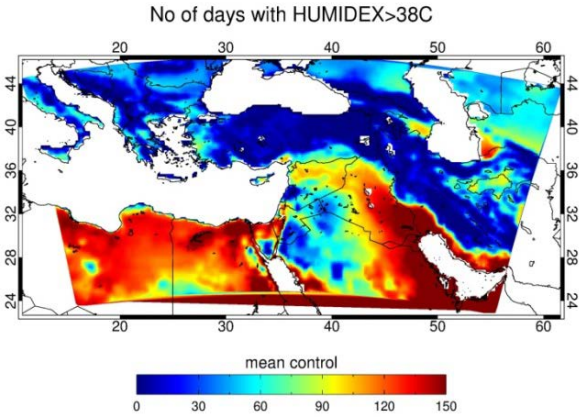

Figure 1. Number of days with HUMIDEX > 38°C for the control period using PRECIS RCM Model

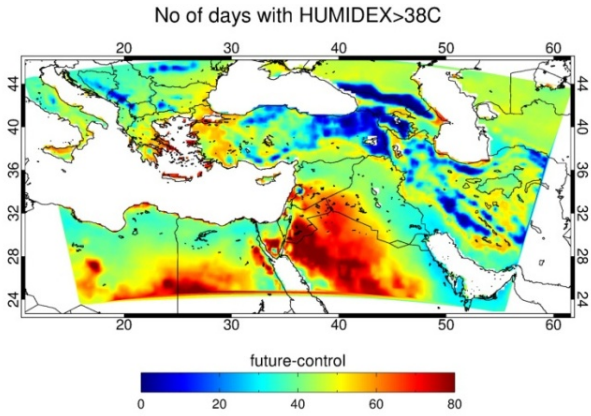

Figure 2. Potential near future changes in the number of days with HUMIDEX > 38°C using PRECIS RCM model

For coastal regions in the Eastern parts of Greece, Crete, western/central Turkey and Cyprus, the duration of HUMIDEX >38°C is projected to increase by as many as 50 days in 2020-2050 (Figure 2). Increases of 80 days are projected for the Arabian Peninsula. Smaller changes are evident in mountainous areas (e.g. Balkans, Anatolia) i.e. their cool summer climate should be maintained.

References

D'Ippoliti, D., Michelozzi, P., Marino, C., de'Donato, F., Menne, B., Katsouyanni, K., Kirchmayer, U., Analitis, A., Medina-Ramón, M., Paldy, A., Atkinson, R., Kovats, S., Bisanti, L., Schneider, A., Lefranc, A., Iñiguez, C., Perucci, A.C. (2010) The impact of heat waves on mortality in 9 European cities: results from the EuroHEAT project. *Environmental Health* 9(1): 37.

Donaldson, G., Kovats, R.S., Keatinge, W.R., McMichael, A. (2001) Heat-and-cold-related mortality and morbidity and climate change. Health effects of climate change in the UK. London: Department of Health. pp. 70-80.

Jones, C.G., Willén, U., Ullerstig, A., Hansson, U. (2004). The Rossby Centre regional atmospheric climate model part I: model climatology and performance for the present climate over Europe. *Ambio* 33:199-210.

Kuglitsch, G.F., Toreti, A, Xoplaki, E., Della-Marta, M.P., Zerefos, S.C., Türkeş, M., Luterbacher, J. (2010). Heat wave changes in the eastern Mediterranean since 1960. *Geophys Res Lett* 37:1-5.

Nakićenović, N., Swart, R. (2000) IPCC Special Report on Emissions Scenarios. A Special Report of Working Group III of the Intergovernmental Panel on Climate Change (eds., N. Nakićenović, R. Swart). Cambridge University Press, Cambridge, UK.

Parry, M.L., Canziani, O.F., Palutikof, J.P., van der Linden, P.J., Hanson, C.E. (2007) Climate Change Impacts, Adaptation and Vulnerability. In: Contribution of Working Group II to the Fourth Assessment Report of the Intergovernmental Panel on Climate Change (eds., M.L. Parry, O.F. Canziani, J.P. Palutikof, P.J. van der Linden, C.E. Hanson) Cambridge University Press, Cambridge, UK.

Paz, S., Xoplaki, E., Gershunov, A. (2010). Scientific Report: Workshop on Impacts of Mediterranean Climate Change On Human Health. Energy, Environment and Water Research Center, the Cyprus Institute.

J. Black Sea/Mediterranean Environment
Special Issue: 41-47 (2015)

Mediterranean model response to enhanced resolution at Gibraltar and tidal forcing

Gianmaria Sannino[1*], Adriana Carillo[1], Giovanna Pisacane[1], Mario Adani[1], Massimiliano Palma[1], Cristina Naranjo[2], Maria Vittoria Struglia[1]

[1] ENEA, via Anguillarese 301, 00123, Rome, ITALY
[2] Physical Oceanography Group, University of Málaga-CEIMAR, Avda. Cervantes 2, 29071, Málaga, SPAIN

[*]**Corresponding author:** gianmaria.sannino@enea.it

Abstract

The Mediterranean Sea circulation has been simulated by means of three different implementations of the MITgcm (MIT General Circulation Model). The three model domains extend over the same model domain and share the same surface forcing and lateral boundary conditions. The first model has been implemented at a horizontal resolution of 1/12° with 72 vertical z-levels, while the remaining two models use a non-uniform curvilinear orthogonal grid, having a maximum horizontal resolution of about 1/200° in the Strait of Gibraltar, degrading eastward down to a regular grid with a 1/16° resolution, and 72 vertical levels. The last two models differ in the inclusion/exclusion of tidal forcing. Comparison with observed data shows that the overall surface and intermediate circulation simulated by the 1/12° model reproduces the main features of the basin-scale circulation reasonably well. From the comparison of the two additional higher resolution experiments performed with and without tidal forcing, it appears that the tidal forcing has a not negligible impact on the simulated circulation.

Keywords: numerical ocean modelling, Mediterranean, tidal forcing, Strait of Gibraltar

Introduction

The Mediterranean Sea is a mid-latitude, semi-enclosed marginal sea connected to the Atlantic Ocean through the Strait of Gibraltar and located in a topographically complex region, where orographically enhanced intense local winds induce strong turbulent air-sea fluxes, thus causing substantial heat and mass exchanges at the air/sea interface. The excess evaporation over precipitation is compensated by water supply from the Atlantic, and sustains a heterogeneous thermohaline circulation which makes the Mediterranean Sea a "miniature ocean", which deserves attention for both experimental observations and numerical modeling.

Over the last decades, many observational campaigns have been conducted in the Mediterranean and Black Seas in the framework of several different international initiatives (MODB, MEDAR/MEDATLAS, EU/MATER, POEM), providing more comprehensive datasets of temperature and salinity profiles, bio-chemical parameters and revised climatological statistics. However, a detailed study of the physical processes in the Mediterranean Sea and an assessment of the relative roles of external forcing and internal variability in determining the observed circulation need to also include the information provided by the constantly improving numerical modelling simulations that have been carried out over the last years. Recent studies have focused on externally-induced climatic variability by exploiting the available multi-decadal numerical hindcasts of mass and energy exchanges at the air-sea interface, thus allowing new insights into the decadal and inter-annual variability of the ocean, and into episodic phenomena such as the Eastern Mediterranean Transient (EMT), (see for example Beuvier *et al.* 2010;Vidal-Vijande *et al.* 2011).

In the present work we present the main results of a 1/12° resolution Mediterranean hindcast covering the period 1958-2004. A preliminary assessment of the effects induced by both increasing resolution at Gibraltar and including tidal forcing will be presented.

Data and Methods

The numerical simulation has been initially performed with the MITgcm implemented at a horizontal resolution of 1/12º, with 72 unevenly spaced vertical levels. The model (hereinafter MedMIT12) is forced by the downscaled surface fluxes provided by a REMO/MPI simulation driven by the ECMWF/ERA40 reanalysis. The simulation is initialized using the MEDATLAS-II monthly climatology data. Model results have been validated using the temperature and salinity observational dataset developed by Rixen *et al*. (2005), consisting of 50 years of Mediterranean and Black Sea climatology. Observed temperature and salinity profiles have been quality checked according to international standards and interpolated at 25 standard vertical levels on a 0.2°x0.2° grid.

A shorter hindcast (1958-1967) for the Mediterranean has been successively performed by the MITgcm using a non-uniform curvilinear orthogonal grid, having a maximum horizontal resolution of about 1/200° in the Strait of Gibraltar, and degrading eastward down to a regular grid with a 1/16° resolution, and 72 vertical levels (same as 1/12° model) (hereinafter MedMIT16). The resolution adopted for SoG follows the recommendations suggested by Sannino *et al.* (2014) to correctly represent the hydraulic behavior in the Strait. An additional hindcast (1958-1967) has been performed using MedMIT16 in which the tidal forcing has been explicitly included (hereinafter MedMIT16T). We would like to stress that these experiments represent an

absolute novelty for the Mediterranean ocean modeling community, as Mediterranean tides and thermohaline circulation have always been studied separately and in different contexts.

Results and Discussion

The time mean general circulation simulated by the 1/12° model (Figure 1) is well reproduced and it is in good agreement with results from other authors (Pinardi *et al.* 2013; Brossier *et al.* 2011; Beuvier *et al.* 2010). The surface circulation is shown in panel (a) as represented by currents and mean Sea Surface Height (SSH) averaged over the period 1958-2004. The Atlantic Water (AW) flows into the Mediterranean Sea and, following an overall cyclonic path, meanders around the Alboran anti-cyclonic gyres, spreading northward as far as the Balearic Islands. An organized current flows along the African Coast (Algerian Current), and then bifurcates, partly entering the Eastern basin through the Sicily Channel and partly proceeding to the northwest along the Tyrrhenian Coast and recirculating westward as the Northern Current. The inflow into the Levantine basin describes a major cyclonic basin wide gyre developing unstable eddies along the Southern Coast and then being transformed into the salty and warm Levantine Intermediate Water (LIW) off the Turkish Coast, where the structure of the Rhode gyre is also evident. The Adriatic Sea circulation is also well represented. The newly formed LIW recirculates westward spreading into the Ionian basin and the Southern Adriatic Sea, being then conveyed into the Western Basin through the Sicily Channel, where it bifurcates into a Tyrrhenian branch and a direct current heading to Gibraltar (panel b).

The Mediterranean basin circulation is driven by the heat and water mass fluxes that determine the unbalance compensated by the inflowing Atlantic Water. Temperature and salinity interannual variations have been investigated at different depth layers and over the entire Mediterranean basin as well as for the Western and Eastern sub-basins separately, and compared to the reference observed data (Rixen *et al.* 2005). Figure 2 shows temperature and salt content averaged over the entire volume of the basin, temperature is in good agreement with the observations and its variations are mainly related to those of the intermediate layer (100 to 600 m) with the exception of the period 1960-1975. Such discrepancy is mostly due to the positive bias (0.9°C over the entire Mediterranean and 1.2°C over the Eastern basin) between observation and model in the first layer (0-100m) until the year 1990, partially compensated by the negative bias of the deep layer (figures not shown). On the other hand the mean salt content over the entire basin agrees with observation but the model shows significantly less interannual variability than the observations.

Despite the encouraging results of MedMIT12, there remains need for the advancement in the Mediterranean models concerning the physically based

representation of the flow exchange through the Strait of Gibraltar (hereinafter SoG), the Mediterranean eddy-dominated flow field, and the formation rates and transports of water masses involved in the Med Thermohaline Circulation (hereinafter MTHC). Despite the key role played by the SoG (Sannino *et al.* 2004; 2009a; 2009b) on the MTHC, none of the ocean models implemented in the last 15 years for the Mediterranean Sea was able to fully simulate the Strait dynamics. The main limiting factors were the coarse horizontal resolution adopted for the SoG and the omission of tidal forcing. Here we fill this modeling gap performing the two eddy-resolving experiments: MedMIT16 and MedMIT16T. A preliminary analysis of results obtained comparing the MedMIT16 and MedMIT16T shows that tides strongly affect the hydrological properties of the Atlantic inflow. The effect of tide induced mixing in the Strait is to increase salinity and decrease temperature in the upper layer, the reverse occurring in the underlying water, thus giving rise to a thicker interfacial layer with respect to MedMIT16. The altered characteristics of the inflowing Atlantic water have a non-negligible impact on the surface circulation in the Western basin, by influencing the processes occurring within the accumulation area of eddies in the western Algerian, their variability and the resulting paths of the Modified Atlantic water, with repercussions on the winter convection events that lead to deep water formation in the Gulf of Lions (Figures 3 and 4).

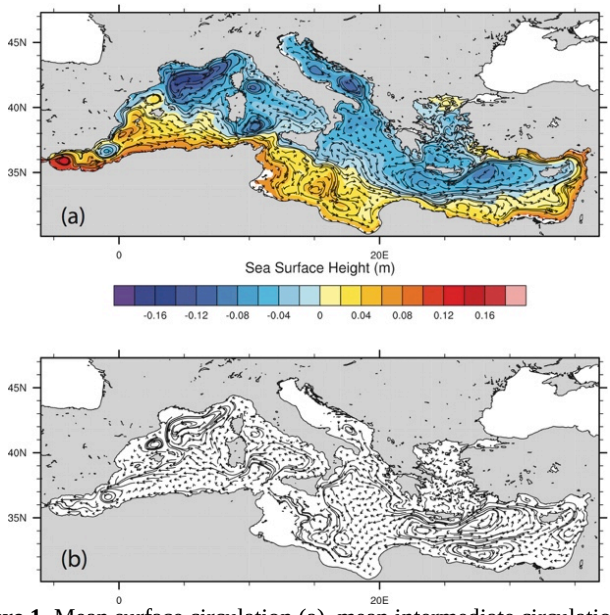

Figure 1. Mean surface circulation (a), mean intermediate circulation (b)

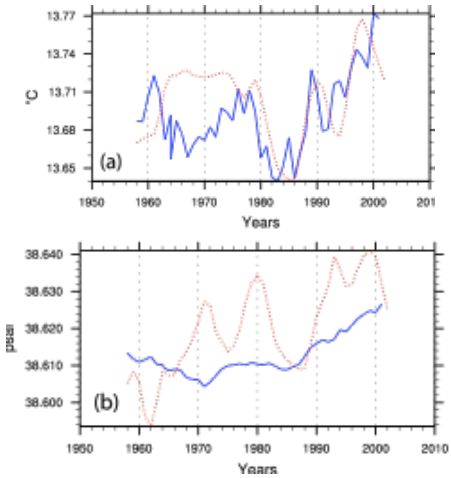

Figure 2. Variability of temperature (a) and salt (b) content over the basin volume Observations (red) and model (blue)

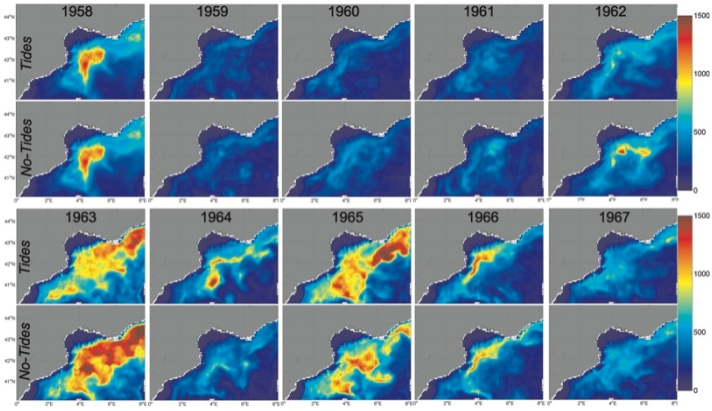

Figure 3. Mixed Layer Depth in meters (color bar) in the Gulf of Lion area computed using a threshold value for the vertical diffusion coefficient of $0.04 m^2 s^{-2}$. Upper and lower rows correspond to tidal and non-tidal runs, respectively. The plots represent the January-to-April average.

Our experiments represent a first attempt to investigate the weight of tidal forcing in determining the main features of the Mediterranean thermohaline circulation, although they are too short to fully describe both its direct impact and the mechanisms of the feedbacks it triggers within the bulk of the fluid. Longer simulations have been planned, as well as the development of ad-hoc diagnostics to be applied to critical areas of the basin. However, even at such a preliminary stage, we can conclude that the inclusion of explicit tidal forcing in

an eddy resolving Mediterranean model has non-negligible effects on the simulated circulation, in addition to the intensification of local mixing processes. The signal induced in the MAW crossing SoG in fact propagates into the basin interior and concurs to determine the dispersal paths of the main water masses, with consequences on critical processes such as deep water formation in the Gulf of Lion and LIW recirculation.

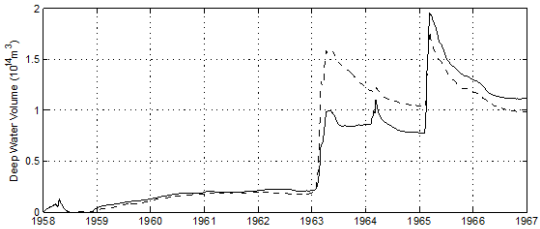

Figure 4. Total deep water volume ($\rho > 29.10$ kgm^{-3}) stored in the Gulf of Lion area. Comparison of the MedMIT16T (solid line) and MedMIT16 (dashed line). Units of $10^{14}m^3$

References

Beuvier, J., Sevault, F., Herrmann, M., Kontoyiannis, H., Ludwig, W., Rixen, M., Stanev, E., Béranger, K., Somot, S. (2010) Modeling the Mediterranean Sea interannual variability during 1961–2000: focus on the Eastern Mediterranean transient. *J. Geophys. Res.* 115: C08017.

Brossier, C.L., Beranger, K., Deltel, C. Drobinski, P. (2011) The Mediterranean response to different space–time resolution atmospheric forcings using perpetual mode sensitivity simulations. *Ocean Modeling* 36:1-25.

Pinardi, N., Zavatarelli, M., Adani, M., Coppini, G., Fratianni, C., Oddo, P., Simoncelli, S., Tonani, M., Lyubartsev, V., Dobricic, S., Bonaduce, A. (2013) Mediterranean Sea large-scale low-frequency ocean variability and water mass formation rates from 1987 to 2007: A retrospective analysis. *Prog. Oceanogr*. doi: http://dx.doi.org/10.1016/j.pocean.2013.11.003

Rixen, M., Beckers, J.M., Levitus, S., Antonov, J., Boyer, T., Maillard, C., Fichaud, M., Balopoulos, E., Iona, S., Dooley, H., Garcia, M.J., Manca, B., Giorgetti, A., Manzella, G., Mikhailov, N., Pinardi, N., Zavatarelli, M. (2005) The Western Mediterranean deep water: a proxy for climate change. *Geophys. Res. Lett.* 32:1-4.

Sannino, G., Bargagli, A., Artale, V. (2004) Numerical modeling of the semidiurnal tidal exchange through the strait of gibraltar. *J. Geophys. Res*. 109.

Sannino, G., Herrmann, M., Carillo, A., Rupolo, V., Ruggiero, V., Artale, V., Heimbach, P. (2009a) An eddy-permitting model of the mediterranean sea with a two-way grid refinement at the Strait of Gibraltar. *Ocean Modelling* 30(1): 56-72.

Sannino, G., Pratt, L., Carillo, A. (2009b) Hydraulic criticality of the exchange flow through the Strait of Gibraltar. *J. Phys. Oceanogr*. 39 (11): 2779–2799.

Sannino, G., Sanchez Garrido, J.C., Liberti, L., Pratt, L. (2014) Exchange flow through the Strait of Gibraltar as simulated by a σ-coordinate hydrostatic model and a z-coordinate nonhydrostatic model. Inc.*Geographical Monograph Series* 202: 25–50.

Vidal-Vijande, E., Pascual, A., Barnier, B., Molines, J.,Tintoré, J. (2011) Analysis of a 44-year hindcast for the Mediterranean Sea: comparison with altimetry and in situ observations. *Scientia Marina* 75(1): 71-86.

J. Black Sea/Mediterranean Environment
Special Issue: 48-53 (2015)

Assessment of temperature and precipitation extremes with climate indices by using high resolution climate simulation

Fulden Batıbeniz, Barış Önol*

Meteorological Engineering, Aeronautics and Astronautics Faculty,
Istanbul Technical University, Istanbul, TURKEY

***Corresponding author:** onolba@itu.edu.tr

Abstract

In this study, the performance of regional climate model in terms of simulating temperature and precipitation extremes is investigated. In order to assess the changes in the extreme events over Turkey and the neighboring region, high resolution regional climate simulation (double nested from 50-km to 10-km) forced by NCEP/NCAR Reanalysis has been accomplished by using ICTP-RegCM3 for the period of 1961-2008. Daily temperature and precipitation simulations are used to calculate extreme weather indices and their trends. The selected extreme indices, which are defined by World Meteorological Organization (WMO) and World Climate Research Programme (WCRP), have been mainly analyzed into two groups: Extreme hot days (TX35), summer days (SU), warm nights (TN90p), warm days (TX90p), extreme warm days (TX99p) as temperature indices and very wet days (R95p), wet days (RR1), heavy rainy days (R10mm), excessive heavy rainy days (R20mm), consecutive dry days (CDD) as precipitation indices. 187 Meteorological stations of Turkey are used to compare with the model results. The model results have been analyzed inter-annually to define the trends in extremes.

Keywords: extreme events, regional climate modeling, climate indices

Introduction

Climate has an undeniable impact on human and natural systems. Extreme weather events depending on climate change are more frequent and severe in recent decades. In addition to long-term climate conditions, extreme values and extreme weather events should be known to reach more comprehensive information in terms of assessing climate change. Thus, the aim of this study is to analyse extreme events, calculating indexes and possible trends of extremes and testing model skills in terms of simulating extremes.

According to the IPCC's Managing the Risks of Extreme Events and Disasters to Advance Climate Change Adaptation Report (2012), heavy rains intensity

and frequency will increase at the end of 21st century. Furthermore, heat waves duration, frequency and intensity will also expand gradually. World Meteorological Organization (WMO) and World Climate Research Program (WCRP) defined a set of 27 indices to characterise extremes and pointed out a increase in the number of warm days since 1990 and a decrease (fewer station than temperature) in the number of cold days since 1970 for Middle East region (Zhang *et al.* 2005). Another study focused on summer heat waves over western Turkey (Unal *et al.* 2013), pointed out that number of warm days, number and frequency of heat waves have increased between 1965 and 2006. Türkeş *et al.* (2004) analyzed trends in the diurnal temperature ranges (DTRs) over Turkey for the period 1929-1999. Some of the results of this study indicate that daytime maximum temperatures have shown weak warming and cooling. On the other hand, night-time minimum temperatures have shown warming in some of the regions. In addition, the study by Kuglitsch *et al.* (2010) focused on the changes in heat wave number, length and intensity by using the homogenized daily maximum and minimum summer air temperatures in the eastern Mediterranean region (covering Cyprus, Greece, Turkey, Albania etc.) for the period 1960-2006. According to this study, western, southwestern and central Turkey and the eastern parts of the Turkish Black Sea coastline have experienced changes in "Hot spots" of heat wave. Kostopoulou and Jones's (2005) determined possible changes in extreme temperature and precipitation, which is connected with climate change, over Eastern Mediterranean for the period of 1958-2000. Analysis of heat waves, consecutive dry days, heavy rainy days showed increasing trend, on the other hand number of the warm nights showed decreasing trend.

In this study, daily-based analyses have been performed to investigate regional climate model skills over Anatolian Peninsula and its surrounding area. Daily maximum, minimum temperatures and daily precipitations produced by regional climate model (ICTP-RegCM3) have been analyzed over Turkey. The model forced with NCEP/NCAR re-analysis data for period of 1961-2008 and the horizontal resolution of simulation is 10 km (Önol 2012). The model skills have been tested in terms of capability of RegCM to capture extreme events.

Materials and Methods

The extreme indices have been selected from WMO and WCRP climate indices. Accordingly, extreme hot days (TX35), summer days (SU), warm nights (TN90p), warm days (TX90p) and extreme warm days (TX99p) are used as temperature indices. Very wet days (R95p), wet days (RR1), heavy rainy days (R10mm), excessive heavy rainy days (R20mm) and consecutive dry days (CDD) are used as precipitation indices. Available temperature and precipitation records of Turkish State Meteorological Service (MGM) have been controlled for 187 meteorological stations. 107 of 187 stations for the period of 1961-2008 have more than %99 of available daily records (63 stations do not have missing

data). The remaining stations have more than %90 of available daily values. Therefore, selected stations are suitable to make comparison between model results and observational data.

Q-Q plot analyses of extremes have been accomplished for meteorological stations and corresponding grid points of model. In order to define simulated temperature values at station coordinates, bilinear interpolation method (weighted average of the nearest 4 grid points) is applied. On the other hand, simulated precipitation values are obtained from the nearest grid point. The Q-Q plot analyses have been performed by using values greater than 90th percentile of temperature data and 95th percentile of precipitation data. According to the Q-Q plot analysis of top percentiles, precipitation and minimum temperature data of model and station are consistent with each other. However, there is a discrepancy between model and station maximum temperature values (Figure 1a). Since the same inconsistency has been observed in TX35 analysis over the Mediterranean region stations (not shown here), we eliminated these stations for only Q-Q plot analysis (17310-Alanya, 17320-Anamur, 17330-Silifke, 17340-Mersin, 17370-İskenderun, 17372-Antakya, 17958-Erdemli, 17960-Ceyhan, 17962-Dörtyol, 17979-Yumurtalık, 17981-Karataş, 17986-Samandağ) and reproduced Q-Q plot called the corrected maximum temperature (Figure 1b). The model and the observation are highly consistent after this correction. We still have been investigating the source of the model failure based on extreme temperatures over the Mediterranean coastal region. The trend analyses of temperature and precipitation indices have been accomplished to define decadal tendency of selected extremes over Turkey. Linear regression method is applied and time is selected as an independent variable.

Consequently, time series of annual mean temperature and precipitation indices have been analysed. The recent temperature trends have been captured quite well by the model. On the other hand, time series of precipitation shows decreasing trend at some of the station points both in model and observation. Since this paper is shortened version of our study, we only represent two of the indices, CDD and SU, in eight-panel plot (Figure 2).

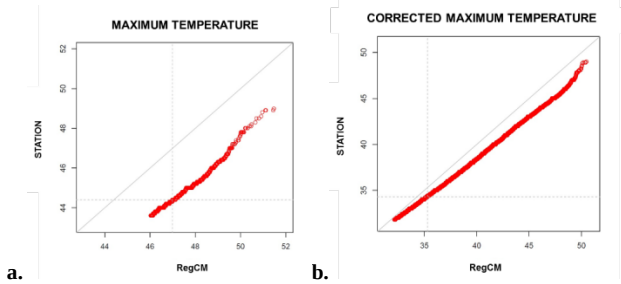

a. **b.**

Figure 1. a) Q-Q plot for the maximum temperature b) Q-Q plot for the corrected maximum temperature

Results and Discussion

Long-term averages, which are calculated from selected indices covering the period of 1961-2008, demonstrate that the model is consistent with observations for precipitation and temperature variables. The model generally overestimates all precipitation indices. Especially for RR1, the model has positive biases in the range of 50-150 days. The biases of CDD indicate that the model especially overestimates for inland stations of the southern Turkey but the general pattern of precipitation (not shown) and CDD are captured well by the model (Figure 2a). Inter-annually analysed temperature indices produced by the model also consistent with observations except TX99p. Especially on SU, the model has negative biases in the range of -10 and 10 days at Aegean, Marmara and Black Sea Regions (Figure 2b). In terms of point wise analysis, the spatial distributions of model and observation are similar. The spatial distribution of grid wise analyses of the precipitation indices produced by the model reveals significant information for the regions where the station coverage is sparse. This is especially critical over the mountainous regions. The model results capture general pattern and distribution of precipitation indices.

Additionally, trend analyses have been performed to reveal decadal tendency of temperature and precipitation indices. Decadal analyses of all precipitation indices demonstrate decreasing trend. RR1 decadal trend shows decreasing tendency in the range of 1-4 days in all regions of Turkey. Additionally, R10mm and R20mm show decreasing trend in the range of 1-3 days in Aegean and Black Sea region. On the other hand, drought index (CDD) shows increasing trend in the southern part of Anatolian Peninsula (Figure 2c). Trend analyses of all temperature indices indicate positive signal. Particularly, TX90p, TN90p and SU (Figure 2d) increase in the range of 2-10 days. Decadal tendency of extreme warm days also increases but the range is 1-2 day over Turkey. The trend analysis of TX35 shows increasing signals especially at Aegean region and the southern coastlines of Turkey in the range of 5-25 days. The western coastlines of Greece, Syria and Iraq has also significant positive trend. In terms of trend analyses, accuracy of the model has been proven with regard to capturing skill in both increasing tendency of temperature indices and decreasing tendency of precipitation indices.

Consequently, using high-resolution regional climate simulations results is considerably reliable to determine climate extremes. Point-wise analyses between the model simulations and observations indicate good agreement and spatial consistency. According to outcomes of this study, the regional climate model results can be performed for future extremes in scenario studies. Therefore, it is possible to produce new indices by determining new thresholds in order to make detailed analysis in impact studies.

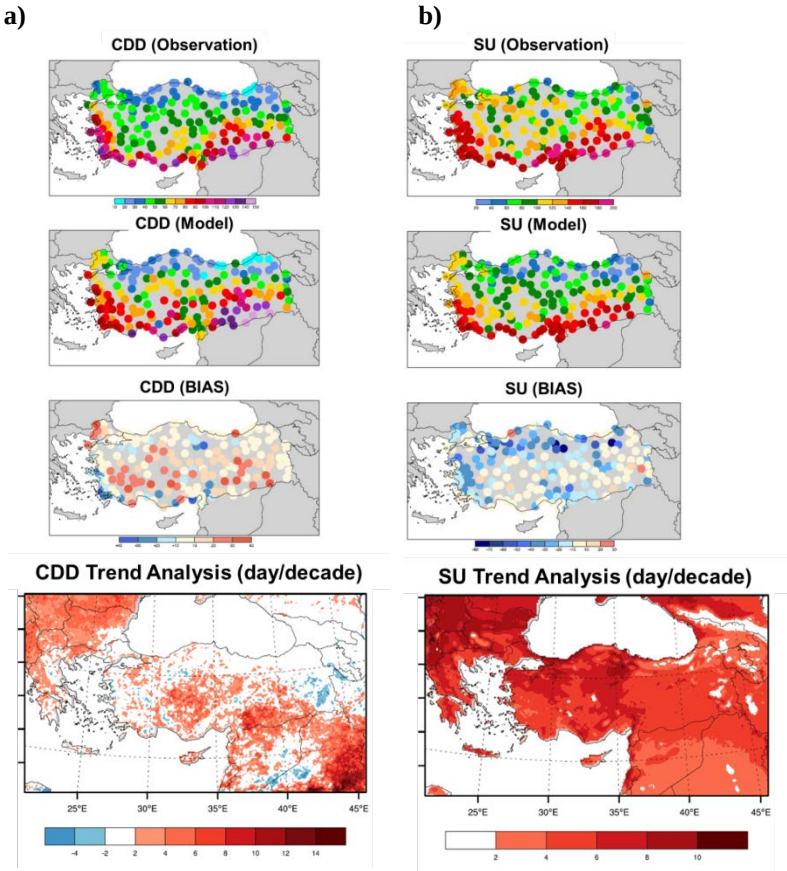

Figure 2. a) Climatology for observation, model and model-observation for CDD b) Climatology for observation, model and model-observation for SU c) Trend Analysis of CDD d) Trend Analysis of SU

References

IPCC (2012) Summary for policymakers. In: Managing the Risks of Extreme Events and Disasters to Advance Climate Change Adaptation (eds. C.B. Field, V. Barros, T.F. Stocker, D. Qin, D.J. Dokken, K.L. Ebi, M.D. Mastrandrea, K.J. Mach, G.-K. Plattner, S.K. Allen, M. Tignor, P.M. Midgley) A Special Report of Working Groups I and II of the Intergovernmental Panel on Climate Change. Cambridge University Press, Cambridge, UK-New York, USA, 1-19.

Kostopoulou, E., Jones, P.D. (2005) UK Assesment of climate extremes in Eastern Mediterranean. the East Anglia University Climatic Research Unit. *Geophys. Research Letters* 37.

Kuglitsch, F.G., Toreti, A., Xoplaki, E., Della-Marta, P.M., Zerefos, C.S., Türkeş, M., Luterbacher, F. (2010) Heat wave changes in the eastern Mediterranean since 1960. *Geophys. Research Letters* 37. doi: 10.1029/2009GL041841.

Önol, B. (2012) Effects of coastal topography on climate: high-resolution simulation with a regional climate model. *Climate Res.* 52: 159-174.

Türkeş, M., Sümer, U.M. (2004) Spatial and temporal patterns of trends and variability in diurnal temperature ranges of Turkey. *Theor. Appl. Climatol.* 77: 195-227.

Unal, Y.S., Tan, E., Menteş, S.S. (2013) Summer heat waves over western turkey between 1965-2006. *Theo. and Appl. Clim.* 112:339-350.

Zhang, X.E., Aguilar, S., Sensoy, H., Melkonyan, U., Tagiyeva, N., Ahmed, N., Kutaladze, F., Rahimzadeh, A., Taghipour, T.H., Hantosh, P., Albert, M., Semawi, M.K., Ali, M.H.S., Al-Shabibi, Z., Al-Oulan, T., Zatari, I.A.D., Khelet, S., Hamoud, R., Sagir, M., Demircan, M., Eken, M., Adiguzel, L., Alexander, T.C., Peterson, T.W. (2005) Trends in Middle East climate extreme indices from 1950 to 2003. *Journal of Geophysical Research* 110. doi: 10.1029/2005JD006181.

J. Black Sea/Mediterranean Environment
Special Issue: 54-57 (2015)

Climate trends of sea surface and air temperatures in the Eastern Mediterranean Basin

Karam Mansour[1*], Ahmed El-Gindy[1], Fahmy Eid[1], Mohamed Shaltout[1,2]

[1] Oceanography Department, Faculty of Science, Alexandria University, 21511 Alexandria, EGYPT
[2] Earth Science Department, Gothenburg University, P.O. Box 460, 40530, Göteborg, SWEDEN

[*]**Corresponding author:** karam.mansour@alexu.edu.eg

Abstract

The recent sea surface temperature (SST) and air temperature (T2m) for the Eastern Mediterranean Basin (EMB) are analyzed using 0.75 degree gridded ERA-Interim dataset, in the period 1979–2010. The results indicate that these data have a significant positive trend. During the period of study, the annual average values (trends) of SST and T2m in the EMB were 20.03±1.25°C (0.39±0.1°C/decade) and 18.79±1.52°C (0.43±0.06°C/decade) respectively. Finally, these variables are linked with the North Atlantic Oscillation Index.

Keywords: Mediterranean, trend analysis, climatic changes, ERA-Interim

Introduction

The Eastern Mediterranean Basin (EMB) extends from 11° to 36° E and 30° to 46 °N. It is a semi-enclosed basin with a negative water balance (i.e. evaporation greater than precipitation plus river runoff). The Sicily Channel (149 km wide and depth about 300 m) and Strait of Messina (4 km wide and maximum depth is 250 m) connect the Eastern and Western Mediterranean basins. The Bosporus-Marmara-Dardanelles system connects the Black Sea with the EMB (Aegean Sea). Several studies demonstrated the rapid surface warming of the Mediterranean Sea during the last decades and dealt with the variability of the air temperature regime in the Mediterranean region during the last century. Some earlier relevant studies are available. The AVHRR-SST, which is used by (Nykjaer 2009) indicated that, the SST in the EMB increased by about 1 °C in the last 2 decades. The satellite-derived mean annual warming rate is about 0.42 °C/decade for the EMB over 1985–2008; this is suggested by (Skliris *et al.* 2012). The modeled SST showed a positive trend of 0.3 °C decade^{-1} over the period 1985–2008, this is done by (Shaltout and Omstedt 2012). Finally, Shaltout and Omstedt (2013) found that, the Mediterranean SST is significantly

warming by 0.35°C/decade, with a seasonal trend variability peaking in spring at 0.38 °C/decade followed by 0.32 °C/decade in summer, 0.22 °C/decade in autumn and 0.16 °C/decade in winter during the period 1982–2012. Study of T2m and SST is used as significant indicators of climate change effect on the world. The present study aims to describe the EMB climate variability through analyzing the time series in different scales (monthly, seasonal and annual), discussing the spatial distributions of averages and linear trends (monthly and annual) and studying the effect of the North Atlantic Oscillation Index (NAOI) on SST and T2m.

Data sources

The used data are: the NAOI is extracted from the National Oceanic and Atmospheric Administration (NOAA) National Weather Service database (http://www.cpc.ncep.noaa.gov/) and gridded data of SST and T2m are extracted from the European Centre for Medium-Range Weather Forecasts (ECMWF) data server (http://www.ecmwf.int/).

Results and discussions

Thirty-two year (1979-2010) of ERA-Interim reanalyzed data are used to describe the spatial and temporal variability of SST and T2m over the EMB. The results showed that, the SST and T2m displayed large monthly, seasonal, annual, and long-term variability. Increasing SST and T2m is the most important changes. The spatial distributions of averaged SST and T2m show a strong seasonal signal occurred over the EMB characterized by zonal distribution during cold winter (November to March) and meridional distribution over the hot summer (June to August) together with transition distribution during the spring and autumn. The transition from cold to hot season occurred during spring (April and May) while the transition from hot to cold season occurred during autumn (September and October). The similarity between T2m and SST distributions may indicate the significant correlation between SST and T2m [0.85-0.97]. This may indicate that T2m is the significant source, rather than the water exchange through Sicily Channel, of the EMB heating.

The monthly and annual climatic linear trend distributions of SST and T2m indicated that the rate of warming of SST and T2m are so different in general pattern. Generally, over the EMB the monthly rate of warming of T2m is significantly larger than SST, as seen in Table 1 and Figure 1. The results indicated a strong southward increasing sea surface warming trend. The SST and T2m exhibit a strong warming for all months. The annual trend of SST over the EMB was 0.39±0.1 °C decade^{-1}. This increase in SST is not constant throughout the year. The monthly mean increase of SST ranged from 0.17±0.11 $^{\circ}$C/decade in April to 0.43±0.16 $^{\circ}$C/decade in July. The annual trend

of T2m over the EMB was 0.43±0.06 °C/decade, ranged from 0.24±0.15 C/decade in February to 0.48±0.11 °C/decade in July.

Table 1. Annual and seasonal characteristics of SST and T2m in the EMB during the period from 1979 to 2010 based on yearly means; all linear trend analyses were tested for significance using the t-test at a 95% significance level

	Sea Surface Temperature (SST)				Air Temperature (T2m)			
	Trend [°C/year]	Mean ± SD [°C]	Minimum [°C] (year)	Maximum [°C] (year)	Trend [°C/year]	Mean ± SD [°C]	Minimum [°C] (year)	Maximum [°C] (year)
Annual	0.031	20.03 ±0.36	19.33 (1980)	20.71 (2003)	0.036	18.79 ±0.41	17.99 (1980)	19.48 (2010)
Winter	0.022	15.38 ±0.33	14.63 (1981)	16.19 (2001)	0.028	13.35 ±0.57	12.30 (1993)	14.77 (2001)
Spring	0.031	19.10 ±0.49	17.96 (1980)	19.94 (2003)	0.038	18.95 ±0.54	17.68 (1980)	19.85 (2003)
Summer	0.039	25.36 ±0.50	24.35 (1984)	26.57 (2003)	0.042	24.85 ±0.54	23.81 (1984)	26.04 (2003)
Autumn	0.033	20.17 ±0.43	19.49 (1983)	20.96 (1999)	0.035	17.93 ±0.52	16.94 (1988)	18.85 (2010)

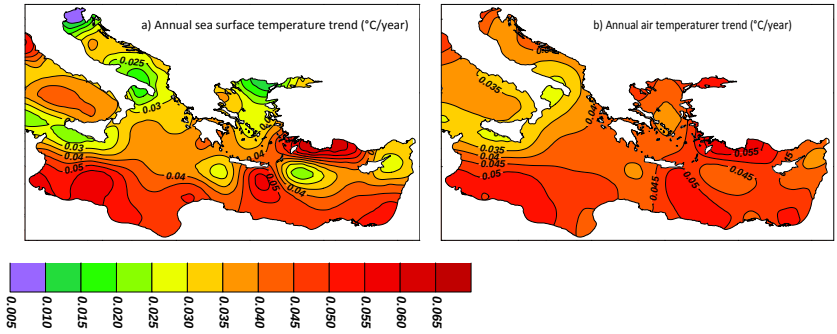

Figure 1. Spatial distribution of annual SST and T2m trends over the EMB during 1979–2010 period; all linear trends are statistically significant at 95% confidence interval

Over the whole EMB, the maximum (minimum) value of annual SST occurred during the year 2003 (1980) which corresponds to the heat wave over Europe. The warmest (coldest) T2m occurred during the year 2010 (1980), see Table 1. Finally, the NAOI show a negative significant correlation with SST and T2m everywhere in the EMB. This is in agreement with (Shaltout and Omstedt 2012; Skliris *et al.* 2012).

Conclusion

The main conclusions of this study are:
a- The ERA-Interim data can describe significantly the large-scale features of the EMB climate and show good agreements with observations, remote sensing

and modeling techniques. However, it is poorly describing the mesoscale features that may be due to its low spatial resolution,
b- The EMB is exposed to climate change especially the warming of SST and T2m, and
c- The NAO is significantly affected on the EMB climate.

Acknowledgments

The author appreciates the great efforts of master supervision committee.

References

Nykjaer, L. (2009) Mediterranean Sea surface warming 1985–2006. *Clim Res.* 39: 11–17.

Shaltout, M., Omstedt, A. (2012) Calculating the water and heat balances of the Eastern Mediterranean Basin using ocean modeling and available meteorological, hydrological and ocean data. *Oceanologia* 54 (2): 199–232.

Shaltout, M., Omstedt, A. (2013) Recent sea surface temperature trends and future scenarios for the Mediterranean Sea. *Oceanologia* 55 (3): 1–33.

Skliris, N., Sofianos, S., Gkanasos, A., Mantziafou, A., Vervatis, V., Axaopoulos, P., Lascaratos, A. (2012) Decadal scale variability of sea surface temperature in the Mediterranean Sea in relation to atmospheric variability. *Ocean Dynamics* 62: 13-30.

J. Black Sea/Mediterranean Environment
Special Issue: 58-61 (2015)

Forty years of geostrophic currents in the Ligurian Sea

Simona Aracri[1*], Harry L. Bryden[1,2], Jacopo Chiggiato[1], Elaine McDonagh[2], Simon A. Josey[2], Katrin Schroeder[1], Mireno Borghini[1]

[1] ISMAR - Istituto di Scienze Marine, Arsenale - Tesa 104 Castello 2737/F, 30122, Venezia, ITALY
[2] NOC- National Oceanography Institute, Empress Dock, SO14 3ZH, Southampton, UK

[*]**Corresponding author:** simona.aracri@ve.ismar.cnr.it

Abstract

An analysis is made of the historical datasets covering almost 40 years (1976 - 2014) in the Ligurian Sea, in the North-Western Mediterranean. Two transects are studied: one at the boundary with the Tyrrhenian sea, in the Corsica Channel, the other between Nice on the French coast and Calvì on Corsica. The variability in the circulation patterns and changes in the hydrological properties of the water masses on seasonal and interannual time scales are investigated. For every cruise we chose the closest transect to the chosen ideal sections.

Keywords: Ligurian Sea, Corsica Channel, geostrophic velocities

Introduction

The North Western Mediterranean Sea is a well-known location where deep water formation (DWF) events occur, sustaining the Mediterranean overturning circulation. The main DWF site in the Western Mediterranean is the Gulf of Lion. The Ligurian Sea in the north-eastern part of the Western Mediterranean is occasionally involved in DWF events. The first evidence of deep convection in the Ligurian basin was recorded in February 1969 down to a depth of 1200 m; other events were observed in 1991 (Sparnocchia *et al.* 1995) and from 2003 to 2006 (Marty and Chiaverini 2010) almost every year.

In the Ligurian Sea, the cyclonic circulation pattern of the Ligurian-Provençal Current (LPC) co-exists with a marked frontal structure. This current is fed by the Eastern Corsica Current (ECC) and by the Western Corsica Current (WCC) shown in Figure 1.

There is evidence (Astraldi *et al.* 1994) that the inflows and the outflows of the Ligurian Sea are undergoing strong variability. Similar changes are also expected in the characteristics of the main water masses, i.e. Levantine

Intermediate Water (LIW), the Atlantic Water (AW) and the Western Mediterranean Deep Water (WMDW).

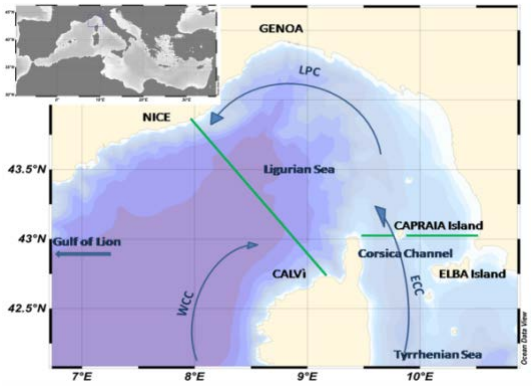

Figure 1. Map of the Ligurian Sea. Green lines identify the chosen transects.

Materials and Methods

A total of 191 hydrographic stations obtained from the MEDAR/MEDATLAS project, as well as others collected in the more recent cruises have been examined for the present study (Figure 2).

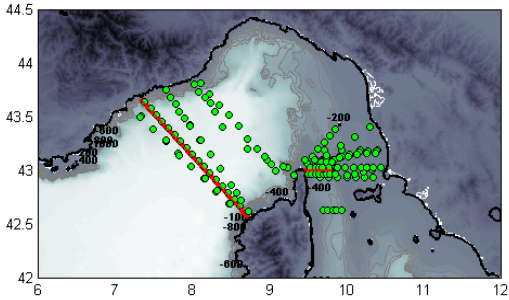

Figure 2. Map of hydrographic stations (green) and ideal chosen sections (red) for the analyses

Geostrophic velocities (GV) have been computed from the horizontal gradients of density, based on the salinity and temperature profiles extracted at each station. In calculating the GV the depth of no motion has been selected at the bottom, where water is considered to be at rest, a good approximation considering that 80% of the transport in the Corsica Channel has been found to occur in the surface layer (Astraldi *et al.* 1994). The GV are calculated every decibar, between every pair of stations. The component of the velocity is normal to the line joining the two stations, it is the difference between the current at each pressure and the current at the bottom, the reference level velocity, which

is assumed to be 0. The velocity is the average velocity between two consecutive stations, so the vector velocity is in the middle of the two stations. First the transports are calculated across each section, where the transport equals the vertically and horizontally integrated GV. Then we divide the transport by the section area to plot the average GV for each section.

To identify the cores of water masses we used the relative maximum in salinity for the LIW and the relative minimum in salinity for the AW. To identify the WMDW we looked for the minimum in temperature.

Results and Discussion

Observations of the interannual variability of GV in the Corsica Channel (Figure 3) show that in summer velocities are lower (Astraldi *et al.* 1994), while in winter velocities are higher. The increase in winter, especially in the latest winters is thought to compensate for the convection occurring in the Gulf of Lion. Exceptions to this trend are observed to occur in Nov-1991 and Jul-1976.

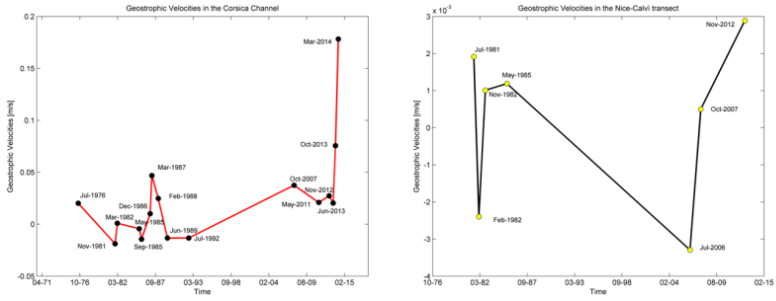

Figure 3. Interannual variability of average GV in the Corsica Channel and in the Nice - Calvì section

Most of the variability in the Nice - Calvì transect is given by the LPC, which is typically double the magnitude of the WCC (Astraldi *et al.* 1994). The WCC velocities increase in winter, meanwhile the Ligurian front displaces compressing the WCC against the coast (Astraldi *et al.* 1994). To conserve the volume inside the chosen box, the LPC, which is dominating the trend of the velocities through the section needs to decrease in this period of the year, making the graph descend, for instance in Feb-1982.

According to the interpretation of the data (not shown here), in the Nice - Calvì section in winter, the salinity content is higher, possibly due to the influence of evaporation caused by the northern winds, Mistral and Tramontane, that blow on this part of the basin.

In the fall season, the LIW salinity presents a maximum, apparently as a result of the increased stratification in summer. On the other hand, in winter, especially after deep-water formation or convection events, the LIW can be mixed with the AW, which lowers its salinity.

The WMDW potential temperature seems to be higher in fall and its core becomes deeper. It has been suggested that the new WMDW formed in more recent years is saltier and warmer (Schroeder *et al*. 2010) than the core of the old WMDW, which is being eroded and therefore is becoming thinner.

Further studies and calculations are required to quantify the transiting water masses and the evolution of the WMDW and to better estimate the level of no motion for the geostrophic calculations. A study on the level of reliability of estimates and statistical measures of variability is undergoing.

To better estimate the temporal variability in the Ligurian Sea, this study is now being extended to examine time series profiles in the Corsica Channel taken over the past decade.

References

Astraldi, M., Gasparini, G.P., Sparnocchia, S. (1994) The seasonal and interannual variability in the Ligurian-Provencal Basin. In: Seasonal and Interannual Variability of the Western Mediterranean Sea (ed., P.E. La Viollette), American Geophysical Union, Washington, D.C., 93-113.

Marty, J.C., Chiavérini, J. (2010) Hydrological changes in the Ligurian Sea (NW Mediterranean, DYFAMED site) during 1995–2007 and biogeochemical consequences. *Biogeosciences* 7: 2017-2028.

Schroeder, K., Josey, S.A., Herrmann, M., Grignon, L., Gasparini, G.P., Bryden, H.L. (2010) Abruptwarming and salting of the Western Mediterranean deep water after 2005 atmospheric forcings and lateral advection. *Journal of Geophysical Research* 115, C08029.

Sparnocchia, S., Picco, P., Manzella, Giuseppe, M.R., Ribotti, A., Copello, S., Brasey, P. (1995) Intermediate water formation in the Ligurian Sea. *Oceanologica Acta* 18: 151-162.

J. Black Sea/Mediterranean Environment
Special Issue: 62-65 (2015)

Climate projections of maximum water level during storms along the coasts of the Mediterranean Sea for the 2021-2050 period

Piero Lionello[1,2*], Dario Conte[2], Luigi Marzo[1], Luca Scarascia[2]

[1] DiSTeBA, Università del Salento, CoNISMa, 73100, Lecce, ITALY
[2] CMCC Euro-Mediterranean Center on Climate Change, 73100, Lecce, ITALY

[*]**Corresponding author:** piero.lionello@unisalento.it

Abstract

This contribution describes projections of the maximum level that water will reach during a storm along the coast of the Mediterranean Sea in the next decades (2021-2050). The computation accounts for changes of marine storminess (maximum wave amplitude and maximum storm surge level) and for the steric contribution (thermosteric expansion, halosteric contraction) to the mean sea level, but not for addition of water mass to the basin through the Gibraltar Strait. This analysis is based on an ensemble of regional climate model simulations (produced by the CIRCE fp6 project) covering the period 1951-2050 under the A1B emission scenario, whose results have been used for forcing a hydro-dynamical shallow water mode and a wave model, obtaining estimates of storm surge levels and maximum amplitude of ocean waves, respectively. Data produced by high resolution models of the Mediterranean Sea circulation have been used for diagnosing the steric sea level change. The climate change signal is computed as the difference between maximum water level statistics in the 1971-2000 and 2021-2050 periods. Results show that the decrease of storm surge level and wave height will compensate for the positive steric effects in the next decades.

Keywords: maximum water level, climate change, storms, coastal management, Mediterranean Sea

Introduction

This contribution describes the results of a practical methodology for estimating the maximum water level that is reached at the coastline during a storm and how it will be affected by global climate change in the future. Results are expected to be relevant for planning coastal and harbor defenses (dams, sea walls, breakwaters and structures such as jetties and docks).

The analysis is carried out accounting for several factors, which in the Mediterranean Sea are actually expected to act in different directions. Previous studies show that storm surge levels and significant wave height will likely

decrease (Conte and Lionello 2013; Lionello *et al.* 2008), while steric effects are positive (Tsimplis *et al.* 2008), though recent criticism have been raised on their interpretation in term of sea level rise (Jordà and Gomis 2013). However, no study has up to now attempted to consider the net result of the superposition of these different effects.

Materials and Methods

The procedure adopted in this study consists in 3 main steps: i) to produce an estimate of the various factors responsible for the water level, ii) to add the different contributions iii), to build indicators of water level maxima, whose values are used for estimating the climate change signal (see Lionello *et al.* 2014 for details).

Input data for this analysis are provided by seven climate simulations that have been produced by different institutions (CMCC, MPI, ENEA, CNRM, IPSL) within the CIRCE fp6 project (Climate Change and Impact Research: the Mediterranean Environment) and cover the period 1951-2050 under the A1B emission scenario (Gualdi *et al.* 2013). Six out of seven simulations have been carried out with coupled atmosphere ocean models including a high resolution model of the Mediterranean Sea circulation. The data of these simulations have been used for 3 sets of computations. The surface wind fields have been used for driving the wave model WAM and producing projections of maximum wave amplitude. The SLP (Sea Level Pressure) and wind fields have been used for driving the hydro-dynamical shallow water model HYPSE (Hydrostatic Padua Sea Elevation model) and producing sea level projections. The sea temperature and salinity fields have been used for computing sea water density and the steric sea level variation.

The practical recipe adopted here for computing the maximum water level is to assume a maximum individual wave height $h_{max}=1.8h_{1/3}$, where $h_{1/3}$ is the significant wave height, and add the maximum wave amplitude $a_{max}= 0.5\ h_{max}$ to the change of sea level produced by the storm surge and steric effects. Note that this is valid if the waves are symmetric. This addition is performed at 3-hourly steps and the resulting time series is used for identifying water level maxima and computing relevant indicators, such as the mean annual maxima.

Results

Figure 1 shows the Mediterranean coastline (panel in the top-right corner) and the change (2021-2050 versus 1971-2000) of the average annual maximum along its coastline. Figure 1 shows also the effect of waves only, of waves and surges together (without the steric contribution). Differences are considered significant (thick coloured parts of the lines in the figure) when the climate

change signal is larger than its standard deviation. Only the model ensemble mean is shown (see Lionello *et al.* 2014 for details).

Results show that the reduction of storm intensity (green and blue parts of the lines) will compensate for the positive thermosteric effect (the halosteric effect is marginal), so that in the next decades the maximum water levels will significantly increase at very few points (black parts of the line) and changes in the Adriatic Sea and along the coast of the Middle East are negative even including the positive steric effect.

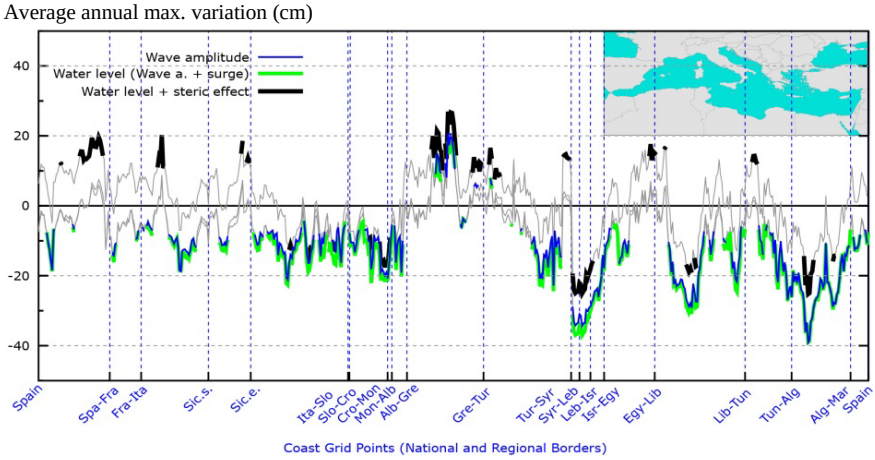

Figure 1. Change of annual max water level along the coast of the Mediterranean Sea (coastal points are ordered clockwise from Spain to Morocco). Significant changes are marked using a thick black line. The figure shows also changes computed considering only the wave amplitude (significant changes in blue), wave amplitude and surges (significant changes in green).

Discussion

This contribution has analysed the future evolution of maximum water level, which will be produced by two contrasting factors: decrease of storminess and increase of mean sea level. In fact, the analysed simulations agree that maxima of storm surge and wave amplitude along the coast of the Mediterranean Sea will decrease in the future and that mean sea level will increase due to the thermosteric effect. Adding these factors shows that changes of water level maxima will be likely small in the next few decades. However, mass addition caused by melting of ice-caps will introduces a large and positive contribution that needs to be included in the actual sea level projections.

References

Conte, D., Lionello, P. (2013) Characteristics of large positive and negative surges in the Mediterranean Sea and their attenuation in future climate scenarios. *Glob.Planet. Change* 111:159-173.

Gualdi, S., Somot, S., Li, L., Artale, V., Adani, M., Bellucci, A., Braun, A., Calmanti, S., Carillo, A., Dell'Aquila, A., Déqué, M., Dubois, C., Elizalde, A., Harzallah, A., Jacob, D., L'Hévéder, B., May, W., Oddo, P., Ruti, P., Sanna, A., Sannino, G., Scoccimarro, E., Sevault, F., Navarra, A. (2013) The CIRCE simulations: a new set of regional climate change projections performed with a realistic representation of the Mediterranean Sea. *Bull. Am. Meteorol. Soc.* 94:65–81.

Jordà, G., Gomis, D. (2013) On the interpretation of the steric and mass components of sea level variability: The case of the Mediterranean basin. *J. Geophys. Res. Oceans* 118: 953–963.

Lionello, P., Cogo, S., Galati, M.B., Sanna, A. (2008) The Mediterranean surface wave climate inferred from future scenario simulations. *Glob.Planet. Change* 63:152-162.

Lionello, P., Conte, D., Marzo, L., Scarascia, L. (2014) A comprehensive climate projection of the maximum water level during storms along the coast of the Mediterranean Sea in the mid 21st century (in preparation).

Tsimplis, M.N., Marcos, M., Somot, S. (2008) 21st century Mediterranean Sea level rise. Regional model predictions. *Glob. Planet.Change* 63:105-111.

J. Black Sea/Mediterranean Environment
Special Issue: 66-69 (2015)

Changes in the contribution of moisture from the Mediterranean Basin to the continental precipitation from 1980 onwards: a Lagrangian analysis

Anita Drumond[1*], Luis Gimeno[1], Ricardo Garcia-Herrera[2], Raquel Nieto[1]

[1] EPhysLab, Facultade de Ciencias de Ourense, Universidade de Vigo, 32004, Ourense, SPAIN
[2] Departamento de Astrofísica y Ciencias de la Atmósfera, Universidad Complutense, Madrid, SPAIN

[*]**Corresponding author:** anitadru@uvigo.es

Abstract

In this work we use an objective 3-D Lagrangian method to identify possible changes in the moisture contribution from the Mediterranean basin to the continental precipitation during the extended winter season (October-April) for the 1980-2012 period. We tracked air parcels from the Mediterranean forward in time along the 10-day trajectories to investigate the role of the basin as source of moisture. Climatologically, the contribution of moisture from the basin to the winter precipitation occurs over a domain expanding from the northern Africa towards Europe and the western Asia. The differences of the decadal composites point out that the 90's was characterized by enhanced moisture contribution from the basin towards central/western Europe.

Keywords: moisture transport, Lagrangian analysis, decadal changes

Introduction

Observational analysis suggests increasing in the evaporation averaged over the Mediterranean basin during the extended winter for the last three decades (Gomez-Hernandez *et al.* 2013 and references therein).

In this work we use an objective 3-D Lagrangian method to identify possible changes in the moisture contribution from the Mediterranean basin source to the continental precipitation during the extended winter season (October-April) for the 1980-2012 period.

Materials and Methods

We used the method developed by Stohl and James (2004), based on the Lagrangian model FLEXPART v9.0 forced by the 1º ERA-Interim reanalysis (Dee *et al.* 2011) available every 3 hours.

The method divides the atmosphere into air parcels, which are transported using the wind field. The changes of the specific moisture of an air parcel (of mass m) along its trajectory can be expressed as: $e - p = m\, dq/dt$, where (e-p) can be interpreted as the freshwater flux in the parcel (the difference of evaporation and precipitation). By adding (e – p) for all the parcels in the vertical atmospheric column over an area, we obtain the surface freshwater flux (E – P).

The lagrangian data set used comes from a global simulation in which the atmosphere was divided into approximately 2.0 million parcels. We track (E-P) from the Mediterranean basin (MED) forward in time along the 10-day trajectories (the average residence time of water vapour in the atmosphere). We analyse negative values of (E-P) integrated over the 10-day trajectories at the seasonal scale. They indicate the sinks of moisture that, under the necessary dynamical conditions, can be converted into surface precipitation.

Differences of the 90´s (1991-2000) and 80´s (1981-1990) and of the 2000´s (2001-2010) and 90´s were calculated for the precipitation (GPCP; 2.5º; Huffmann *et al*. 2009), the vertically integrated moisture flux (VIMF; ERA-INTERIM) and the (E-P) fields. A bootstrap test with 90% of significance was applied in the decadal differences of the (E-P).

Results

Climatologically, the rainy season for most of Europe occurs during October-April, when higher precipitation and convergence of VIMF are observed (fig 1, left and central top panels, respectively). Divergence of VIMF over Mediterranean suggests its role as a moisture source. The contribution of moisture from MED to the precipitation occurs towards the northern Africa, Europe and the western Asia (Figure 1, right top panel).

The 90's - 80's differences (Figure 1, central panels) show a dipole over MED and Europe: reduced (increased) precipitation and higher divergence (convergence) of VIMF over MED (central/north Europe). The moisture contribution from MED increased towards western and central Europe.

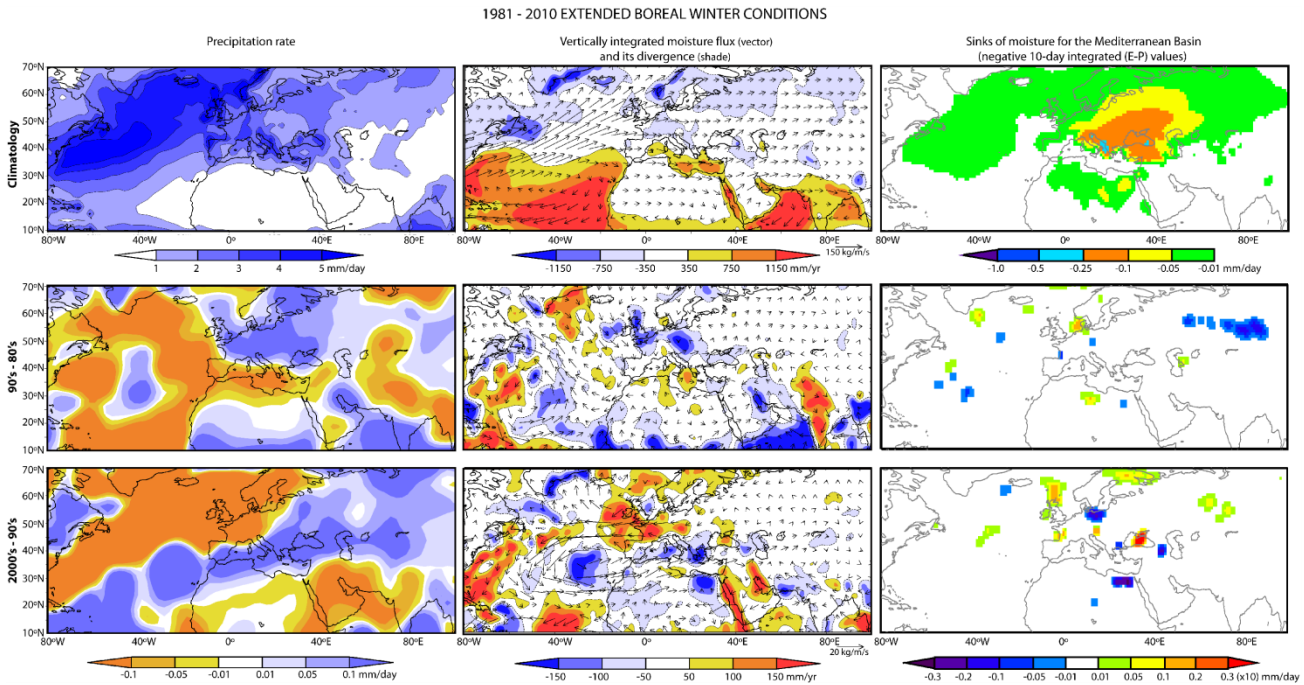

Figure 1. Top (from left to right columns): 1981–2010 extended boreal winter climatology of the precipitation rate (mm/day, GPCP), of the Vertically Integrated Moisture Flux (vector; kg/m/s) and its divergence (mm/year, Era-Interim), and of the negative E-P (sinks of moisture) (mm/day). Central: same as top, but for decadal differences of 90's and 80's. Bottom: same as top, but for 00's and 90's. Only decadal differences of sinks of moisture significant at the 90% confidence level are plotted (Bootstrap Test).

The dipolar structure of precipitation and VIMF over MED and Europe observed in the 90's - 80's was inverted during 00's – 90's (Figure 1, bottom panels). In comparison to the 90's, enhanced moisture contribution from MED towards Egypt and areas of Turkey was configured during the 00's. However, the moisture contribution from MED was reduced towards Black Sea and regions of western/Central Europe.

Discussion

The differences of the decadal composites suggest that the patterns over the Mediterranean basin and Europe have changed during the last thirty years. It seems that the 90's was characterized by the enhancement of the divergence of the VIMF over the basin and by the intensified moisture contribution from this source towards central/western Europe.

Acknowledgement

To the Spanish Government (the TRAMO project) and to FEDER.

References

Dee, D.P.,Uppala, S.M., Simmons, A.J., Berrisford, P., Poli, P., Kobayashi, S., Andrae, U., Balmaseda, M.A., Balsamo, G., Bauer, P., Bechtold, P., Beljaars, A.C.M.,van de Berg, L., Bidlot, J., Bormann, N., Delsol, C., Dragani, R., Fuentes, M., Geer, A.J., Haimberger, L., Healy, S.B., Hersbach, H., Hólm, E.V., Isaksen, L., Kållberg, P., Köhler, M., Matricardi, M., McNally, A.P., MongeSanz, B.M., Morcrette, J.-J., Park, B.-K., Peubey, C., de Rosnay, P., Tavolato, C., Thépaut, J.N.,Vitart, F. (2011) The ERA Interim reanalysis: configuration and performance of the data assimilation system. *Quart. J. Roy. Meteor. Soc.* 137: 553–597.

Gomez-Hernandez, M., Drumond, A., Gimeno, L., Garcia-Herrera, R. (2013) Variability of moisture sources in the Mediterranean region during the period 1980–2000. *Water Resour. Res.* 49: 1-21

Huffman, G.J, Adler, R.F., Bolvin, D.T., Gu, G. (2009) Improving the global precipitation record: GPCPversion2.1. *Geophys.Res.Lett.* 36:L17808. doi: 10.1029/2009GL040000

Stohl, A., James, P.A. (2004) Lagrangian Analysis of the atmospheric branch of the global water cycle. Part I: Method description, validation, and demonstration for the August 2002 flooding in Central Europe. *J. Hydrometeor* 5: 656-678.

J. Black Sea/Mediterranean Environment
Special Issue: 70-73 (2015)

Cyclone-precipitation analysis for the island of Crete

Vasiliki Iordanidou[1], Aristeidis G. Koutroulis[1], Ioannis K. Tsanis[1,2*]

[1] Department of Environmental Engineering, Technical University of Crete, Chania, Crete, GREECE
[2] Department of Civil Engineering, McMaster University, Hamilton, Ontario, CANADA

[*]**Corresponding author**: tsanis@mcmaster.ca

Abstract

The characteristics of cyclones over Eastern Mediterranean that cause precipitation in the island of Crete are studied examining potential forecasting applications. The datasets used for this study are ECMWF reanalysis (ERA-Interim) for the time period 1979-2011 and local precipitation records from a dense rain gauge network in Crete. The Melbourne University algorithm (MS-scheme) is used for identification of the cyclones' characteristics and tracks from Mean Sea Level Pressure (MSLP) fields. Cyclone pressure, intensity and other characteristics are examined in different seasons in combination with three rain severity categories. Results show that the most cyclones that affect Crete approach from the southwest direction during the spring period while during the other seasons they originate from north-northwest direction. Decrease in pressure as well as increase in cyclone intensity, depth, radius and propagation velocity result in an increased rain accumulation. Probability maps of the cyclone tracks over a gridded mesh of the domain of interest provide short term forecast of an affecting cyclone pathway. The rain diagnostic potential of the estimated probability maps reach 50-80% scores in the statistical tests of sensitivity, specificity and accuracy.

Keywords: cyclones, rain, probability maps, Crete Island

Introduction

Socioeconomic damages in organized societies are highly depended on natural hazards such as floods, and landslides (Real and Lionello 2013). Cyclonic activity is the main triggering factor for rain events and especially extreme precipitation in Mediterranean region. Cyclone identification, analysis and tracking is a subject of research for many scientists and many algorithms have been developed for the study of these problems (Neu *et al.* 2013). In this work, cyclone-rain association is investigated for the island of Crete as well as cyclone rain diagnosis potential.

Materials and Methods

The European Centre for Medium-Range Weather (ECMWF) 0.5x0.5 Era-Interim MSLP fields for the years 1979-2011 are used for the extraction of cyclones as well as their tracks and characteristics with the aid of MS Scheme (Murray and Simmonds 1991). Rain records are gathered from 69 rain gauge stations over the island of Crete. The MSLP fields have 6-hour temporal resolution while rain records are daily. The domain of study covers middle-eastern Europe (4°–33°E and 32° –43°N) and Crete (area of interest) is enclosed within the boundaries of 23.4°-26.4°E and 34.8°-35.7°N.

Rain is classified in three accumulation categories: mild (10-50mm/day), strong (50-100mm/day) and heavy (>100mm/day) rain. The thresholds for the rain categories are chosen from the daily average of the gauging stations for the 50^{th}, 90^{th} and 99.5^{th} percentile of rain. If at least one station has a daily rain accumulation in the rain range of the defined rain categories then it is considered that we have a rain event of the corresponding rain category. Spatiotemporal correlation of a cyclone to the rain event is accepted when the cyclone center distance from Crete boundary is smaller than the cyclone radius (spatial correlation) and the cyclone appears within the day of the rain record (temporal correlation).

Cyclones correlated to the rain events are referred as 'hitting' and their previous instances are referred to as 'affecting' cyclones. Probability maps (PMs) over the study domain are estimated by the number of affecting/hitting cyclones to the total number of cyclones, on a gridded 0.5x0.5 mesh. Weighted-normalized probability maps (WNP) are also estimated weighting PMs with the number of affecting/hitting cyclones. WNPs are normalized to 1 to be comparable with simple PMs. Relevant PMs are also estimated for cyclones with extreme characteristics of depth, radius and intensity. In every case estimations are made for every rain category and for every distinct cell of the gridded mesh.

In order to predict whether a passing cyclone could in the near future trigger a rain event in Crete, probability thresholds are selected for each rain category over which an alarm of possible affecting cyclone is turned on. Statistical measures of sensitivity, specificity and accuracy are used to evaluate the success rate of the probability maps to predict rain events. Validation of the PMs is achieved using a combination of 10-fold cross validation and Monte Carlo technique. More details on the methodology of this work can be found in Iordanidou *et al.* (2014).

Results and Discussion

The cyclone-rain analysis showed that more than 70% of rain events and up to 80% of heavy rain events are triggered by cyclones in agreement with (Reale

and Lionello 2013) who found an increasing probability of cyclone detection with the rain increase. In accordance to the geographical location of Crete the majority of affecting cyclones originate northwest in autumn and winter for all rain categories. In spring this changes, as the difference between northwest and southwest cyclones gets smaller and this difference gets even smaller for the rain categories of higher rain accumulation. Hitting cyclones are mainly located north of Crete. However difference of impacts between cyclones located north and south is small for events in the heavy rain category. In particular, heavy rain events are mainly triggered by south originating cyclones during spring. Differences in cyclone characteristics are also observed for the mild, strong and heavy rain events as well as for the tree examined seasons of autumn, winter and spring. An increase in intensity, depth, radius and propagation velocity causes a decrease in rain accumulation while the opposite is true for pressure.

Regarding the probability maps, southern positioned affecting and hitting cyclones have greater probability to trigger heavy rain events than those located in other directions. WNPs compared to PMs, better emphasize the so-called 'hot spots' as the number of affecting cyclones passing by is used as weight for the probability. The region south of Italy has high probability to trigger rain in Crete in WNP probability maps (Figure 1), especially mild rain events. Validation results are promising, giving sensitivity-specificity in the range 0.6-0.8, with the higher results achieved for heavy rain events. WNPs have both good sensitivity and specificity results for all rain categories compared to the other combinations of the PMs. An example of the rain prediction use of the PMs and the statistical measures is shown in Figure1.

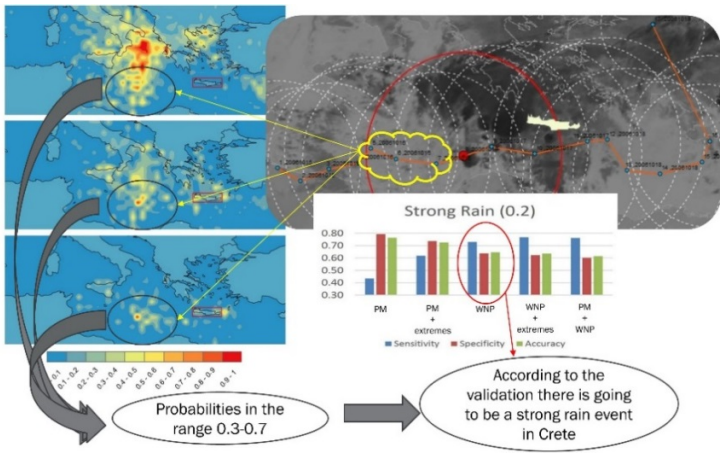

Figure 1. Example of rain prediction via PMs use (Almirida flood event). On the left are illustrated the WNPs for mild, strong and heavy rain categories and on the right the METEOSAT image at 00:00 UTC in 17/10/2006. Below those images is presented the bar diagram showing for different PM and WNP combinations the sensitivity-specificity and accuracy scores.

Finally, the rain events in Crete are associated with cyclones, especially those of high rain accumulation. The results can be interesting from the perspective of storm-track regimes that favour different categories of precipitation in the area of interest. Also, giving fair results in sensitivity-specificity statistics, the PMs could be a useful tool for rain prediction complementary to conventional WNPs.

References

Iordanidou, V., Koutroulis, A.G., Tsanis, I.K. (2014) A probabilistic rain diagnostic model based on cyclone statistical analysis. *Adv. Meteorol.* 1-11.

Murray, R., Simmonds, I. (1991) A numerical scheme for tracking cyclone centres from digital data. Part I: Development and operation of the scheme. *Aust. Meteorol. Mag.* 39: 155–166.

Neu, U., Akperov, M.G., Bellenbaum, N., Benestad, R., Blender, R., Caballero, R., Cocozza, A., Dacre, H.F., Feng, Y., Fraedrich, K., Grieger, J., Gulev, S., Hanley, J., Hewson, T., Inatsu, M., Keay, K., Kew, S.F., Kindem, I., Leckebusch, G.C., Liberato, M.L.R., Lionello, P., Mokhov, I.I., Pinto, J.G., Raible, C.C., Reale, M., Rudeva, I., Schuster, M., Simmonds, I., Sinclair, M., Sprenger, M., Tilinina, N.D., Trigo, I.F., Ulbrich, S., Ulbrich, U., Wang, X.L., Wernli, H. (2013) IMILAST- A community effort to intercompare extratropical cyclone detection and tracking algorithms. *Bull. Am. Met. Soc*. 94:529- 547.

Reale, M., Lionello, P. (2013) Synoptic climatology of winter intense precipitation events along the Mediterranean coasts. *Nat. Hazards Earth. Syst. Sci.* 13: 1707-1722.

J. Black Sea/Mediterranean Environment
Special Issue: 74-77 (2015)

Investigating deep-water formation variability in the Aegean Sea and its influence in the adjacent basins deep circulation

Sarantis Sofianos[1*], Vassilios Vervatis[1,2], Anneta Mantziafou[1], Michael Ravdas[1], Sotiria Georgiou[1]

[1] University of Athens, Faculty of Physics, GREECE
[2] Laboratoire d'Etudes en Géophysique et Océanographie Spatiales, CNRS, Toulouse, FRANCE

[*]**Corresponding author:** sofianos@oc.phys.uoa.gr

Abstract

Based on the observed variability of the deep-water characteristics in the Eastern Mediterranean Sea, multi-decadal high-resolution model simulations were carried out in order to identify the major patterns of deep-water formation variability in the Aegean Sea and its influence to the adjacent basins. Water mass characteristics and deep-water formation processes in the Aegean Sea present very large temporal and spatial variability. This is related to the variability of the atmospheric forcing, the complex topography and the fact that the Aegean Sea receives very diverse water masses from the adjacent basins. The central Aegean plays an important role in the structure of the thermohaline cells. It is the combination of the high salinities of the waters reaching the central basin with the enhanced winter buoyancy loss that makes this area favorable for dense water formation. Interannual to multi-decadal variability is present in all Eastern Mediterranean sub-basins. Water column variability and circulation pattern are strongly affected by both the atmospheric forcing and the lateral fluxes through the boundaries with adjacent basins.

Keywords: Aegean Sea, oceanic variability, thermohaline circulation

Introduction

The Aegean Sea is one of the four major basins of the Eastern Mediterranean Sea, situated in the northeastern Mediterranean, to the northeast of the Ionian Sea and to northwest of the Levantine Sea. The Aegean Sea is connected with the Marmara and Black Seas through the Turkish Strait system (Dardanelles and Bosphorus). At its southern end it is connected with the Levantine and Ionian Seas through a series of six straits (the Cretan Arc Straits). Despite the progress in direct observations and modeling efforts, the circulation of the Aegean Sea is yet far from being well defined and understood. The basic water masses in the Aegean are: the brackish Black Sea Water (BSW) outflowing from the Dardanelles, the highly saline and warm waters of Levantine origin (Levantine

Surface Water – LSW and Levantine Intermediate Water - LIW), and the dense deep and intermediate waters of that are formed locally and fill the deepest layers. The exchange between the Aegean Sea and the Levantine and Ionian basins, through the Cretan Arc Straits, is very complex, presenting strong seasonal and interannual variability.

The importance of Aegean Sea to the thermohaline circulation of the Mediterranean Sea has acquired attention during the last decades due to the changes related to the Eastern Mediterranean Transient (EMT), when the stratification of the Aegean Sea changed dramatically and large amounts of very dense waters of Aegean origin outflowed from the basin and sank to the bottom of the Eastern Mediterranean Sea (Roether *et al.* 1996). It is, thus, very important to identify the major pattern and processes of deep-water formation variability in the Aegean Sea and the consequent influence in the adjacent basins deep circulation.

Data and Methods

Focusing on identifying the patterns and variability of water mass formation in the Aegean Sea the analysis of the in situ measurement is concentrated in the deeper layers of the basin (below the 800 m). Annual mean potential temperature, salinity and sigma-theta values were computed from temperature and salinity profiles acquired and quality controlled from a comprehensive data set (Ozsoy *et al.* 2014; Georgiou *et al.* 2014). Since the temporal and spatial resolution of the observations is rather sparse, the identification of the water mass formation patterns and its variability is difficult to make. For this reason the analysis is complemented with numerical experiments that cover the Aegean Sea and the adjacent basins. Two 40-years experiments (1960-2000) where carried out, one for the Aegean-Levantine basins (Vervatis *et al.* 2013) with horizontal resolution 1°/30 and one for the Ionian Sea (Ravdas *et al.* 2013) with horizontal resolution 1°/20. The experiments were validated towards the in situ observations and the results are discussed in the following section.

Results and conclusions

The time series of the mean annual thermohaline properties of the deep-water mass in the Aegean Sea demonstrate large variability (salinity variations are of the order of around 0.3 and temperature variations are of the order of 1°C). It is related to the small size and the complex topography of the sub-basins and the important open boundaries, which allow large lateral flows between the Aegean, the Levantine and the Ionian basins. The largest variability is observed during the EMT but other important events were also recorded. These events are related with deep-water formation processes that modify the structure of the Aegean water column and the thermohaline cells inside the basin. These waters outflow from the Aegean and subsequently modify in the thermohaline circulation

patterns of the other Mediterranean basins.

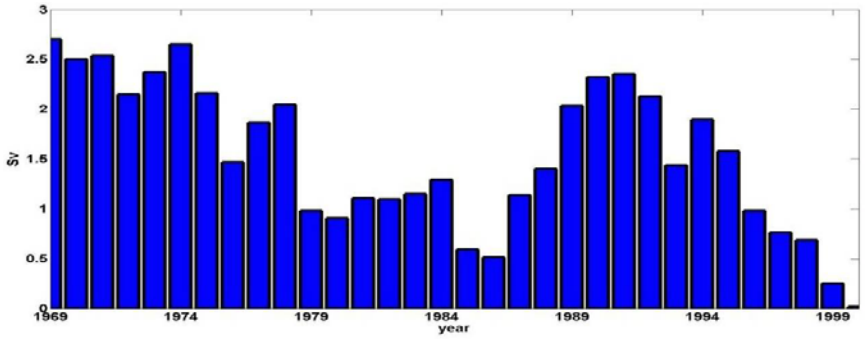

Figure 1. Annual mean intermediate layer transport through the Ionian Sea eastern boundary, derived from the modeling results

The magnitude of the variability of the deep-water characteristics differs between the various sub-basins of the Aegean (Georgiou *et al.* 2014). The central part of the basin seems to play a crucial role in determining the structure of the thermohaline circulation in the Aegean Sea. It is the area where the combination of lateral salinity input, of Levantine origin, with relatively strong winter atmospheric forcing creates the appropriate conditions for dense water mass formation. This was verified through direct observations (Vervatis *et al.* 2011) and numerical experiments (Vervatis *et al.* 2013). In contrast, although the atmospheric forcing in North Aegean is of comparable strength, the presence of the BSW, with larger buoyancy, strengthens the stratification and prohibits water mass formation processes. Salinity preconditioning, in the Aegean Sea, is mostly related to lateral salt flux while temperature preconditioning and intense mixing, associated with formation processes, is related to the heat flux from the sea surface.

Exchange flow of intermediate and deep waters between the Eastern Mediterranean basins is very important for the circulation and the water-mass formation. As an example we present here (Figure 1) the flux of saline waters (S > 38.9) at intermediate depths (200 - 500 m) through the eastern boundary of the Ionian Sea. This lateral flux variability together with the possible accumulation of water masses inside each basin can significantly change the stratification and thus the circulation and water mass formation processes.

Reference

Georgiou, S., Mantziafou, A., Sofianos, S., Gertman, I., Özsoy, E., Somot, S., Vervatis, V. (2014) Climate variability and deep water mass characteristics in the Aegean Sea. *Atmos. Res.* (in press). doi: 10.1016/j.atmosres.2014.07.023.

Özsoy, E., Gertman, I., Mantziafou, A., Aydoğdu, A., Georgiou, S., Tutsak, E., Lascaratos, A., Hecht, A., Latif, M.A. (2014) Deep-water variability and inter-basin interactions in the Eastern Mediterranean Sea. In: The Mediterranean Sea: Temporal Variability and Spatial Patterns. *Geophysical Monograph Series* 202: 85-112.

Ravdas, M., Mantziafou, A.,Vervatis, V. (2013) The dynamics of the Ionian Sea and its climatic implication: Interannual simulation for the period 1960-2000. Geophysical Research Abstracts Vol. 15, EGU2013-4909, 2013, EGU General Assembly, Vienna.

Roether, W., Manca, B.B., Klein, B., Bregant, D., Georgopoulos, D., Beitzel, V., Kovacevic, V., Luchetta A. (1996) Recent changes in Eastern Mediterranean deep waters. *Science* 271: 333–335.

Vervatis, V.D., Sofianos, S., Skliris, N., Somot, S., Lascaratos, S., Rixen, A.M. (2013) Mechanisms controlling the thermohaline circulation pattern variability in the Aegean–Levantine region A hindcast simulation (1960–2000) with an eddy resolving model. *Deep-Sea Res. I* 74:82–97.

Vervatis, V.D., Theocharis, A. (2011) Distribution of the thermohaline characteristics in the Aegean Sea related to water mass formation processes (2005-2006 winter surveys). *J. Geophys. Res.* Vol.116,C09034.

J. Black Sea/Mediterranean Environment
Special Issue: 78-83 (2015)

Late Pleistocene-Holocene climate transition in the western Mediterranean: a view from the stable isotopes of land snail shells

André Carlo Colonese[1*], Giovanni Zanchetta[2,3,4], Anthony E. Fallick[5], Russell Drysdale[6]

[1] BioArCh, Department of Archaeology, University of York, Biology S. Block, York YO10 5DD, UK
[2] Dipartimento di Scienze della Terra, University of Pisa, Via S. Maria, 53, 56126 Pisa, ITALY
[3] IGG-CNR Via Moruzzi, 1 56100 Pisa, ITALY
[4] INGV sez. Pisa, Via della Faggiola 32, 56126 Pisa, ITALY
[5] Scottish Universities Environmental Research Centre, East Kilbride G75 0QF, Glasgow, SCOTLAND
[6] Department of Resource Management and Geography, University of Melbourne, Victoria 3010, AUSTRALIA

[*]**Corresponding author:** andre.colonese@york.ac.uk

Abstract

Late Pleistocene and Holocene archaeological deposits from the central Mediterranean regions contain abundant terrestrial gastropod shell remains. Stable isotope studies of their shell carbonate are valuable proxies for various aspects of climate and environmental change such as temperature, hydrological sources and balance, as well as vegetation. Here we present stable carbon and oxygen isotope data of snail shells from several archaeological deposits in the western Mediterranean (Iberian, Italian Peninsula and Sicily). Isotope ratios differ remarkably between the Late Pleistocene, Holocene and modern shells. The results can be interpreted in terms of hydrological variations and changes in vegetation over time. Fossil shells offer the opportunity to examine the effects of past climate change on local and regional environments.

Keywords: Western Mediterranean, archaeological record, land snail shells, stable isotopes, palaeoclimate, palaeoenvironment

Introduction

Late Pleistocene - Holocene archaeological deposits around the Mediterranean have preserved numerous shells of land snails and offer the exceptional opportunity to explore shell isotopic response to late Quaternary climate change. Land snails are sensitive to environmental conditions and the stable isotopes (oxygen and carbon) composition of their shells are valuable sources for

reconstructing local hydrological balance and vegetation cover. Shell $\delta^{18}O$ has been related to atmospheric conditions, and in particular to the oxygen isotope ratio of precipitation, relative humidity and temperature (Balakrishnan and Yapp 2004). However, the imprinting of atmospheric conditions on the shell oxygen isotope ratio is not straightforward and it is shown as distinctive regional relations (e.g. Zanchetta *et al*. 2005). Shell $\delta^{13}C$ is mainly a function of respired CO_2 from the diet, which for most of the species means vegetation (e.g. Stott 2002). Shell $\delta^{13}C$ thus reflects vegetation type (e.g. C3, C4), but also species-specific feeding behaviour (calciophilous) and potentially the effect of environmental conditions on the plants carbon isotope fractionation.

Here we analyse the stable carbon and oxygen isotope of shells from several archaeological sites of the Iberian and Italian Peninsula and Sicily (Figure 1; Table 1). Through a comprehensive compilation of previously published data (n = 854) we explore shell isotope variations between the Late Pleistocene (~14.5 to 10.7 ka cal BP) and the early-late Holocene (~10.7 to 2.5 ka cal BP) and discuss their implications to understand millennia-scale changes in hydrological conditions and vegetation dynamics. This work also aims at stimulating research efforts to complement the land snail archive with other environmental proxies from multiple sites (speleothems, lake cores etc.).

Table 1. Archaeological sites reported in Figure 1

Site	^{14}C age (ka cal BP)	Reference
1 - Los Castillejos	~7.2 – 4.0	Yanes *et al.* 2011
2 - Marroquíes	~4.1	Yanes *et al*. 2013a
3 - Arena de la Virgen and Casa Corona	~8.5 – 12.2	Yanes *et al.* 2013b
4 - Bauma del Serrat del Pont	~2.5 – 9.0	Colonese *et al*. 2013
5 - Grotta di Latronico 3	~7.8 – 8.8	Colonese *et al*. 2010a
6 - Grotta del Romito	~13.0 – 14.5	Colonese *et al*. 2007
7 - Grotta della Serratura	~7.2 – 12.1	Colonese *et al.* 2010b
8 - Grotta d'Oriente	~7.8 – 14.2	Colonese *et al*. 2011

Materials and Methods

Archaeological and modern shell values are compared at the regional scale. The comparison also includes modern shell isotope data from Italian Peninsula and Sicily (e.g. Zanchetta *et al.* 2005; Colonese *et al.* 2014) not associated with archaeological sites (Figure 2A). Variations in shell isotope composition are also analysed on a site-by-site basis by correcting archaeological values for the modern average shell isotope data at each site ($\Delta\delta$ = archaeological-modern; Figure 2B).

Results and discussion

Early to late Holocene shells in general are depleted in ^{18}O and ^{13}C compared to Late Pleistocene and modern counterparts. By contrast Late Pleistocene shells

fall within the range of isotope values of modern specimens from the western Mediterranean (Figure 2A). Δδ adjusts values for site-specific environmental condition (e.g. elevation, $\delta^{18}O$ of rainfall, temperature) and species-specific

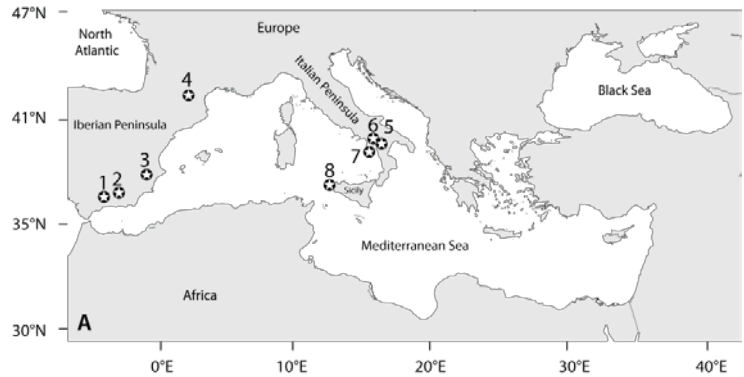

Figure 1. Study area showing the location of the archaeological sites (Table 1)

feeding behaviour (i.e. $\delta^{13}C$). Late Pleistocene $\delta^{18}O$ and $\delta^{13}C$ are similar to higher than modern counterparts (up to 4‰ and 2‰ for $\delta^{13}C$ and $\delta^{18}O$ respectively), whilst Holocene $\delta^{18}O$ and $\delta^{13}C$ values are variably lower (up to 6‰ in both $\delta^{18}O$ and $\delta^{13}C$). $\Delta\delta^{18}O$ and $\Delta\delta^{13}C$ values are positively moderately correlated ($r = 0.63$; $R^2 = 0.40$; Figure 2B), implying a major mechanism that is driving changes in both $\delta^{18}O$ and $\delta^{13}C$ values over time. Variations between dry and wet conditions would explain the $\delta^{18}O$ and $\delta^{13}C$ values between the Late Pleistocene and Holocene. Higher $\delta^{18}O$ and $\delta^{13}C$ values in the Late Pleistocene generally reflect a negative water balance, which in turn increases the $\delta^{18}O$ values of rainfall (Bard *et al.* 2002) and the $\delta^{13}C$ of vegetation (e.g. Khon 2010). However other factors are likely to be involved as $\delta^{18}O$ changes in the source of precipitation.

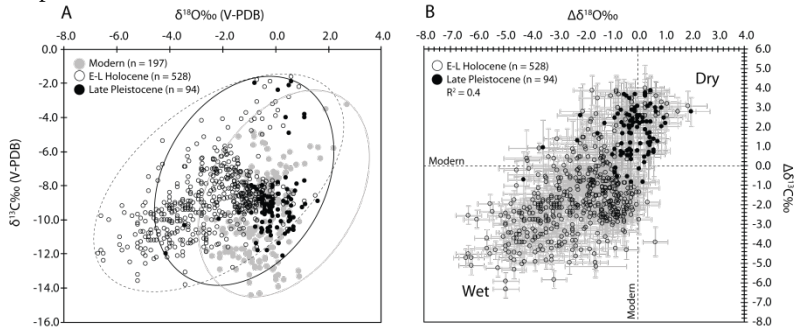

Figure 2. A) Shell $\delta^{18}O$ and $\delta^{13}C$ distribution in Late Pleistocene, early to late Holocene and modern snails. B) Corrected shell $\delta^{18}O$ and $\delta^{13}C$ values between archaeological and modern counterparts for each site. Δδ value of 0‰ means no difference between archaeological and modern shells.

Shells are remarkably depleted in ^{18}O and ^{13}C during the Holocene in response to positive hydrological balance (and decreased evaporation) and dilution of the western Mediterranean Sea (source of precipitation), as well as taxonomic and isotopic changes in vegetation. Holocene $\delta^{18}O$ in are in broad agreement with palaeohydrological scenarios provided by pollen records from Iberian Peninsula, lake records from SW and N Mediterranean regions, speleothems in NW Italian Peninsula at the time of decreasing summer insolation maxima in the N Hemisphere (e.g. Pérez-Obiol *et al.* 2011; Zanchetta *et al.* 2013).

The results emphasize the validity of $\delta^{18}O$ and $\delta^{13}C$ signatures in fossil snail shells from archaeological records as complementary information for the study of past climate and environmental conditions. Furthermore, stable isotope composition of fossil shells can assist the translation of complex and large-scale climate conditions into local-regional opportunity and limits to human societies.

Acknowledgement

The authors wish to thank T. Donnelly, J. Dougans, A. Tait, E. Rigattiere, I. Baneschi, N. Hausmann, F. Serchisu, H. Hobson. This work is partially funded by the University of Pisa (ex 60% G. Zanchetta) and the Society of Antiquaries of London (http://www.sal.org.uk/).

References

Balakrishnan, M., Yapp, C.J. (2004) Flux balance model for the oxygen and carbon isotope compositions of land snail shells. *Geochimica et Cosmochimica Acta* 68: 2007-2024.

Bard, E., Delaygue, G., Rostek, F., Antonioli, F., Silenzi, S., Schrag, D. (2002) Hydrological conditions over the western Mediterranean basin during the deposition of the cold Sapropel 6 (ca. 175 ka BP). *Earth and Planetary Science Letters* 202: 481–494.

Colonese, A.C., Zanchetta, G., Dotsika, E., Drysdale, R.N., Fallick, A.E., Grifoni Cremonesi, R., Manganelli, G. (2010a). Early Holocene land snail shell stable isotope record from Grotta di Latronico 3 (Southern Italy). *Journal of Quaternary Science* 25 (8): 1347-1359.

Colonese, A.C., Zanchetta, G., Drysdale, R.N., Fallick, A.E., Manganelli, G., Lo Vetro, D., Martini, F., Di Giuseppe, Z. (2011) Stable isotope composition of Late Pleistocene-Holocene *Eobania vermiculata* (Müller, 1774) (Pulmonata, Stylommatophora) shells from the Central Mediterranean basin: data from Grotta d'Oriente (Favignana, Sicily). *Quaternary International* 244: 76-87.

Colonese, A.C., Zanchetta, G., Fallick, A.E., Manganelli, G., Lo Cascio, P., Hausmann, N., Baneschi, I., Regattieri, E. (2014) Oxygen and carbon isotopic

composition of modern terrestrial gastropod shells from Lipari Island, Aeolian Archipelago (Sicily). *Palaeogeography, Palaeoclimatology, Palaeoecology* 394: 119–127.

Colonese, A.C., Zanchetta, G., Fallick, A.E., Manganelli, G., Saña, M., Alcade, G., Nebot, J. (2013) Holocene snail shell isotopic record of millennial-scale hydrological conditions in western Mediterranean: Data from Bauma del Serrat del Pont (NE Iberian Peninsula). *Quaternary International* 303: 43-53.

Colonese, A.C., Zanchetta, G., Fallick, A.E., Martini, F., Manganelli, G., Drysdale, R.N. (2010b). Stable isotope composition of *Helix ligata* (Müller, 1774) from Late PleistoceneeHolocene archaeological record from Grotta della Serratura (Southern Italy): palaeoclimatic implications. *Global and Planetary Change* 71: 249-257.

Colonese, A.C., Zanchetta, G., Fallick, A.E., Martini, F., Manganelli, G., Lo Vetro, D. (2007) Stable isotope composition of Late Glacial land snail shells from Grotta del Romito (Southern Italy): palaeoclimatic implications. *Palaeogeography, Palaeoclimatology, Palaeoecology* 254 (3-4): 550-560.

Kohn, M.J. (2010) Carbon isotope compositions of terrestrial C3 plants as indicators of (paleo)ecology and (paleo)climate. *Proceedings of the National Academy of Sciences* 107 (46) 19691-19695.

Pérez-Obiol, R., Jalut, G., Julià, R., Pèlachs, A., Iriarte, M.J., Otto, T., Hernández-Beloqui, B. (2011) Mid-Holocene vegetation and climatic history of the Iberian Peninsula. *The Holocene* 21 (1): 75-93.

Stott, L.D. (2002) The influence of diet on the $\delta^{13}C$ of shell carbon in the pulmonate snail *Helix aspersa*. *Earth and Planetary Science Letters* 195: 249-259.

Yanes, Y., Gómez-Puche, M., Esquembre-Bebia, M.A., Fernández-López-de-Pablo, J. (2013b) Younger Dryas-early Holocene transition in the south-eastern Iberian Peninsula: insights from land snail shell middens. *Journal of Quaternary Science* 28 (8): 777-788.

Yanes, Y., Riquelme, J.A., Cámara, J.A., Delgado, A. (2013a) Stable isotope composition of middle to late Holocene land snail shells from the Marroquíes archeological site (Jaén, southern Spain): paleoenvironmental implications. *Quaternary International* 302: 77-87.

Yanes, Y., Romanek, C.S., Molina, F., Cámara, J., Delgado, A. (2011) Holocene paleoenvironment (~7200-4000 cal BP) of the Los Castillejos

archaeological site (SE Spain) inferred from the stable isotopes of land snail shells. *Quaternary International* 244: 67-75.

Zanchetta, G., Bini, M., Cremaschi, M., Magny, M., Sadori, L. (2013) The transition from natural to anthropogenic-dominated environmental change in Italy and the surrounding regions since the Neolithic: an introduction. *Quaternary International* 303: 1-9.

Zanchetta, G., Leone, G., Fallick, A.E., Bonadonna, F.P. (2005) Oxygen isotope composition of living land snail shells: data from Italy. *Palaeogeography, Palaeoclimatology, Palaeoecology* 223: 20-33.

J. Black Sea/Mediterranean Environment
Special Issue: 84-88 (2015)

A 600 year-long drought index for central Anatolia

Hakan Yiğitbaşıoğlu[1], Jonathan R. Dean[2], Warren J. Eastwood[3], Neil Roberts[4*], Matthew D. Jones[5], Melanie J. Leng[2,5]

[1] Department of Geography, Ankara University, Ankara, TURKEY
[2] NERC Isotope Geosciences Facilities, British Geological Survey, Nottingham NG12 5GG UK
[3] School of Geography, Earth and Environmental Sciences, University of Birmingham, Birmingham B15 2TT UK
[4] School of Geography, Earth and Environmental Sciences, University of Plymouth PL4 8AA UK
[5] Centre for Environmental Geochemistry, School of Geography, University of Nottingham, University Park, Nottingham NG7 2RD UK

[*]**Corresponding author:** cnroberts@plymouth.ac.uk

Abstract

We have used sediments from Nar lake in central Turkey to reconstruct climatic variability over timescales longer than can be obtained from direct meteorological observations. Because the sediments of this lake are annually layered and precisely dated, it has been possible to calibrate sedimentary climate proxies against meteorological records to derive a drought index; this has then been applied to time periods before instrumental data are available. In this study, $\delta^{18}O$ from Nar lake carbonates have been used to generate a decadal average P/E index for central Anatolia, which highlights major drought events since 1400 AD.

Keywords: Anatolia, lake sediments, varves, calibration, Little Ice Age, oxygen isotopes

Introduction

In the context of a changing global climate, it is important to understand Mediterranean hydro-climatic variability over timescales longer than those that can be obtained from direct monitoring and observations (i.e. >100 years). The long-term frequency, duration and intensity of drought periods are especially significant for rain-fed agriculture, water supply, and other key human needs. Our objective in this study is a reconstruction of hydro-climatic conditions for the last 600 years for central Anatolia, one of the driest regions of Turkey and consequently especially sensitive to hydro-climatic variations. We have used the oxygen isotope composition ($\delta^{18}O$) of individual carbonate layers from Nar Gölü, a small volcanic lake whose sediments are annually laminated, or varved. Analysis of historical meteorological data suggests that climatic trends at this

site are likely to be representative of the central Anatolian climate region (Türkeş *et al*. 2009) (Figure 1).

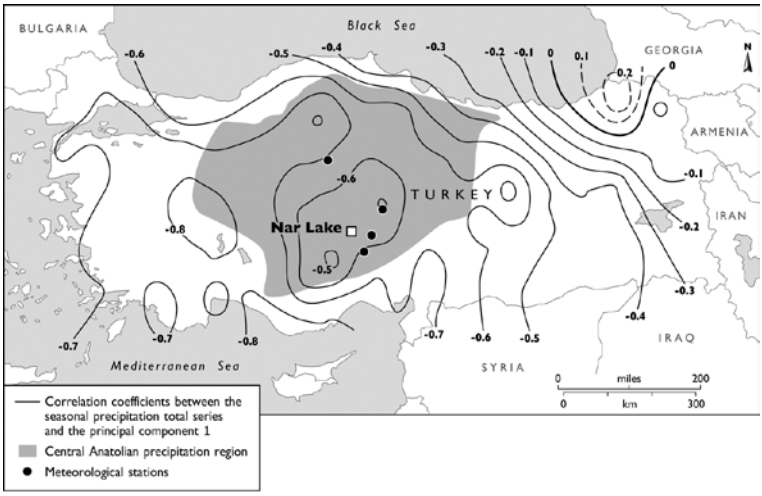

Figure 1. Spatial correlations in winter precipitation for Turkey 1953-2002 (see Türkeş *et al.* 2009 for detailed explanation. PC1 explains 46.5% of variance)

Central and western Anatolia shows good coherency in the pattern of precipitation (Pearson's correlation coefficients r ≥0.5). The Central Anatolian precipitation region is shown along with the location of the Nar lake study site and meteorological stations used for P/E index calibration.

Materials and methods

We have calibrated $\delta^{18}O$ of carbonates from individual Nar lake varves against temperature, precipitation, etc. for four central Anatolian meteorological stations for the last ~70 years (Ankara, Nevşehir, Derinkuyu, Niğde) to derive a regional drought index; viz. Precipitation/Evaporation (or P/E). Because of the multi-year residence time of the Nar lake water, sedimentary proxy data represent an 8-year average of lake water balance (Jones *et al.* 2005). They therefore allow past droughts of decadal or longer duration to be identified, but year-to-year weather variations are less clear.

We have used 1940-1976 as the reference period for this "calibration in time" approach. After 1980, shifts in the lake system, marked by a change in carbonate mineralogy between aragonite and calcite, altered isotopic balance in the lake, and complicate any linear calibration. For the calibration period there is an R^2 correlation of 0.76 between $\delta^{18}O$ in lake sediments and the 8-year running mean index for P/E. We have confirmed this relationship by annual

monitoring of Nar lake since 1998, a time period which has included a fall in lake level, increase in salinity and rise in $\delta^{18}O$ (Dean *et al.* in press).

Results

Our P/E calibration has been applied to $\delta^{18}O$ on individual carbonate laminae from long lake sediment cores from Nar lake (Figure 2). Although this Late Holocene record extends back to ~300 AD, we focus here on drought events during the Little Ice Age and modern times (1400-1980 AD), for which the lake carbonate mineralogy is mono-specific (i.e. aragonite) and we are confident of the linear relationship between $\delta^{18}O$ and climate.

Overall, the Little Ice Age in Anatolia was a period of relatively dry climate, compared to the preceding Medieval times and to the late 20th century. Within it, there were extended phases of drier than average climate during the 15th century (1410-1495 AD), in the 19th century (1810-1900 AD), and also in the mid-20th century (1920-1965 AD), including a number of important drought years during the 1930s. The 16th and 17th centuries were notable for the lack of major dry events, an exception being a severe drought at the end of the 16th century which is registered in Anatolian tree ring widths (Kuniholm 1990; Touchan *et al.*, 2007) as well as in the Nar isotope record (Roberts *et al.* 2012). The historical links between this late 16th-century drought and the Ottoman Celâli rebellion have been studied in detail by White (2011, chapters 6 and 7).

There is no clear relationship between the time interval between droughts and drought severity. Some dry phases included multiple events, for example, there were drought peaks in the 1850s, late 1860s-1870s (which led to the death of 81% of cattle, 97% of sheep, and almost 40% of the human population in Ankara province; Kuniholm 1990) and again in the late 1880s.

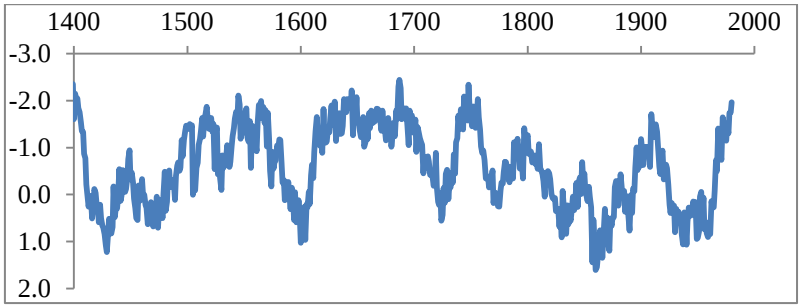

Figure 2. Oxygen isotope values for individual carbonate laminae from Nar Lake cores (1400-1980 AD). Data taken from Jones *et al.* (2006). More positive isotopes indicate dry climatic conditions, more negative values indicate a wetter climate.

Discussion

Because of their annual chronology, it is possible with lake varves (in a similar way to tree rings) to calibrate climate proxies against meteorological records to derive a drought index which can be applied to time periods before instrumental data become available. In this study, $\delta^{18}O$ from lake carbonates have been used to generate a decadal average P/E index for central Anatolia, which highlights major drought events since 1400 AD. This provides a long-term context for understanding future hydro-climatic changes in the eastern Mediterranean region.

Acknowledgements

This project has been supported by the British Institute in Ankara (Climate History thematic programme) and by the NERC Isotope Geoscience Facilities Steering Committee.

References

Dean, J., Eastwood, W.J., Roberts, N., Jones, M.D., Yiğitbaşıoğlu, H., Allcock, S.L., Woodbridge, J., Metcalfe, S.E., Leng, M.J. Tracking the hydro-climatic signal from lake to sediment: a field study from central Turkey, *J. Hydrol*. (in press)

Jones, M.D., Leng, M.J., Roberts, C.N., Türkeş, M., Moyeed, R. (2005) A coupled calibration and modelling approach to the understanding of dry-land lake oxygen isotope records. *J. Paleolimnol*. 34: 391-411.

Jones, M.D., Roberts, C.N., Leng, M.J., Türkeş, M. (2006) A high-resolution late Holocene lake isotope record from Turkey and links to North Atlantic and monsoon climate. *Geology* 34: 361-364.

Kuniholm, P.I. (1990) Archaeological evidence and non-evidence for climate change. *Phil. Trans. R. Soc. Lond.* 330:645-655.

Roberts, N., Moreno, A., Valero-Garcés, B.L., Corella, J.P., Jones, M., Allcock, S., Woodbridge, J., Morellón, M., Luterbacher, J., Xoplaki, E., Türkeş, M. (2012) Palaeolimnological evidence for an east-west climate see-saw in the Mediterranean since AD 900. *Global and Planetary Change* 84-85: 23–34.

Touchan, R., Akkemik, Ü., Hughes, M.K., Erkan, N. (2007) May-June precipitation reconstruction of south-western Anatolia, Turkey during the last 900 years from tree rings. *Quaternary Research* 68: 196-202.

Türkeş, M., Koç, T., Sarış, F. (2009) Spatiotemporal variability of precipitation total series over Turkey. *Int. J. Climatol.* 29: 1056–1074.

White, S. (2011) The Climate of Rebellion in the Early Modern Ottoman Empire. Cambridge University Press. 345 pp.

J. Black Sea/Mediterranean Environment
Special Issue: 89-92 (2015)

Modeling of near future air temperature and precipitation climatology of Turkey and surrounding regions

M. Tufan Turp[1,2]*, Tuğba Öztürk[2,3,5], Murat Türkeş[2,4], M. Levent Kurnaz[2,3]

[1] Department of Environmental Sciences, Institute of Environmental Sciences, Boğaziçi University, 34342, İstanbul, TURKEY
[2] Climate Change and Policies Research Center, Boğaziçi University, 34342, İstanbul, TURKEY
[3] Department of Physics, Faculty of Science and Arts, Boğaziçi University, 34342, İstanbul, TURKEY
[4] Affiliated Faculty at the Department of Statistics, Middle East Technical University (METU), 06800, Ankara, TURKEY
[5] Department of Physics, Faculty of Science and Arts, Işık University, 34980, İstanbul, TURKEY

*Corresponding author: tufan.turp@boun.edu.tr

Abstract

Projected future changes in mean air temperature and precipitation for 2020 – 2050 were assessed with respect to the control period 1970 – 2000 via regional climate model simulations, using a regional climate model driven by three different global climate models, dynamically downscaled to 50 km for Turkey and surrounding regions, using the IPCC emission scenario outputs of global climate models.

Keywords: Turkey, climate change, regional climate model

Introduction

Estimating future climatic conditions is crucial for the Mediterranean region including Turkey, a region most sensitive to impacts of climate change (Öztürk *et al.* 2013; Önol and Semazzi 2009; Şen *et al.* 2012; Trigo *et al.* 2006; Türkeş *et al.* 2011; Türkeş 2012).

Materials and Methods

Expected changes in air temperature and precipitation were assessed for the region surrounding Turkey for the period 2020-2050 with respect to the control period 1970-2000. The output of the Regional Climate Model (RegCM4.3.5) of ICTP (International Centre for Theoretical Physics) was used to analyze future

projections with respect to simulated present climate conditions. HadGEM2 global climate model of the Met Office Hadley Centre, MPI-ESM-MR of the Max Planck Institute for Meteorology, GFDL-ESM2M of the National Oceanic and Atmospheric Administration Geophysical Fluid Dynamics Laboratory were downscaled to 50 km for Turkey and surrounding regions by using the regional climate model (Taylor *et al.* 2012). Two emission scenarios were considered in this study: the high-emission scenario RCP8.5 and the mid-range mitigation emission scenario RCP4.5 of the IPCC. To validate model performance, mean air temperature and precipitation obtained from the regional climate model forced by the above global circulation models were compared with the observational datasets of the Climatic Research Unit (CRU) for the reference period of 1970-2000. For parameterization, best agreement with observational data was obtained by using the Grell scheme with the Fritsch-Chappell type closure.

Results

Even though the model outputs show warm and/or cold biases for the different seasons, the magnitude of the biases is low and results can be accepted as reasonable and reliable when the domain's geographical and climatic features were taken into account (Figure 1).

Based on spatial mean biases with respect to the CRU dataset, HadGEM2 displays better performance amongst the three global circulation models. According to the different model and scenario results, an increase between 0.5 °C and 4 °C in seasonal mean air temperatures of Turkey is expected for the period of 2020 – 2050 with respect to the period of 1970-2000. This warming will be more severe in warm than in cold seasons. We only present mean air temperature for 2020 – 2050 with respect to 1970-2000 according to the RCP 8.5 scenario outputs of global climate model HadGEM2 (Figure 2). Seasonal mean of total precipitation is expected to decrease by -0.4 mm/day and -2 mm/day. Increases in precipitation are expected at coastlines of the region especially in the winter season.

Discussion

In accordance with the different model outputs, it is obvious that in the near future Turkey will be exposed to the warmer and drier climate conditions compared to that in the reference period and Turkey is in the group of most vulnerable countries to climate change. These results are of crucial importance mostly in terms of hydrological systems, forestry and agricultural production, among others.

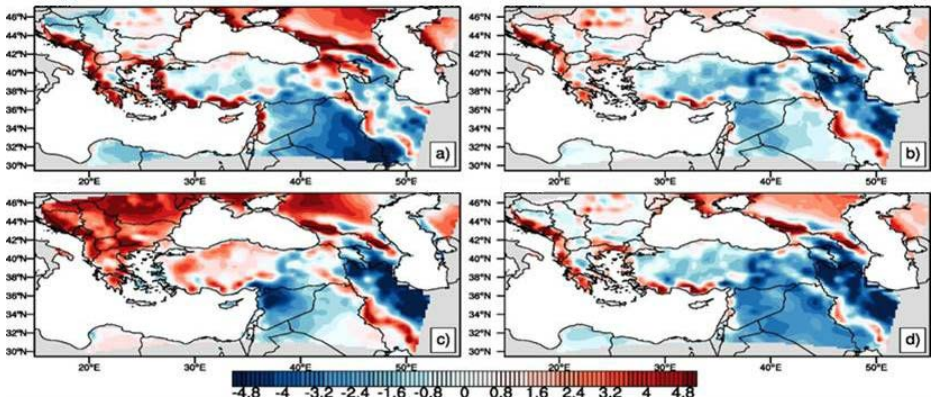

Figure 1. Comparison of the seasonal air temperatures of the RegCM4.3.5, which is forced by the HadGEM2, with respect to CRU dataset for the period 1970 - 2000: (a) winter, (b) spring, (c) summer and (d) autumn

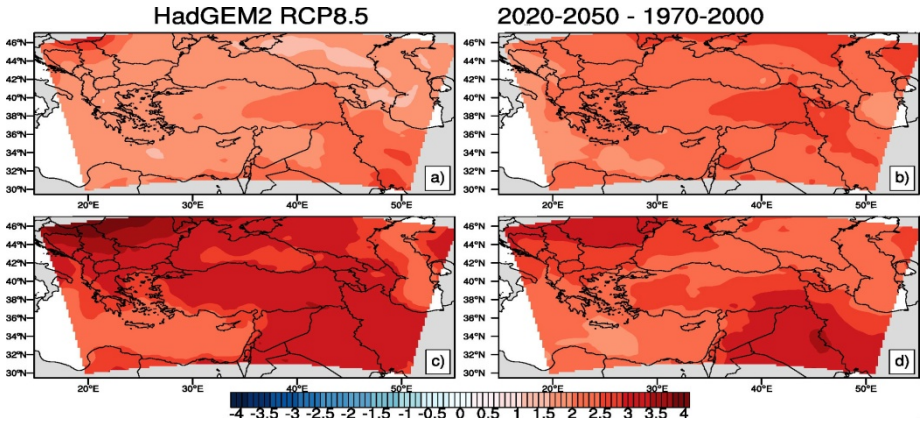

Figure 2. Geographical distribution patterns of changes in projected mean air temperatures over Turkey and surrounding regions from the RegCM4.3.5, which is forced by the HadGEM2 with RCP8.5 scenario for the climatology of 2020 - 2050 period with respect to 1970 - 2000: (a) winter, (b) spring, (c) summer and (d) autumn seasons

Acknowledgements

This study was supported by BAP 7362.

References

Önol, B., Semazzi, F.H.M. (2009) Regionalization of climate change simulations over the Eastern Mediterranean. *Journal of Climate* 22: 1944-1960.

Öztürk, T., Türkeş, M., Kurnaz, M.L. (2013) Projected changes in air temperature and precipitation climatology in Turkey by using RegCM4.3. *In:* Proceedings of European Geosciences Union General Assembly 2013, April 2013: Vienna. pp 07–12.

Şen, B., Topçu, S., Türkeş, M., Şen, B.,Warner, J.F. (2012) Projecting climate change, drought conditions and crop productivity in Turkey. *Climate Research* 52: 175–191.

Taylor, Karl E., Stouffer, R.J., Meehl, G.A. (2012) An overview of CMIP5 and the experiment design. *Bulletin of the American Meteorological Society* 93(4): 485–498.

Trigo, R., Xoplaki, E., Zorita, E., Luterbacher, J., Krichak, S., Alpert, P., Jacobeit, J., Saenz, J., Fernandez, J., Gonzalez-Rouco, F., Garcia-Herrera, R., Rodo, X., Brunetti, M., Nanni, T., Maugeri, M., Türkeş, M., Gimeno, L., Ribera, P., Brunet, M., Trigo, I., Crepon, M., Mariotti, A. (2006) Relations between variability in the Mediterranean region and mid-latitude variability. In: Mediterranean Climate Variability (eds., P., Lionello, P., Malanotte-Rizzoli, R., Boscolo), Elsevier Developments in Earth & Environmental Sciences 4: Amsterdam, pp.179-226.

Türkeş, M. (2012) Global Climate Change and Desertification, In: Current Global Problems- An Interdisciplinary Approach (ed., N. Özgen). Eğiten Kitap, Ankara, pp.1-42. (in Turkish).

Türkeş, M., Kurnaz, M.L., Öztürk, T., Altınsoy, H. (2011) Climate changes versus 'security and peace' in the Mediterranean macro climate region: are they correlated? In: Proceedings of International Human Security Conference on Human Security: New Challenges, New Perspectives, CPRS Turkey, 27-28 October 2011: İstanbul, pp. 625-639.

J. Black Sea/Mediterranean Environment
Special Issue: 93-96 (2015)

Assessment of projected changes in air temperature and precipitation over the Mediterranean region via multi-model ensemble mean of CMIP5 models

M. Tufan Turp[1,2*], Tugba Öztürk[2,3,5], Murat Türkeş[2,4], M. Levent Kurnaz[2,3]

[1] Department of Environmental Sciences, Institute of Environmental Sciences, Bogazici University, 34342, Istanbul, TURKEY
[2] Climate Change and Policies Research Center, Bogazici University, 34342, Istanbul, TURKEY
[3] Department of Physics, Faculty of Science and Arts, Bogazici University, 34342, Istanbul, TURKEY
[4] Affiliated Faculty at the Department of Statistics, Middle East Technical University (METU), 06800, Ankara, TURKEY
[5] Department of Physics, Faculty of Science and Arts, Isik University, 34980, Istanbul, TURKEY

[*]**Corresponding author:** tufan.turp@boun.edu.tr

Abstract

A multi-model ensemble mean approach was followed in order to investigate the projected changes in near surface air temperatures and precipitation total over the Mediterranean region. Among sixty seven different models of thirty modeling groups all around the world participating in the World Climate Research Programme (WCRP) Coupled Model Intercomparison Project (CMIP5), fourteen models were used. In this respect, we focused on two distinct scenarios (i.e. RCP4.5 and RCP8.5) for three different future periods (i.e. 2016-2035, 2046-2065 and 2081-2100) to examine accurately the foreseen changes in two fundamental climate variables (near surface air temperature and precipitation total) for the Mediterranean region.

Keywords: Mediterranean, climate change, CMIP5, ensemble mean

Introduction

Harmful impacts of climate change have been becoming more severe on different spatial and temporal scales in this century. The results of climate change and variability studies for the Mediterranean basin indicate that Mediterranean basin will be affected adversely by climate change in the future (Giorgi and Lionello 2008; Lelieveld *et al.* 2012; Ozturk *et al.* 2014; Türkeş *et al.* 2011). Because of the importance of the region and its vulnerability to global climate change, the studies including the investigation of projected changes in

the climate of Mediterranean basin play a crucial role in order to struggle with the negative effects of climate change.

Materials and Methods

The projected changes in air temperature and precipitation over the Mediterranean region are examined based on the multi-model ensemble mean of the Coupled Model Intercomparison Project Phase 5 (CMIP5) historical, RCP4.5 and RCP8.5 experiments with 14 different coupled global climate models (GCMs) (Taylor *et al.* 2012). The models used in this study are ACCESS1.0, ACCESS1.3, CMCC-CMS, CNRM-CM5, EC-EARTH, HadGEM2-AO, HadGEM2-CC, HadGEM2-ES, MIROC-ESM, MIROC-ESM-CHEM, MPI-ESM-MR, MPI-ESM-LR, MRI-CGCM3, CMMC-CM. Among the studied models, the CMCC-CM has the highest resolution. So, model outputs interpolated bilinearly 0.75 degree grid resolution. In the 14 models used in this study, CMMC-CM's horizontal resolution was the highest, hence we interpolated all the models to the highest resolution available. Firstly, to detect biases in the data, we calculated the temperature difference (and precipitation ratio) between the observational dataset from the Climatic Research Unit (CRU) for the reference time period (1981-2000) and the outputs of each model and the ensemble averages of them. Thereafter the projections of each model and their ensemble means were computed using delta bias correction method for near- (2016-2035), mid- (2046-2065), and long-term (2081-2100), respectively.

Results

With regard to multi-model ensemble mean, a mainly cold bias was found for the southern parts of the study region (North Africa - Levant) and a warm bias characterizes the Caucasus and Alpine areas. Besides, for precipitation overestimated results for winter and spring over North Africa, the Central Anatolia region of Turkey, and Western Spain were seen. Seasonal projected changes obtained by the GCM ensembles are given in Figure 1. In average, more dry seasons in all three future periods for both scenarios (up to 0.18 mm/day) were found with the exception of the Caucasus region on winter for the mid- and far future periods. Generally, temperature is expected to increase in all seasons and projections (between 1.1 and 6.2 °C). Temperature rise was found particularly strong in the summer season.

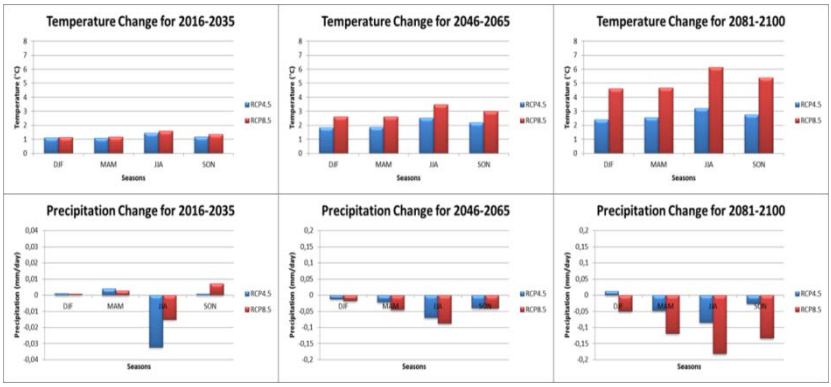

Figure 1. Projected temperature and precipitation changes for three different future periods based on two different scenarios by GCM ensembles. DJF, MAM, JJA and SON denote winter, spring, summer and autumn, respectively.

Discussion

The results briefly shown above indicate that the Mediterranean region is expected to experience warmer and drier climate conditions in the near to far future study periods. Since the Mediterranean basin already has a semi-arid, semi-humid with strong and long summer dryness climate, any decrease in precipitation strongly affects the region. One should also consider the adverse effects on hydrology, ecosystems among others. Therefore especially the changes in the rainy season have stronger impacts. Furthermore, hotter and drier conditions might enhance the desertification processes which can also stimulate the erosion, salinization and forest fires.

Acknowledgements

This study was supported by BAP 7362.

References

Giorgi, F., Lionello, P. (2008) Climate change projections for the mediterranean region. *Global and Planetary Change* 63: 90-104.

Lelieveld, J., Hadjinicolaou, P., Kostopoulou, E., Chenoweth, J., Giannakopoulos, C., Hannides, C., Lange, M.A., El Maayar, M., Tanarthe, M., Tyrlis, E., Xoplaki, E. (2012) Climate change and impacts in the eastern Mediterranean and the Middle East. *Climatic Change* 114: 667-687.

Ozturk, T., Türkeş, M., Kurnaz, M.L. (2014) Analysing projected changes in future air temperature and precipitation climatology of Turkey by using

RegCM4.3.5 climate simulations. *Aegean Geographical Journal* 20(1): 17-27 (in Turkish with an English abstract, figure and table captions).

Taylor, Karl E., Stouffer, R.J., Meehl, G.A. (2012) An overview of CMIP5 and the experiment design. *Bulletin of the American Meteorological Society* 93: 485-498.

Türkeş, M., Kurnaz, M.L., Öztürk, T., Altınsoy, H. (2011) Climate changes versus 'security and peace' in the Mediterranean macro climate region: are they correlated? In: Proceedings of International Human Security Conference on Human Security: New Challenges, New Perspectives, CPRS Turkey, 27-28 October 2011: İstanbul, pp. 625-639.

J. Black Sea/Mediterranean Environment
Special Issue: 97-103 (2015)

Changing climate: a great challenge for Turkey

Ömer Lütfi Şen[1*], Ozan Mert Göktürk[1], Deniz Bozkurt[2]

[1]Eurasia Institute of Earth Sciences, Istanbul Technical University, Istanbul, TURKEY
[2]Department of Geophysics, Center for Climate and Resilience Research, University of Chile, Santiago,CHILE

[*]**Corresponding author:** senomer@itu.edu.tr

Abstract

Turkey lies in a region that is highly vulnerable to climate change, and the indicators show that climate is changing in Turkey. The station observations show that temperatures are increasing throughout the country. Summer temperatures increase more than those of the other seasons. There are significant shifts in the timing of the snowfed river discharges, which indicates that snow melts earlier in response to the elevated temperatures. No significant coherent change has yet been detected in precipitation observations. Future climate change projections agree on an increase in temperatures throughout the country and a reduction in precipitation in the southern half of the country. There is no doubt that these changes will impact the country's water resources negatively by reducing the water potentials in the southern basins. The projections that were based on the high emissions scenarios indicate water potential reductions up to 37% in the Mediterranean basins, up to 70% in Konya basin and up to 10% in the Euphrates and Tigris basins by the mid twenty first century. The decline in the water resources has the potential to influence the agriculture, energy and tourism that are significant sectors in Turkey.

Keywords: Turkey, climate change, water resources, agriculture, energy, tourism

Introduction

Observations indicate that the Earth's climate has been changing as a result of human activities (IPCC 2013). Most visibly, the air is getting warmer (close to 1 °C since 1900), the land and sea ice are melting, and consequently the sea level is rising (about 19 cm since the beginning of twentieth century). Climate change projections suggest that these changes will continue throughout the twenty first century.

Turkey is located in the eastern parts of the Mediterranean Basin, which is identified as one of the most vulnerable regions to the future climate change by the recent Assessment Reports (AR4 and AR5) of IPCC (IPCC 2007; IPCC 2013). The General Circulation Model (GCM) simulations largely agree on a basin-wide precipitation reduction in the Mediterranean Basin (IPCC 2007;

IPCC 2013). Some studies (e.g., Giorgi and Lionello 2008) suggest that the Atlantic cyclone tracks will shift northward as a result of the strengthening of the subtropical high over the Mediterranean region. This change is expected to increase the precipitation in the Black Sea basin, while decreasing it in the Mediterranean basin. Based on the A2 scenario simulation of NASA's fvGCM model, Önol and Semazzi (2009) investigated the future climate change over the eastern Mediterranean for the last 30 years of the 21st century. They reported drying for the Mediterranean and Aegean coastal regions of Turkey, while wetting for the Black Sea coastal areas. Hemming *et al.* (2010) pointed out that magnitude of precipitation decrease (5-25%) for all the model ensembles is highly consistent in western coasts of Turkey during the first-half of the 21st century. Önol *et al.* (2014) reported the most comprehensive climate change study for Turkey using several model-scenario combinations, and their results also confirm the finding of the previous studies that the precipitation will decrease in the southern half of Turkey in response to climate change.

The present study, by compiling and analysing the available data, provides an integrated picture of climate change (both historical and future) in Turkey and its effects on Turkey's water resources. It also discusses how primary sectors, including agriculture, energy and tourism, could be affected by these changes.

Study area and data

Turkey is a Eurasian country, lying between the latitudes 36° and 42° N and longitudes 26° and 45° E. Anatolian Peninsula consists of much of the territory in the Asian side. It is surrounded by seas on three sides: Black Sea to the north, Aegean Sea to the west, and Mediterranean Sea to the south. Turkey has a fairly mountainous landscape. It consists of a high central plateau that lies between two mountain ranges: the Pontic Mountain range to the north and Taurus Mountains to the south. The average elevation of Turkey is about 1000 metres. The elevation increases eastward. Highlands of eastern Turkey comprise the headwaters of the important rivers such as Euphrates and Tigris.

Turkey is situated in the mid-latitudes, therefore it is under the influence of the westerly air flow with respect to the atmospheric general circulation. For this reason, the western-facing sides of mountain ranges and coastal areas receive, in general, more precipitation than the other sides. According to the Köppen–Geiger climate classification, there are three primary climate types in Turkey. The Mediterranean and Aegean coastal areas of the country experience a temperate Mediterranean climate, which is characterized by hot and dry summers and mild and wet winters. The Black Sea coastal region experiences the features of a temperate maritime climate, which are warm and wet summers and cool and wet winters. The interior parts of Turkey are under the influence of a continental climate, which has hot summers and cold winters. This region usually receives comparatively less precipitation, much of which is in the form of snow in winter.

Many different data sets are used in this study. The observational precipitation and temperature data are obtained from the General Directorate of Meteorology. The water potential data are acquired from the State Hydraulic Works. The sector data (agriculture, tourism and energy) are acquired from the Turkish Statistical Institution. Climate change projections used in this study are based on the A2 scenario simulation of ECHAM5, the General Circulation Model of Max Planck Institute in Germany. Downscaling its outputs to a higher resolution (27 km) was achieved by employing a Regional Climate Model called ICTP-RegCM3, the regional climate model of International Centre for Theoretical Physics in Trieste, Italy (Bozkurt *et al.* 2012; Önol *et al.* 2014).

Results

Figure 1a illustrates the past (1970-2013) changes in the hydro-climatic variables. Temperatures are rising almost everywhere in Turkey. The summer temperatures have increased more than the temperatures in other seasons (not shown). The average summer temperature of 2000s is about 1.5 $^{\circ}$C higher than that of 1960s or 1970s. Spring and fall temperatures have also increased in recent decades, but the increases are not as large as that in summer. Precipitation has not changed much in Turkey except for the northeastern parts where it shows a coherent regional increase. The observations indicate important changes in two more hydro-climatic variables (mountain glacial retreat and the streamflow timing), which could be considered as a response to the increasing temperatures. A study by Sarıkaya (2011) suggests that the mountain glaciers in Turkey have been retreating at a rate of about 10 m/year. The eastern Anatolian highlands, which feed important rivers such as Euphrates and Tigris, are covered by snow during the cold period, and the snow starts to melt in March when the temperatures rise over freezing point in the region. The recent warming is causing snow to start melting earlier, and this could be observed in the stream discharges as they start to rise earlier in response to this event. A study by Sen *et al.* (2011) analysed the discharge data in the unregulated basins in the region and assessed that the peak discharge timing has already shifted to earlier days. The magnitude of the shift they calculated is about 5 days. It is not directly related to the climate change in Turkey, but the observations show that the sea level is rising between 3.8 and 7.7 mm/year along the coasts of Turkey (Demir *et al.* 2005).

Figure 1b shows the changes in the annual temperatures of the 2071-2099 period over those in 1961-1990 reference period. According to the A2 scenario simulation, the temperatures in Turkey are projected to increase between 2.5 $^{\circ}$C and 5.0 $^{\circ}$C by the end of the century. The changes are not uniformly distributed. The eastern and southeastern parts of Turkey illustrate comparatively larger increases in temperatures. Figure 1c shows the changes in the annual precipitation of the 2071-2099 period over that in 1961-1990 reference period. The projections indicate that the annual precipitation will tend to decrease in the

southern parts of Turkey while it will tend to increase in the northern parts, especially in the northeastern parts. The reductions along the Mediterranean coastlines could be as large as 30% by the end of the century. Similar magnitudes could be stated for the increases along the northeastern coastal areas of Turkey. The map in Figure 1d shows the changes of the water potentials for individual basins in Turkey. It seems that there will be substantial reductions in the southern basins, while little or no changes in the northern basins will occur. The projections that were based on the high emissions scenarios indicate water potential reductions up to 37% in the Mediterranean basins, up to 70% in Konya basin and up to 10% in the Euphrates and Tigris basins by the mid twenty first century.

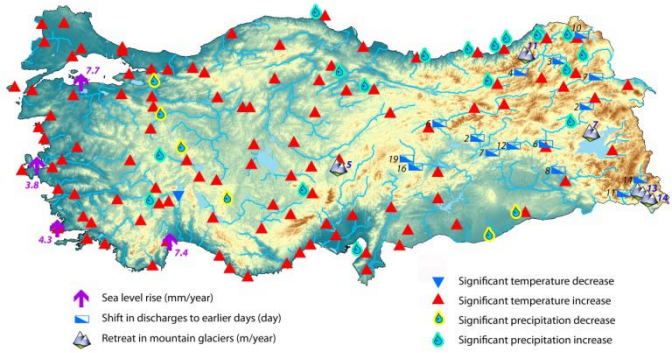

a.

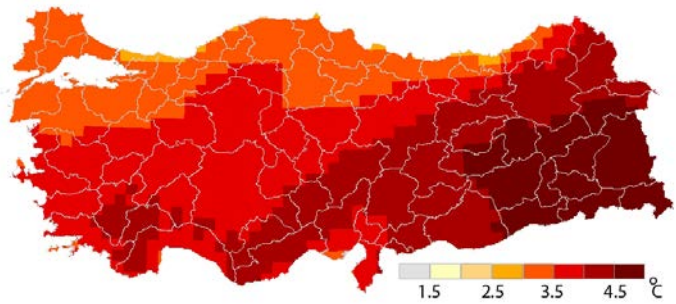

b.

Figure 1. (a) Historical (1970-2013) changes in temperature, precipitation, sea level, river discharges and mountain glaciers in Turkey, (b) future (2071-2099 period) temperature change over 1961-1990 period

c.

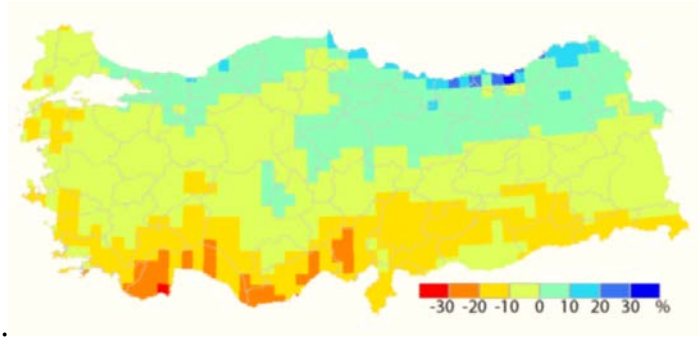

d.

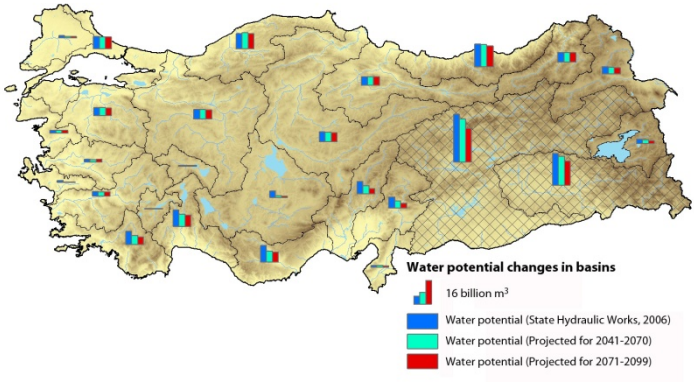

Figure1. (c) future (2071-2099 period) precipitation change over 1961-1990 period, (d) water potential changes in the basins of Turkey. Blue bar shows the water potentials based on the observations of State Hydraulic Works. Green and red bars show the projected water potentials for the mid-century and the end of the century, respectively.

Discussion

Turkey lies in a region that is highly vulnerable to climate change, and the indicators show that climate is changing in Turkey. The station observations show that temperatures are increasing throughout the country. Summer temperatures increase more than those of the other seasons. There are significant shifts in the timing of the snowfed river discharges, which indicates that snow melts earlier in response to the elevated temperatures. No significant coherent change has yet been detected in precipitation observations. Future climate change projections agree on an increase in temperatures throughout the country and a reduction in precipitation in the southern half of the country. There is no doubt that these changes will impact the country's water resources negatively by reducing the water potentials in the southern basins. The decline in the water resources will, first and foremost, influence the agriculture and animal husbandry and the related sectors. Hydroelectric energy production is another

sector that will be negatively affected by the water potential reduction in Turkey. Besides, Turkey will be subjected to more droughts, heat waves and forest fires. The wider prevalence of Mediterranean climate in Turkey in the future (together with the expansion of warm summer period) may have positive effects in terms of both human life and tourism. The winter tourism will be negatively influenced by the climate change as a result of reduced snow cover. In order to mitigate the negative impacts and benefit from the positive impacts of climate change, Turkey should certainly include the climate change projections in all future planning. Switching to water efficient irrigation techniques, extending the irrigated fields, recycling water, saving water and energy, adopting climate compatible cropping patterns, distributing crop cultivation to different regions, replacing the forest areas with drought and temperature resilient trees, planning urbanization in such a way to minimize urban heat island effect, using more renewable energy will certainly help Turkey cope better with the adverse effects of climate change.

References

Bozkurt, D., Turunçoğlu, U., Şen, Ö.L., Önol, B., Dalfes, H.N. (2012) Downscaled simulations of the ECHAM5, CCSM3 and HadCM3 global models for the eastern Mediterranean–Black Sea region: evaluation of the reference period. *Clim Dyn* 39(1–2): 207–225.

Demir, C., Yıldız, H., Cingöz, A., Simav, M. (2005) Long-term sea level change along the Turkish coasts. 5th National coastal Engineering Symposium, 5-7 May 2005, Bodrum (in Turkish).

Giorgi, F., Lionello, P. (2008) Climate change projections for the Mediterranean region. *Glob Planet Chang* 63: 90-104.

Hemming, D., Buontempo, C., Burke, E., Collins, M., Kaye, N. (2010) How uncertain are climate model projections of water availability indicators across the Middle East. *Phil Trans R Soc A* 368:5117-5135.

IPCC (2007) In Climate Change 2007: Synthesis Report. Contribution of Working Groups I, II and III to the Fourth Assessment Report of the Intergovernmental Panel on Climate Change [Core Writing Theme], (eds., R.K.Pachauri, A. Reisinger). IPCC: Geneva; 104 pp.

IPCC (2013) Working Group I Contribution to the IPCC Fifth Assessment Report, Climate Change 2013: The Physical Science Basis, Summary for Policymakers.

Önol, B., Bozkurt, D., Turunçoğlu, U., Şen, Ö.L., Dalfes, H.N. (2014) Evaluation of the 21st century RCM simulations driven by multiple GCMs over

the Eastern Mediterranean-Black Sea region. *Climate Dynamics* 42:1949-1965.

Önol, B., Semazzi, F.H.M. (2009) Regionalization of climate change simulations over the Eastern Mediterranean. *J. Climate* 22: 1944–1961.

Sarıkaya, M.A. (2011). Present glaciers of Turkey. In: Research in Physical Geography: Systematic and Regional (ed. D. Ekici). Turkish Geographical UnionPublications, İstanbul, 6: 527-544. (in Turkish).

Şen, Ö.L., Ünal, A., Bozkurt, D., Kindap, T. (2011) Temporal Changes in Euphrates and Tigris Discharges and Teleconnections, *Environmental Research Letters* 6:024012. doi:10.1088/1748-9326/6/2/024012.

J. Black Sea/Mediterranean Environment
Special Issue: 104-109 (2015)

The early Holocene Black Sea reconnection with the Mediterranean: implications for benthic ecological changes on the Caucasian shelf

Elena Ivanova[1*], Maria Zenina[1,2], Fabienne Marret[3], Ivar Murdmaa[1], Andrey Chepalyga[4], Lee Bradley[3], Maria Zyryanova[1]

[1] P.P. Shirshov Institute of Oceanology, Russian Academy of Sciences, 36 Nakhimovsky Prospekt, 117997, Moscow, RUSSIA
[2] A.V. Zhirmunsky Institute of Marine Biology, Far East Division of the Russian Academy of Sciences, St. 17, Palchevskogo Street, 690041,Vladivostok, RUSSIA
[3] School of Environmental Sciences, University of Liverpool, L69 7ZT, Liverpool, UK
[4] Institute of Geography, Russian Academy of Sciences, 29 Staromonetny Pereulok, 119017, Moscow, RUSSIA

[*]**Corresponding author:** e_v_ivanova@ocean.ru

Abstract

The Black Sea reconnection to the Mediterranean, in the early Holocene, is studied with special emphasis on the marine species immigration and occupation on the NE Caucasian shelf as well as the disappearance of species of Caspian origin. The distribution of different groups of fossils is analyzed from three radiocarbon dated sediment cores retrieved from the NE Black Sea shelf. The data provide evidence of sustained cohabitation of benthic species of Caspian and Mediterranean origin from at least ~8.8 to 6.7 cal ka BP. The slow disappearance of brackish species suggests a gradual increase in salinity and most likely a change in salt composition. This study also confirms previous findings of some upward reworking of Caspian elements within the mixed fauna layer. As mollusc shells represent one of the major components of the sediments, the succession of facies from *Dreissena* mud and shell to *Modiolus* mud is outlined and discussed according to changes in dominance of species and their individual ecological preferences.

Keywords: immigration, cohabitation, ostracods, molluscs paleoenvironments, sedimentation

Introduction

We present a continuous multi-proxy record from the core Ak-2575 which spans the last 9.6 cal ka. This new record is correlated to previously studied cores Ak-521 and Ak-2571 to investigate environmental change, during the Holocene, on the relatively under-investigated NE Black Sea shelf. The major changes

occurred during the early Holocene and were initiated by the reconnection of the Black Sea to the Mediterranean. These records contribute to the existing debates on the timing of marine species invasion (e.g. Ivanova *et al.* 2012 and references therein; Yanko-Hombach *et al.* 2014 and references therein) and provide new evidence of temporal cohabitation and slow turn-over of species in benthic assemblages on the NE Black Sea shelf. These are linked to sea level and salinity rises followed by marine species immigration from the Mediterranean to the Black Sea and disappearance of Caspian origin species. For comparison with our previous and other regional studies we used the generally accepted framework by Balabanov (2007, see also Ivanova *et al.* 2012) based on the ^{14}C dated succession of phases of the Black Sea transgression during the Holocene separated by the short-term regressions or the sea level low stand, since the reconnection of the Neoeuxinian Lake to the Mediterranean. In this paper, we focus on the major phases including Bugazian (9.2-7.9 ^{14}C ka BP), Vityazevian (7.9-7 ^{14}C ka BP) and Kalamitian (7-6 ^{14}C ka BP). According to the common practice in the area we consider waters with the salinity 5-12 psu (hereafter unitless) as brackish and with the salinity 18-20 as marine (e.g. Mudie *et al.* 2011; Ivanova *et al.* 2012; Yanko-Hombach *et al.* 2014).

Materials and Methods

Three sediment cores were collected from the northeastern Black Sea outer shelf and shelf edge off Arkhipo-Osipovka village (Figure 1) during the RV *Akvanavt* cruises.The lithology, mollusc and ostracod assemblages are studied from all cores, and benthic foraminifers from two cores (Ak-521 and Ak-2575).

Figure 1. Location of the sediment cores on the NE Black Sea shelf. Study area is marked by a square, Mediterranean water inflow is shown by flashes. Note that sites Ak-521 and Ak-2571 are in close proximity (~ 30 m).

The results from cores Ak-521 and Ak-2571 are published by Ivanova *et al.* (2007, 2012). The new core, Ak-2575 was sampled contiguously in 2 cm slices. The grain size fractions 0.1-2 and > 2 mm were used for lithological and micro-paleontological analyses. All cores are radiocarbon dated and correlated to the regional frame by Balabanov (2007). The radiocarbon dates are calibrated using CALIB7 with Intcal 2013 calibration dataset (Reimer *et al.* 2013) and applying a reservoir correction as described in (Ivanova *et al.* 2012).

Results and Discussion

Analysis of the radiocarbon dates and the stratigraphic frame by Balabanov (2007) suggest only one of the three cores, Ak-521, recovered the Neoeuxinian/Bugazian boundary. It was during this period that the brackish Black Sea was reconnected to the Mediterranean (event 1 in Figure 2) and the two-way circulation in the Bosphorus strait was re-established. However, the Bugazian-Vityazevian benthic assemblages were still strongly dominated by the brackish species of Caspian origin (Figure 2). Molluscs were represented by *Dreissena rostriformis*, *Micromelania* sp., and *Monodacna caspia*, whereas ostracod assemblages from the core Ak-2575 contained 16 species of Caspian origin and *Fabaeformiscandona* sp. of semi-freshwater origin and rare occurrences of three Mediterranean species. Among the species of Caspian origin, *Loxocaspia lepida*, *Loxocaspia sublepida*, *Amnicythere postbissinuata*, *Euxinocythere relicta*, *Amnicythere stepanaitisae*, *Graviacypris schweyeri*, were the most abundant suggesting the salt composition of the water was still similar to that of the Caspian Sea and not of the modern Black Sea. The first mollusc species of Mediterranean origin, *Mytilus* spp., appeared on the NE shelf at ~8.8 (core Ak-521) - 7.8 (core Ak-2575) cal ka BP (event 2 in Figure 2) suggesting a significant increase in bottom-water salinity and gradual change in the salt composition. The diversity of the species of Caspian origin declined after this period before they disappeared from the record by 7-6.7 cal ka BP (event 3 in Figure 2). They were gradually replaced by the species of Mediterranean origin including *Hiltermannicythere rubra*, *Leptocythere multipunctata*, *Palmoconcha agilis*, *Xestoleberis cornelii*, *Cytheroma marinovi* and *Cytheroma variabilis*. The bottom-water salinity on the shelf increased from ~11- to ~18 (Nevessakaya 1965; Yanko-Hombach *et al.* 2014 and references therein), i.e. from the lower limit of the tolerance of Mediterranean ostracods (Schornikov 1969) to almost modern values. It is noteworthy, that the ostracod data from the core Ak-2575, for the first time in the area, demonstrate the cohabitation of two groups in the early Holocene. This lasted until ~6.7 cal ka BP and is confirmed by many species being represented by specimens of different ontogenetic stages (adults and juveniles). Nevertheless, the reworking of several molluscs and ostracods of Caspian origin is also evident and supports data from other locations (Ivanova *et al.* 2012 and references therein; Yanko-Hombach *et al.* 2014 and references therein). In Figure 2, the reworking is demonstrated by AMS-^{14}C dates

measured on *Dreissena* and *Mytilus* from the same samples in the cores Ak-2575 and Ak-2571.

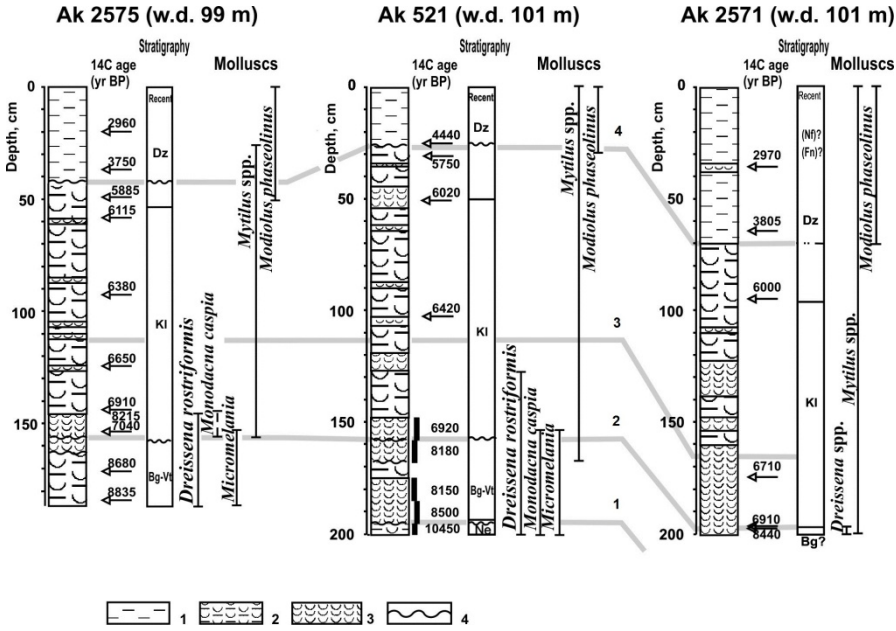

Figure 2. Lithology of sediment cores from the NE shelf, ^{14}C dates, chronostratigraphic units corresponding to transgression phases according to Balabanov (2007) and distribution of key mollusc species of Caspian and Mediterranean origin. Data on cores Ak-521 and Ak-2571 are modified from Ivanova and co-authors (2007, 2012). Correlation of records and peaks of four paleoceanographic events are also shown by grey lines at ~9 cal ka (event 1), ~7.8-8 cal ka (event 2),~ 7 cal ka (event 3) and 4 cal ka (event 4). W.d. – present-day water depth at core location. Lithology: 1 – mud with shell admixture (<10%), 2- shelly mud (10-30%), 3 – shell bed (>30%). 4 – hiatus. Stratigraphic units corresponding to transgression phases by Balabanov (2007): Ne-Neoeuxinian, Bg-Bugazian, Vt-Vityazevian, Kl-Kalamitian, Dz-Dzhemetinian

Accordingly, the following succession of sedimentary facies is distinguished from the cores, some of which are separated by hiatus. *Dreissena* mud and *Dreissena* shell bed in the lowermost part of the records before the event 2 (at water depth ~60-80 m); mixed mollusc fauna shell bed between events 2 and 3; *Mytilus* mud and shell beds between events 3 and 4 (at water depth ~ 70-90 m) and *Modiolus phaseolinus* mud after the event 4 when the sea level and salinity reached modern values of ~20 psu and 100 m, respectively. Our data suggest that the very rapid (likely pulsating) mud accumulation was due to intense terrigenous material supply. This created favorable conditions for the development of the active filtrator *Mytilus galloprovincialis* dominated mollusc assemblage on the outer shelf, much deeper than the common depth of the facies

(~50 m), because of abundant food resources and sufficient oxygen content in the mobile near-bottom nepheloid layer.

Conclusions

The significant discrepancies in the rate of immigration of molluscs, ostracods and foraminifers suggest that although salinity changes were the primary environmental change other factors were also important.

Data from this study indicate that the ostracod assemblages were sensitive to sea water salt composition change during the Early Holocene.

The cohabitation of benthic fauna of Caspian and Mediterranean origin is highlighted during the Early Holocene (Bugazian-Vityazevian interval) along with the upward reworking of several older specimens.

We suggest an explanation for a deep location of *Mytilus* facies on the outer shelf from ~7 to 4 cal ka BP in terms of the specific bottom-water conditions favoring for the species during this period.

Acknowledgement

This study was partly supported by the RFBR grant 12-05-00617a.

References

Balabanov, I.P. (2007) Holocene sea-level changes of the Black Sea. In: The Black Sea Flood Question: Changes in Coastline, Climate, and Human Settlement (eds., V. Yanko-Hombach, A.S. Gilbert, N. Panin, P.M. Dolukhanov). Springer, Dordrecht, pp. 711-730.

Ivanova, E.V., Murdmaa, I.O., Chepalyga, A.L., Cronin, T.M., Pasechnik, I.V., Levchenko, O.V., Howe, S.S., Manushkina, A.V., Platonova, E.A. (2007) Holocene sea-level oscillations and environmental changes on the Eastern Black Sea shelf. *Palaeogeogr., Palaeoclim., Palaeoecol.* 246: 228-259.

Ivanova, E.V., Murdmaa, I.O., Karpuk, M.S., Schornikov, E.I., Marret, F., Cronin, T.M., Buynevich, I.V., Platonova, E.A. (2012) Paleoenvironmental changes on the northeastern and southwestern Black Sea shelves during the Holocene. *Quat.y Int.* 261: 91-104.

Mudie, P.J., Leroy, S.A.G., Marret, F., Gerasimenko, N.P., Kholeif, S.E.A., Sapelko, T., Filipova-Marinova, M. (2011) Nonpollen palynomorphs: indicators of salinity and environmental change in the Caspian ?Black Sea ?Mediterranean corridor. In: Geology and Geoarchaeology of the Black Sea Region: Beyond the

Flood Hypothesis (eds. I.V. Buynevich, V. Yanko-Hombach, A.S. Gilbert, R.E. Martin), Geological Society of America Special Paper 473. pp. 89-115.

Nevesskaya, L.A. (1965) Late Quaternary Bivalvia of the Black Sea, their Systematics and Ecology). Nauka, Moscow (in Russian).

Reimer, P.J., Bard, E., Bayliss, A., Beck, J.W., Blackwell, P.G., Ramsey, C.B., Buck, C.E., Cheng, H., Edwards, R.L., Friedrich, M., Grootes, P.M., Guilderson, T.P., Haflidason, H., Hajdas, I., Hatte, C., Heaton, T.J., Hoffmann, D.L., Hogg, A.G., Hughen, K.A., Kaiser, K.F., Kromer, B., Manning, S.W., Niu, M., Reimer, R.W., Richards, D.A., Scott, E.M., Southon, J.R., Staff, R.A., Turney, C.S.M., van der Plicht, J. (2013) Intcal13 and Marine13 Radiocarbon Age Calibration Curves 0-50,000 Years Cal BP. *Radiocarbon* 55: 1869-1887.

Schornikov, E.I. (2011) Ostracoda of the Caspian origin in the Azov-Black seas basin. *Joannea Geologie Paläontologie*11: 180–184.

Yanko-Hombach, V., Mudie, P.J., Kadurin, S., Larchenkov, E. (2014) Holocene marine transgression in the Black Sea: New evidence from the northwestern Black Sea shelf. *Quat.y Int.* (in press)

J. Black Sea/Mediterranean Environment
Special Issue: 110-116 (2015)

Recent advancements on modelling the exchange flow dynamics through the Turkish Straits System

Gianmaria Sannino[1*], Adil Sözer[2], Emin Özsoy[2]

[1] ENEA, via Anguillarese 301, 00123, Rome, ITALY
[2] Institute of Marine Sciences, Middle East Technical University (IMS-METU), Erdemli, Mersin, TURKEY

[*]**Corresponding author:** gianmaria.sannino@enea.it

Abstract

The system composed by the two narrow Straits, Dardanelles and Bosphorus, and the Marmara Sea is known as the Turkish Straits System (TSS). The scientific questions on the role of the TSS in coupling the adjacent basins of the Mediterranean and Black Seas with highly contrasting properties and in a region of high climatic variability can only be answered by model predictions of the processes that determine the integral properties of the coupled sub-systems. This can only be achieved if the entire TSS is modeled as a finely resolved integral system that appropriately accounts for the high contrasts in seawater properties, steep topography, hydraulic controls, fine and meso-scale turbulence, nonlinear and non-hydrostatic effects, thermodynamic states and an active free-surface in the fullest extent, based on well represented fluid dynamical principles. In this study the MITgcm (MIT General Circulation Model) is used at very high resolution to study this extreme environment that needs to be represented as a whole and with the full details of its highly contrasting properties. The capability of MITgcm to represent the two-layer exchange dynamics both in the straits and in the Marmara Sea is examined. The non-uniform grid and the vertical resolution implemented have demonstrated to be suitable to capture the fine scales within the two Straits and also to well represent mesoscale in the Marmara Sea. The response of the currents and density structure over the water column to different net flow is also examined through the setup of experiment with varying net barotropic volume fluxes.

Keywords: numerical ocean modelling, Turkish Straits System, Bosphorus, Marmara Sea, Dardanelles

Introduction

The Turkish Straits System (TSS) consists of the Sea of Marmara connecting to the Aegean and Black Seas respectively through the Dardanelles (length 75 km, min. width 1.3 km) and Bosphorus (length 35 km, min. width 0.7 km) Straits. The Marmara Sea has three elongated depressions (max. depth ~1350 m) interconnected by sills (depth ~600 m) and adjoining continental shelves. The

nonlinear, turbulent, strongly stratified hydrodynamics of the flow through the narrow straits has made the modeling of the TSS a grand challenge. The coupling of the adjacent basins of highly contrasting properties, in a region of extreme hydro-climatic variability can only be achieved if the entire TSS is modelled as a finely resolved integral system, accounting for steep topography, nonlinear hydraulic controls and turbulent mixing processes, as well as an active free-surface. The nonlinear, turbulent, strongly stratified hydrodynamics of the flow through the narrow straits has made the modeling of the TSS a grand challenge. Here, thanks to a PRACE (Partnership for Advanced Computing in Europe) infrastructure this grand challenge has been achieved. In the following we describe and validate the TSS model together with a discussion on some preliminary results.

Data and Methods

In this work the MITgcm model (http://mitgcm.org) is used to study TSS with full details of its contrasting properties. The model domain chosen extends over the entire TSS, including also parts of the north-east Aegean Sea and the Black Sea at its two ends (Figure 1). A non-uniform curvilinear orthogonal grid covers the domain at variable resolution: from less than 50 m in the two Straits up to about 1 km in the Marmara Sea. To adequately resolve the complex hydraulic dynamics of the TSS, the model grid is made by 100 inhomogeneous distributed vertical z-levels. The thickness exponentially ranges from 1.2 m at the surface to 80 m at the bottom with most of the levels concentrated in the first 100 m.

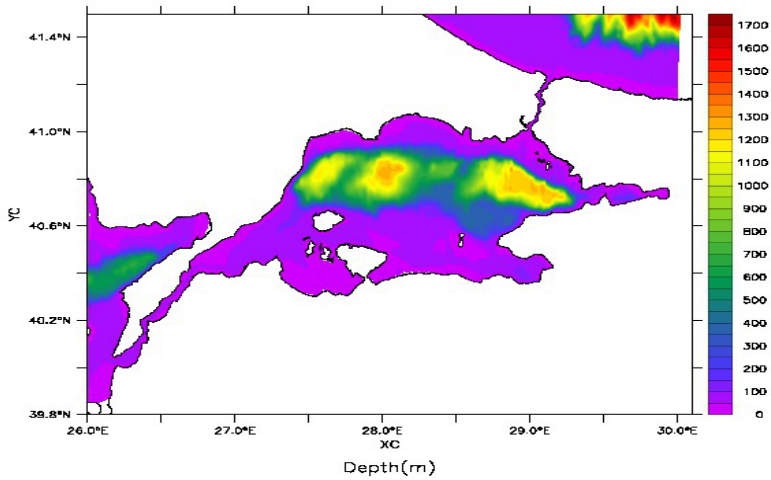

Figure 1. Model bathymetry (colorbar: depth in m)

The very high horizontal resolution adopted in MITgcm, together with the partial cell formulation result in a very detailed description of the bathymetry. The model has been initialized with three different water masses filling the western part of the domain, the Marmara Sea and the eastern side of the domain

respectively, with vertical profiles selected from CTD casts obtained during the cruise of the R/V BILIM of the Institute of Marine Sciences in June-July 2013. With the initial condition specified as lock-exchanges at the two straits, the model is left free to adjust to the expected two-way exchange. No-slip conditions were imposed at the bottom and lateral solid boundaries.

Results

The non-uniform curvilinear orthogonal grid and the vertical resolution implemented have demonstrated to be sufficient to capture the fine scales within the two Straits and also to well represent mesoscale in the Marmara Sea. The response of the currents and density structure over the water column to different net flow is also examined through the setup of experiments with varying net barotropic volume flux values (Q=-9600, 0, 5600, 9600, 18000 and 50000 m^3/s respectively). The expected range of fluxes for testing the TSS behavior with respect to barotropic net flows were guided by our earlier experience based on frequent sampling by past field experiments using in-situ ADCP and CTD measurements of the strait hydrography and currents, covering the TSS under normal and extreme climatic conditions (Beşiktepe *et al.* 1994; Özsoy *et al.* 1998; Gregg *et al.* 2002). Positive values of Q represent flow from the Black Sea towards the Mediterranean, while negative values represent net flow in the opposite direction. The free surface variations in the Marmara Sea, corresponding to configurations initialized with vertical profiles representative of the three basins selected from CTD casts in June-July 2013 and variable values of net barotopic flow values are shown in Figure 2.

Discussion

For the studied flows, characterized to be driven exclusively by the imposition of net flux, an S-shaped current, first moving south from the Bosporus, later turning northwest and finally exiting from the from the Dardanelles Strait, appears to be the basic character of the circulation. With a negative flux of Q=-9600 m^3/s, such that the net flow is towards the Black Sea, the upper layer flow from the Bosphorus into the Marmara Sea is still positive, and sufficient to generate an anticyclonic net circulation in the midst of the Marmara Sea, as shown in Figure 2. For zero net flux, the same structure is preserved and as the positive values of the barotropic flux is increased further the size of the central gyre is reduced and the flow becomes increasingly more attached to the northern coast of the Marmara Sea. As the flux is increased to 9600 m^3/s, the central anticyclonic circulation cell takes an elongated form. For the extreme flux values of Q=18000 m^3/s and Q=50000 m^3/s, the lower layer flow in the Bosphorus becomes blocked, and qualitative changes occur in the circulation of the Marmara Sea, with a smaller anticyclone near the Bosphorus exit, a jet attached to the northern coast, and a secondary anticyclone further west, and a cyclonic circulation emerging in the south. For these cases, the circulation

pattern looks more like the buoyancy driven flow along the coast adjacent to the mouth of a river. The generation of a basic anticyclonic circulation in the Marmara Sea for lower net fluxes, evolving towards a more balanced circulation of cyclonic-anticyclonic eddies appears to be a result of the vorticity balance of the basin.

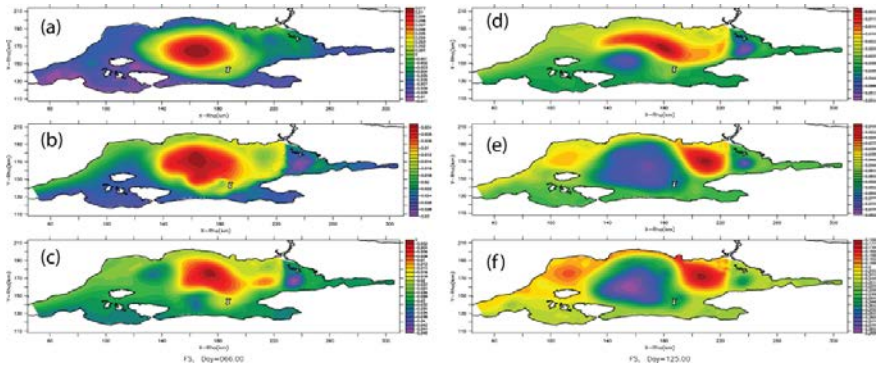

Figure 2. The free surface variations in the Marmara Sea for varying net barotropic volume flux values of:

(a) Q = -9600 m^3/s, day=67, range=2.2 cm
(b) Q = 0 m^3/s, day=100, range=2.7cm
(c) Q = 5600 m^3/s, day=66, range=4.5 cm
(d) Q = 9600 m^3/s, day=22, range=4.8 cm
(e) Q = 18000 m^3/s, day=65, range=6.4 cm
(f) Q = 50000 m^3/s, day=125, range=12.0 cm

As shown by Spall and Price (1998), and studied by Morrison (2011), the net basin circulation is sensitively determined by the potential vorticity (PV) imports and exports of the basin. From this point of view, the reduction of interface depth (or upper layer thickness) from the Black Sea to the Marmara Sea implies a decrease in fluid vorticity, or anticyclonic circulation assuming the input to have zero vorticity. The behaviour of the buoyant plume entering the Marmara Sea, initially shooting south and hitting the opposite coast is displayed in all cases in Figures 2, although the later turning of the flow to the west is typical of buoyant plumes at this scale. Buoyant flows entering the sea are typically attached to the right hand coast (looking out from the exit in the northern hemisphere), especially for initial vorticity zero below a critical limit (e.g. Nof 1978; Stern *et al.* 1982). Often a bulge of the buoyant fluid is formed, as the flow turns right to follow the coast, as often observed at river mouths (e.g. Huq 2013). In a two-layer system with variable bottom topography and dynamically active layers, the circulation may develop differently, with topography influencing the lower layer flow, and the resultant interface topography influencing the upper layer flow (Beardsley *et al.* 1978). As the net flux is increased in Figure 2, the changes in the circulation pattern may be a result of this kind of interactive adjustment of the flow layers to bottom and interface topography. The qualitative change in the circulation towards a series of anticyclonic and cyclonic eddies following the meander of the currents, when the flux is increased to 18000 m^3/s and 50000 m^3/s is reminiscent of the Alboran

Sea, where similar gyres filling the basin develop under high fluxes (Spall and Price 1998).

Table 1. Sea level difference at both edges of the two straits as a function of net flux

Net flux Q (m^3/s)	Bosphorus (TSS) sea level difference Δη (cm)	Dardanelles (TSS) sea level difference Δη (cm)	Bosphorus (ROMS) sea level difference Δη (cm)
-9600	2	1.5	-
0	8	5	14
5600	10	7	18
9600	14	11	22
18000	22	16	30
50000	85	32	-

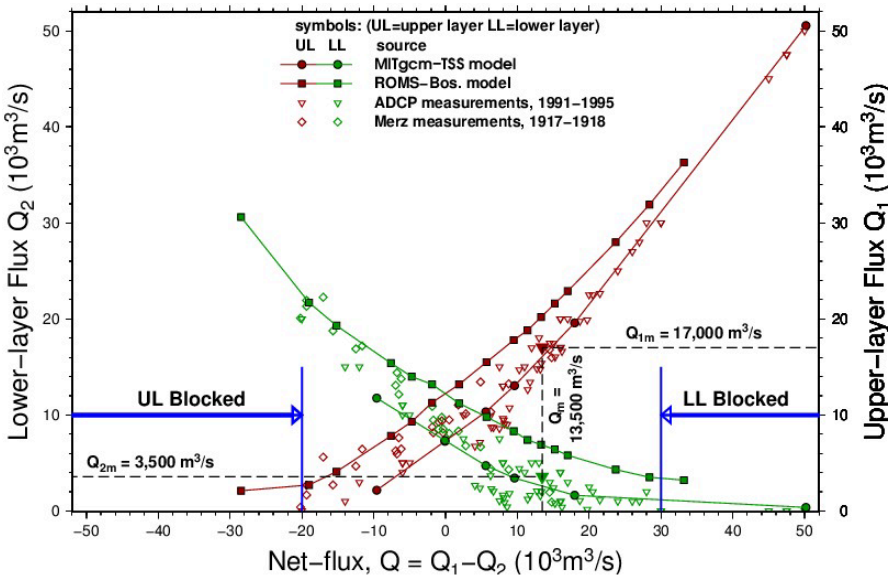

Figure 3. Upper-layer (Q_1) and lower-layer (Q_2) volume fluxes through the Bosphorus as a function of the net flux ($Q=Q_1-Q_2$), based on observational data and compared with the results from the Bosphorus model (ROMS) of Sözer (2013) and the TSS (MITgcm) models

The sea level differences that develop at the two straits, Bosphorus and Dardanelles are given in Table 1, in relation to the net barotropic fluxes and the values obtained from the TSS model are compared with the ROMS model results for the Bosphorus (Sözer 2013). While the total range of sea level in the Marmara Sea between cyclonic and anticyclonic areas varies between 2-12 cm (Figure 1), the net sea level differences across straits are much larger, varying between 2-85 cm in the Bosphorus and 1-32 cm in the Dardanelles, while the

results for the Bosphorus compare well between the two models. These results would imply sea level differences of about 0-120 cm between the Black Sea and the Aegean Sea, for the range of net transport tested. Finally a comparison is made of the upper-layer (Q_1) and lower-layer (Q_2) volume fluxes through the Boshorus (Figure 3), based on observational data and the results from the Bosphorus model (ROMS) of Sözer (2013) and the TSS (MITgcm) models. Although the Bosphorus model is more specific to the Strait and has better resolution, the TSS model results perform even better in comparison with observations.

References

Beardsley, R.C., Hart, J. (1978) A simple theoretical model for the flow of an estuary on to a continental shelf. *J. Geophys. Res.* 83:873-883.

Beşiktepe, Ş., Sur, H.İ., Özsoy, E., Latif, M.A., Oğuz, T., Ünlüata, Ü. (1994) The circulation and hydrography of the Marmara Sea *Prog. Oceanogr.* 34: 285-334.

Gregg, M.C., Özsoy, E. (2002) Flow, water mass changes and hydraulics in the Bosphorus. *J. Geophys. Res.* 107(C3): doi:10.1029/2000JC000485.

Huq, P. (2013) Buoyant outflows to the coastal ocean. In: Handbook of Environmental Fluid Dynamics, Volume One, (ed. H. J. S. Fernando). CRC Press / Taylor & Francis Group, LLC, 1, pp. 207-215.

Morrison, A. (2011) Upstream Basin Circulation of Rotating, Hydraulically Controlled Flows, 2011 Summer Program in Geophysical Fluid Dynamics, WHOI, 429 pp.

Nof, D. (1978) On geostrophic adjustment in sea straits and wide estuaries: theory and laboratory experiments. part ii – two-layer system. *J. Phys. Ocean.* 8: 861-872.

Özsoy, E., Latif, M.A., Beşiktepe, S., Çetin, N., Gregg, N. Belokopytov, V., Goryachkin, Y., Diaconu, V. (1998) The Bosphorus Strait: exchange fluxes, currents and sea-level changes. In: Ecosystem Modeling as a Management Tool for the Black Sea, NATO Science Series 2 (eds., L. Ivanov, T. Oğuz): Environmental Security 47, Kluwer Academic Publishers, Dordrecht, pp. 1-26

Sözer, A. (2013) Numerical Modeling of the Bosphorus Exchange Flow Dynamics, Ph.D. thesis, Institute of Marine Sciences, Middle East Technical University, Erdemli, Mersin, Turkey.

Spall, M., Price, J.F. (1998). Mesoscale variabilty in Denmark Strait: the PV outflow hypothesis. *J. Phys. Ocean.* 28:1598-1623.

Stern, M., Whitehead, J., Hua, B. (1982) The intrusion of a density current along the coast of a rotating fluid. *J. Fluid Mech*. 123:237-265.

J. Black Sea/Mediterranean Environment
Special Issue: 117-124 (2015)

Effects of the Etesian wind regime on coastal upwelling, floods and forest fires in the seas of the old world

Ozan Mert Göktürk[1,4], Sinan Çevik[2], Nathalie Toque[1], Robinson Hordoir[3], Hazem Nagy[1,5], Emin Özsoy[1]

[1] Institute of Marine Sciences, Middle East Technical University, Erdemli, Mersin, TURKEY
[2] Turkish State Meteorology Service, İnebolu, TURKEY
[3] Swedish Meteorological and Hydrological Institute, Norrköping, Sweden
[4] İstanbul Technical University, İstanbul, TURKEY
[5] Oceanography Department, University of Alexandria, Alexandria, EGYPT

[*]**Corresponding author:** ozsoy@ims.metu.edu.tr

Abstract

The Etesian wind regime dominating the climate of the Aegean Sea in summer often influences a larger area extending from the Balkans and the Black Sea to the Levantine Basin of the Eastern Mediterranean. The steady dry northerly winds descending from the Balkans in summer often incite forest fires in the Aegean Sea region, while the moist air picked up from the sea and trapped against the mountainous eastern Black Sea coast results in severe floods. The intense upwelling on the southern Black Sea and the eastern Aegean Sea result from steady winds aligned with the coast. Case studies based on recent observations and model simulations illustrate these events.

Keywords: Etesian, upwelling, floods, forest fires, Aegean, Black Sea, modeling

Introduction

The summer Etesian wind regime often develops to gale force winds, veering from NE to N and NW respectively in the north, central and south Aegean (Tyrlis and Lelieveld 2013; Tyrlis *et al.* 2014), fed by northerly winds from the Balkan gap and northeasterly winds from the Black Sea area. The typical wind pattern affects the entire region, often intensified south, at the elevated island of Crete (Figure 1a).

Data and Methods

Case studies in the present context emphasize the region-wide influence of Etesian winds by making use of surface wind, sea surface temperature and satellite data, as well as atmospheric and ocean models. Operational weather forecasts at the IMS-METU (http://linux-server.ims.metu.edu.tr/metuwrf/) are

used for the analyses. The NEMO model (domain: 40.92°-47.30°N, 27.43°-42.00°E at 2.5 km horizontal resolution and 60 z-levels), developed for Black Sea hincasts and operational use in the MyOcean2 European project, includes inputs from major rivers, seasonal T,S profile boundary conditions specified at the Bosphorus, and is driven by surface fluxes based on the atmospheric data of the University of Athens (IASA) at 1 hr intervals and 0.05° horizontal resolution. SST satellite data are obtained from MHI, Ukraine. Daily observations of sea surface temperature are obtained at the İnebolu (41.98°N 33.76°E) station of the Turkish State Meteorology Service. ERA-interim reanalysis surface atmospheric data for the region have been obtained from the ECMWF.

Results

Strong air-sea interactions during the Etesian wind regime are all too significant in this sensitive region of continental/marine climates. Often the sustained wind pattern is suitable to create forest fires in the region especially in the central and southern Aegean (Koletsis *et al.* 2009; 2010), e.g. in 25 August 2012 when the government of Greece declared a state of emergency as the blaze reached Athens, verified by wind patterns (Figure 1a). It was however rather surprising to evidence a completely different extreme event happening at the same time in the eastern Black Sea, where the winds diverged with a northwesterly orientation. The moisture picked up by winds from the northern steppes was trapped against the steep Anatolian and Caucasian mountain ranges (Figure 1b) and precipitated by orographic uplift against the southeast coast, leading to the extreme flooding event on August 21, 2012 in the southeast (Figure 1c). Precipitation of about 230 mm was received in two days, equivalent to few months of annual rainfall. Several times in the summer of 2012 the pattern was repeated, and a similar flooding extreme event had occurred earlier on July 7, 2012, associated with a small-scale cyclone trapped in the mountainous eastern Black Sea region. The storm created the worst floods in 70 years in Krasnodar and Krymsk, Russia, with rainfall amounting to 270 mm/day and a death toll of more than hundred people.

In the Aegean Sea, circulation features such as the persistent upwelling along the eastern shores and the jet-like boundary currents on the western shores, largely owing their existence to the northerly Etesian winds, are well known (Theocharis *et al.* 1999; Olson *et al.* 2007; Sayın *et al.* 2011). In the Black Sea, the SW-NE oriented section of the southwest coast, aligned with the NW wind pattern in much of summer (Figure 1a) is favorable for Ekman drift currents in offshore direction leading to coastal upwelling (Sur *et al.* 1994).

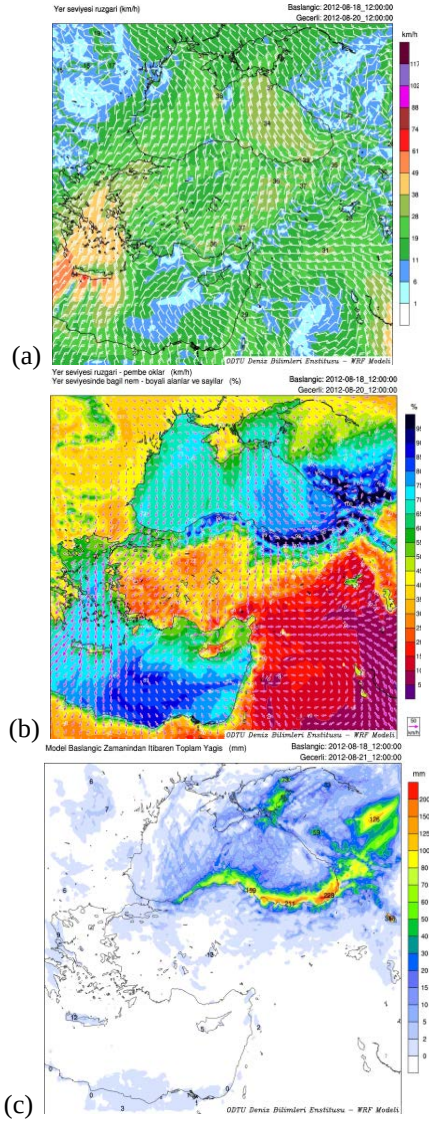

Figure 1. Atmospheric model forecasts of (a) surface winds (km/h), (b) surface relative humidity (%) and wind (km/h) on 20 August 2012 and (c) total precipitation (mm) during 18-21 August 2012

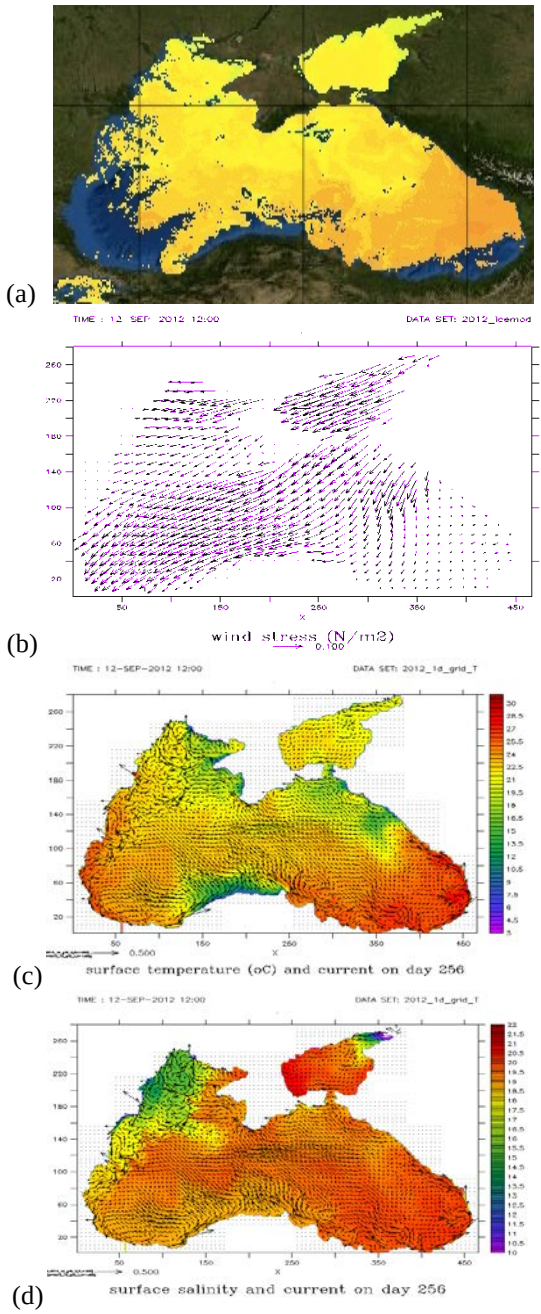

Figure 2. September 12, 2012 (a) satellite SST image, (b) surface winds and ocean model hindcasts of (c) surface currents and temperature, (d) surface currents and salinity

A typical situation is shown in the satellite image of Figure 2a, where cold waters with temperatures of 15°C are detected adjacent to the coast, in contrast to the 22-26°C in the rest of the basin. The upwelling is subject to some intermittency under changing winds, and located downstream of the meandering coastal jet (i.e. the 'rim-current') which often separates from the coast and transits offshore of the upwelling area (Sur *et al.* 1994; Özsoy and Ünlüata 1997, 1998).

The mainly cyclonic circulation of the highly stratified Black Sea is buoyancy and wind driven (Özsoy and Ünlüata 1997, 1998). A distinctive feature of the Black Sea thermal stratification is the subsurface Cold Intermediate Water (CIW) usually found above the pycnocline, upwelled in summer in the southwest as well as around Crimea (Figure 2a). Also shown in the same figure are the surface winds (Figure 2b), temperature (Figure 2c) and salinity (Figure 2d) produced by the NEMO model continuous hindcast for the years 2010-2014, confirming the observed features.

Daily observations of SST at the İnebolu indicate very frequent and persistent upwellings during repeated episodes in the summer season (Figure 3a). What are seen as many spikes and dropouts in the time-series are actually many cases of upwelling, with temperature drops to as low as 11^{o}C, as a result of the cold intermediate water (CIW) surfacing at the coast. SST data high-pass filtered at cutoff period of 30 days indicate high frequency events (Figure 3a). The enlarged plots of the observed SST (Figure 3b, lower panel, blue) reveal sharp dropouts of temperature lasting from few days to few weeks, which differ strongly from the regional average SST in the ECMWF reanalysis (black). Figure 3b, upper two panels display along-shore and cross-shore components of the wind at the ECMWF grid point near the İnebolu station, after the wind vector has been rotated by 40° to be aligned with the coast. It is clear that the main component of the wind is along-shore and blows from the northeast in summer, favorable to upwelling.

Discussion

The regional influences of the Etesian winds are well known, but perhaps not sufficiently appreciated. Forest fires are incited in the Aegean, while floods occur concurrently in the Black Sea. We try to demonstrate the climatic significance of some of these concurrent events. For instance, in continuing fisheries studies in the Black Sea (http://hamsi.ims.metu.edu.tr), the role of upwelling events have not been investigated. Yet, Black Sea fisherman near İnebolu are very well aware that they can not go out to fish Palamut (pelamydes) during periods of persistent northerlies which lead to upwelling. It was only revealed to us during this study that local towns people of İnebolu have been going to the coast at night with searchlights to collect half-dizzy fish suffering shock by the cold waters during upwelling (Figure 4).

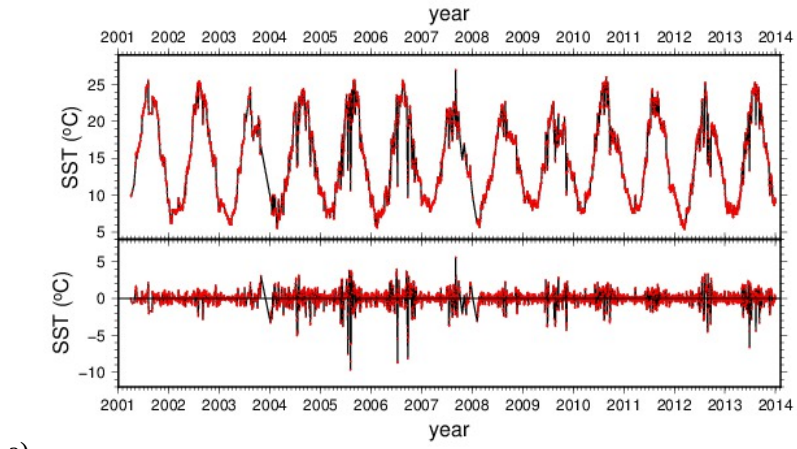

a)

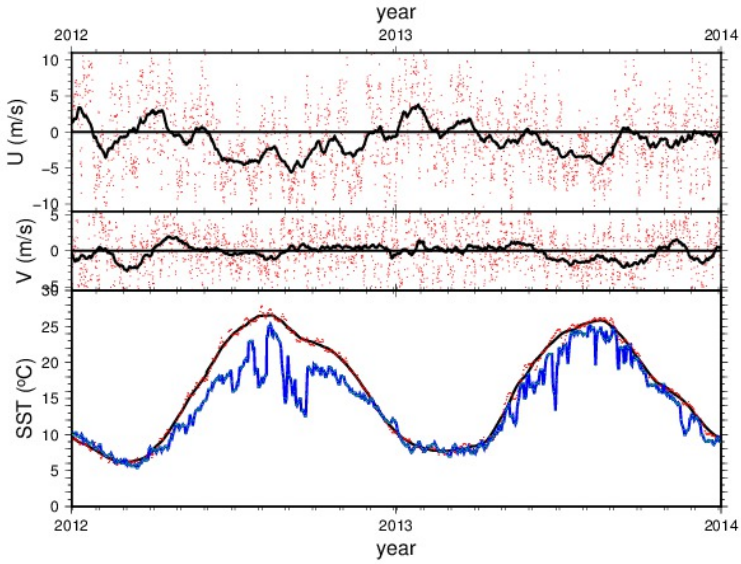

(b)

Figure 3. (a) İnebolu daily (upper) and high-pass filtered (lower) SST time series, (b) along-shore and cross-shore components of wind velocity at 42.2°N, 32°E based on ERA-interim reanalysis (ECMWF) rotated clockwise by 40° (upper two panels, red dots are original unfiltered data points), the SST based on the reanalysis (black) and the İnebolu meteorological station time-series data (blue) (lower panel)

Figure 4. İnebolu people searching for fish near the coast at night (photos: Sinan Çevik)

Acknowledgements

We thank the MyOcean2 European project for making possible this study, and to the Turkish State Meteorological Service for the İnebolu data and for providing access to the ECMWF MARS archives.

References

Koletsis, I., Lagouvardos, K., Kotroni, V., Bartzokas, A. (2009) The interaction of northern wind flow with the complex topography of Crete Island – Part 1: Numerical study. *Nat. Hazards Earth Syst. Sci*. 9: 1845–1855.

Koletsis, I., Lagouvardos, K., Kotroni, V., Bartzokas, A. (2010) The interaction of northern wind flow with the complex topography of Crete Island – Part 2: Observational study. *Nat. Hazards Earth Syst. Sci.* 10: 1115–1127.

Olson, D.B., Kourafalou, V.H., Johns, W.E., Samuels, G., Veneziani, M. (2007) Aegean surface circulation from a satellite-tracked drifter array. *J. Phys. Oceanogr*. 37: 1898–1917.

Özsoy, E., Ünlüata, Ü. (1997) Oceanography of the Black Sea: a review of some recent results. *Earth Sci. Rev.* 42 (4): 231-272.

Özsoy, E., Ünlüata, Ü. (1998). The Black Sea. In: The Sea: The Global Coastal Ocean: Regional Studies and Syntheses (eds., A. R. Robinson, K. Brink), 11, John Wiley and Sons, New York, pp. 889-914.

Sayın, E., Eronat, C., Uçkaç, Ş., Beşiktepe, Ş.T. (2011) Hydrography of the eastern part of the Aegean Sea during the Eastern Mediterranean Transient (EMT). *J. Mar. Sys*. 88: 502-515.

Sur, H.İ., Özsoy, E., Ünlüata, Ü. (1994) Boundary current instabilities, upwelling, shelf mixing and eutrophication processes in the Black Sea. *Prog. Oceanogr*. 33: 249-302.

Theocharis, A., Georgopoulos D., Krestenitis Y., Koutitas, Ch. (1999) Upwellings in the Aegean Sea. *Thalassographika* 13(2): 67-75.

Tyrlis, E., Lelieveld, J. (2013) Climatology and dynamics of the summer Etesian winds over the eastern Mediterranean. *J. Atmos. Sci*. 70: 3374-3396.

Tyrlis, E., Škerlak, B., Sprenger, M., Wernli, H., Zittis, G., Lelieveld, J. (2014) On the linkage between the Asian summer monsoon and tropopause fold activity over the eastern Mediterranean and the Middle East. *J. Geophys. Res. Atmos.* 119: 3202–3221.

J. Black Sea/Mediterranean Environment
Special Issue: 125-130 (2015)

Climate change leads to more frequent but smaller fires in a Mediterranean environment

Marco Turco[1,*], Maria-Carmen Llasat[2], Jost von Hardenberg[1], Antonello Provenzale[1]

[1] ISAC-CNR, Corso Fiume 4, 10133 Torino, ITALY
[2] Department of Astronomy and Meteorology, University of Barcelona, Av. Diagonal 647, 08028 Barcelona, SPAIN

[*]**Corresponding author:** m.turco@isac.cnr.it

Abstract

The analysis of both observed climate and fire data from 1970 to 2007 in a typical Mediterranean environment (i.e., the North-eastern Iberian Peninsula) shows that the warming climate forcing alone would have led to a positive trend in the Number of Fires (NF) and a slightly negative trend in the Burned Area (BA) in summer. This is in contrast to the common expectation that warming should result in larger fires. In fact, for BA, probably less favourable conditions for both fine fuel availability and fuel connectivity counterbalance the increase in fuel flammability. Climate projections from the ENSEMBLES Project indicate that warming will continue up to at least 2050, promoting more numerous fires but of similar or slightly smaller extension. These results suggest the necessity for a more intense fire management effort in order to maintain the number of fires at least at the same level as today.

Keywords: forest fires, Mediterranean regions, climate change, fire management

Introduction

The Mediterranean region is a "Hot-Spot" of climate change and wildfires, where about 50'000 fires burn 500'000 hectares every year (San-Miguel-Ayanz *et al.* 2013). However, in spite of the growing concerns of the climate change impacts on Mediterranean wildfires, there are aspects of this topic that remain largely to be investigated.

The main scientific objective of this study is to analyse the climate-driven changes on fires in a typical Mediterranean environment (Catalonia, NE of Spain). To achieve this goal, the following specific aims have been identified and addressed in this study. First, we analyse the recent evolution of fires. Secondly, we develop a statistical fire-climate model. Finally we estimate the fire impacts of observed and future climate change.

Materials and Methods

Fire data were obtained from the Forest Fire Prevention Service of the "Generalitat de Catalunya" (SPIF) for the period 1970-2010. We focused on the eastern part of Catalonia and we considered two standard fire variables: the total Number of Fires (NF) and the total Burned Area (BA) in the summer months (June, July, August and September; JJAS).

Observed climate data used in this study are provided by the high-resolution ($0.2^{\circ} \times 0.2^{\circ}$, approximately 20 km × 20 km) gridded dataset Spain02 (www.meteo.unican.es/es/datasets/spain02; Herrera *et al.* 2012) covering Spain over the period 1950-2007. This dataset is a reference dataset for climate studies in Spain (see e.g. Herrera *et al.* 2010; Turco and Llasat 2011; Turco *et al.* 2011).

The EU-funded project ENSEMBLES (http://ensemblesrt3.dmi.dk/; van der Linden and Mitchell 2009) produced the biggest available ensemble of latest-generation RCM regional simulations at an unprecedented resolution (25 km). We have analysed three different sets of regional models: (i) the RCMs driven by the ERA40 reanalysis data, available for the period 1961-2000, (ii) the GCM-driven RCMs in the control period 1961-2000 (using the 20C3M scenario, i.e. with observed greenhouse gasses) and (iii) future A1B scenario simulations of GCM-driven RCMs. The RCMs used here has been extensively validated (see Herrera *et al.* 2010; Turco *et al.* 2013a for more details).

Results

First, we examined a homogeneous series of forest fires in the period 1970–2010. We restricted the analysis to fires with a burned area of at least 0.5 ha. Our analysis shows that both the burned area and number of fire series display a significant decreasing trend. We found that BA decreased by about -2 $km^2 year^{-1}$ and NF by about -6 fires $year^{-1}$. A possible driver of the observed fires trend is the increasing effort to fire management. For instance, after the big fires in the 1980s, fire management strategies were improved, with an increase in fire prevention and fire fighting measures, on a European and Spanish level (more details at Turco *et al.* 2013b).

Secondly, we showed that the interannual variability of summer fires is significantly related to antecedent and concurrent climate conditions, highlighting the importance of climate not only in regulating fuel flammability, but also fuel load (Turco *et al.* 2013c; Turco *et al.* 2014a). On the basis of these results, we developed a multiple linear regression model (MLR) through a stepwise regression process (more details in Turco *et al.* 2013c):

$$\log(BA)' = -0.91\ DD'_{(6\text{-}7)} + 0.36\ Tx'_{(6\text{-}7)} - 0.48\ Tn'_{(4\text{-}4)} - 0.75\ Tx'_{(2\text{-}11)(2)} + \varepsilon \quad \text{(Eq.1)}$$

$$\log(NF)' = -0.36\ P'_{(5\text{-}8)} + 0.34\ Tx'_{(6\text{-}9)} - 0.16\ Tn'_{(4\text{-}5)} + 0.08\ P'_{(1\text{-}8)(2)} + \varepsilon \quad \text{(Eq. 2)}$$

where the fire variables (log-transformed and detrended BA and NF in JJAS), are related to the detrended climate variables (precipitation $P'_{(n-m)(\tau)}$, number of dry days $DD'_{(n-m)(\tau)}$, maximum temperature $Tx'_{(n-m)(\tau)}$, and minimum temperature $Tn'_{(n-m)(\tau)}$, during the months from n to m (starting in January) at the time lag τ, in years, omitted if it is equal to 0. These regression models are the simplest empirical models with the largest explanatory power (R^2= 67% for BA and 71% for NF). Our out-of-sample tests confirm that these simple regression models have predictive ability for summer fires in Catalonia (Figure 1).

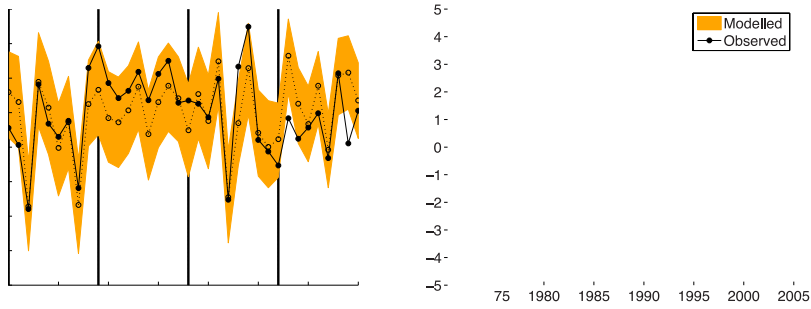

Figure 1. Out-sample prediction for (a) detrended log(NF) and (b) detrended log(BA). The continuous line with solid circles represents the observed data. The dotted line with empty circles is the median of 1000 different out-of-sample predictions; the dashed orange bands include 95% of the members of the ensemble of out-of-sample predictions. Vertical lines show the edges of the 4 test periods considered in a 9-fold cross validation during the 36-years period 1970-2005.

Finally we applied this model to estimate the impacts of observed climate trends on summer fires and the possible fire response to different regional climate change projections. The temperature trend indicates a clear warming, coherent with the observed regional and global warming (Turco *et al.* 2014b and reference therein) while for precipitation no significant trend is observed (Turco and Llasat 2011). Future projections indicate a sustained increase in temperature, particularly in summer, at a rate that continues the historical value. Precipitation projections show a non-significant decreasing trend (Turco *et al.* 2014a).

We assessed the impact of observed climate trends on wildfire statistics by fitting the fire-climate model with two sets of drivers: (i) all drivers: that is, the MLR consider the year-to-year climate variation added to the overall trend and (ii) only the climate drivers. The climate trends lead to a positive trend for NF (+0.16 log(number)/decade). While the actual trend is negative (0.42 log(NF) /decade) climate forcing alone would have led to a positive trend in NF. This suggests that the direct effect of climate (i.e. higher flammability) is more important than the indirect effects (i.e. lower fine fuel availability). In the absence of fire management, which presumably drives the NF decrease, we would have had a significant increase in NF. As an example, in the 70's the annual number of summer forest fires (>0.5 ha) arrived to 250, while at the end of last decade, was approximately near 50, but considering only the climate trend the expected value would be near 400. The climate change impact on BA is more complex. Both the actual fire trends (-0.49 log(BA)/decade) and the parts attributed to climate (-0.13 log(ha)/decade) are negative. In this case a decrease near to 40% in the burned area has been recorded since the 70's. This can be associated with the importance of antecedent climate conditions for this variable. A hypothesis would be that warmer conditions act on the fuel structure by limiting the availability of fine fuel and the spread of large fires.

Finally we analysed the future projections for NF and BA. For future projections, we drive the MLR models using only climate variables as predictors, that is, assuming no further improvement in future fire management. Figure 2 shows the impacts of climate change on BA and NF (as changes of the actual fire series and not of their log-transformed values). This is achieved by plotting the results for 2020-2050 relative to those for 1970-2000. Boxplots show the uncertainty of the ensemble of projections (composed by eleven RCMs) and the uncertainty of the fire-climate model parameters combined with RCM uncertainties (1000 bootstrap replications for each of the eleven RCMs). The results suggest that future warmer conditions should lead to a decrease in BA (the median of the BA is at -50% of the historical value), and to an increase in NF (median at about +50% of the historical value). The overall uncertainty is large, and it is dominated by the RCM spread (Figure 2).

Conclusions

We show that a transition toward warmer conditions has already started to occur and it is possible that these conditions will continue until 2050 (under the A1B scenario). Such an increase in temperature would promote more fires, with similar or lower extension. These results suggest that a warmer climate affects wildfire activity in Mediterranean environments, not only by leading to more favourable conditions for burning, but also modifying the structure of the fuel (availability and continuity) to be burned (Turco *et al.* 2014a).

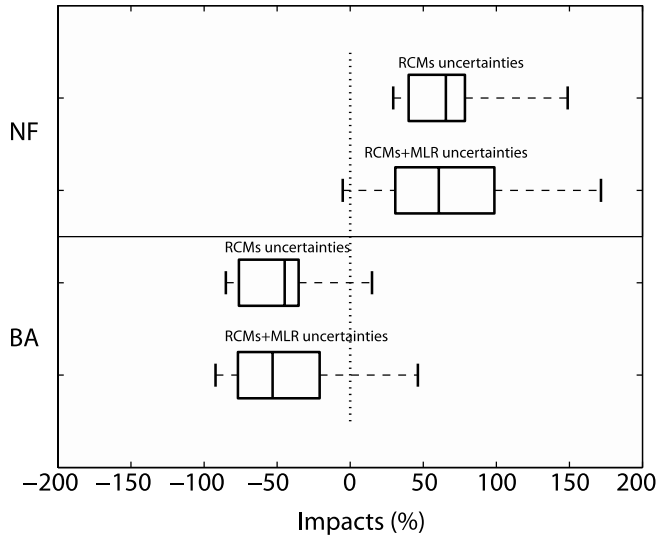

Figure 2. Impacts on BA and NF from climate change in 2020-2050 relative to 1970-2000. Boxplots show the uncertainty associated with the ensemble of model projections (11 RCMs) and the uncertainty of the fire-climate model parameters combined with the RCM uncertainties (1000 bootstrap replications for each one of the 11 RCMs). The median of the fire response is shown as a solid line, the box shows the 25-75 percentile range and the whiskers show the 5-95 percentile range.

Presumably, the complex relationships between climate, human activities, vegetation and fires, hamper the applicability of fire impact models to conditions which are very different from the current ones. For these reasons, we limited our estimate of wildfire response to a few decades in the future, when climatic conditions should not be dramatically different from the current ones. Even on such a limited time span, the ability to quantitatively predict the impact of climate change on wildfires is crucial to provide adequate society adaptation strategies. For example, the increase in NF which we find in future projections indicates the need for a more intense fire management effort in order to maintain the number of fires at least at the same level as today.

Acknowledgement

This work was partially funded by the Project of Interest “NextData” of the Italian Ministry for Education, University and Research.

References

Herrera, S., Fita, L., Fernández, J., Gutiérrez, J.M. (2010) Evaluation of the mean and extreme precipitation regimes from the ENSEMBLES regional climate multimodel simulations over Spain. *J Geophys Res* 115:1–13.

Herrera, S., Gutiérrez, J.M., Ancell, R., Pons, M.R., Frías, M.D., Fernández, J. (2012) Development and analysis of a 50-year high-resolution daily gridded precipitation dataset over Spain (Spain02). *Int J Climatol* 32(1):74–85.

San-Miguel-Ayanz, J., Moreno, J.M., Camia, A. (2013) Analysis of large fires in European Mediterranean landscapes: lessons learned and perspectives. *For Ecol Manag* 294:11–22.

Turco, M., Llasat, M.C. (2011) Trends in indices of daily precipitation extremes in Catalonia (NE Spain), 1951–2003. *Nat Hazards Earth Syst Sci* 11(12):3213-3226.

Turco, M., Quintana-Seguí, P., Llasat, M.C., Herrera, S., Gutiérrez, J.M. (2011) Testing MOS precipitation downscaling for ENSEMBLES regional climate models over Spain. *J Geophys Res* 116(18): 1–14.

Turco, M., Sanna, A., Herrera, S., Llasat, M.C., Gutiérrez, J.M. (2013a) Large biases and inconsistent climate change signals in ENSEMBLES regional projections. *Clim Chang* 120(4): 859–869.

Turco, M., Llasat, M.C., Tudela, A., Castro, X., Provenzale, A. (2013b) Brief communication Decreasing fires in a Mediterranean region (1970–2010, NE Spain). *Nat Hazards Earth Syst Sci* 13(3): 649–652.

Turco, M., Llasat, M.C., von Hardenberg, J., Provenzale, A. (2013c) Impact of climate variability on summer fires in a Mediterranean environment (northeastern Iberian Peninsula). *Clim Chang* 116: 665–678.

Turco, M., Llasat, M.C., von Hardenberg, J., Provenzale, A. (2014a) Climate change impacts on wildfires in a Mediterranean environment. *Clim Chang*: 125 (3-4): 369-380.

Turco, M., Marcos, R., Quintana-Seguí, P., Llasat, M.C. (2014b) Testing instrumental and downscaled reanalysis time series for temperature trends in NE of Spain in the last century. *Reg Environ Chang* 14 (5): 1811–1823.

Van der Linden, P., Mitchell, J. (2009) ENSEMBLES: Climate Change and its Impacts: Summary of research and results from the ENSEMBLES project (eds., P. van der Linden, J. Mitchell). Met Office Hadley Centre, FitzRoy Road, Exeter, UK.